16

CO-tolerant Catalysts

Siyu Ye

16.1 Introduction

Fuel cell systems offer the promise of economically delivering power with environmental and other benefits. Recently, polymer electrolyte membrane fuel cells (PEMFCs) have passed the demonstration phase and have partly reached the commercialization stage due to impressive research efforts. Nevertheless, there are still some technological challenges to be solved. Among those challenges, (i) choice of fuel (gasoline, methanol, or hydrogen), (ii) efficient fuel processing, with reduction of weight, volume, and carbon monoxide (CO) residuals, and (iii) development of anode electrocatalysts tolerant to CO at levels of 50 ppm (with a noble metal loading of 0.1 mg cm^{-2} or less) are deemed to be the most significant barriers that PEMFCs must overcome to achieve complete commercialization. The first and second challenges are closely related to the source and purity of hydrogen as the fuel.

The simplest and highest performing PEMFC systems employ pure hydrogen as the fuel. Since H_2 storage and supply devices are an issue, feeding the anode with the reformate of liquid alcohols, gasoline, or natural gas is the most popular choice, as they are readily available. The alcohols, gasoline, or natural gas are reformed using steam, partial oxidation, or autothermal reforming to produce the reformate – a hydrogen-rich gas stream (H_2, 40–70%) containing carbon dioxide (CO_2, 15–25%), carbon monoxide (CO, 1–2%), and small quantities of inert gases, such as nitrogen and water vapor. However, at current PEMFC stack operating temperatures of around 80 °C, the membrane electrode assemblies (MEAs) within the stack cannot tolerate such high CO levels. Therefore, the reformate must be passed from the reformer to a shift reactor and then to a catalytic preferential oxidation (PROX) reactor to reduce the CO content to less than 100 ppm, and in some cases down to a few ppm. The reformate can then enter the stack and react in the anode electrocatalyst layer of the MEA. The additional reformer, shift and PROX reactors significantly complicate and add extra cost to the PEMFC system [1]. For instance, Cu-based catalysts [2] were ordinarily used as the shift-converter catalysts in plants; however, it is difficult to use a Cu-based catalyst in the domestic-use PEMFC system. The PEMFC system would be frequently turned on

and off, and when it was turned off, the Cu catalyst would be easily oxidized by steam and air, and eventually deactivated. Therefore, precious metal catalysts such as Pt catalysts supported on CeO_2-containing oxides were used in the PEMFC system. On the other hand, Pd [3], Au [3], Pt, or Ru [5] is used as the catalyst for preferential oxidation of CO at low temperature. Among these, the Ru catalyst exhibited high performance for preferential oxidation of CO and long-term stability under a low O_2/CO molar ratio [5]. In any case, considerable amounts of precious metals were used in both a shift converter unit and a CO preferential oxidation unit, resulting in high cost. Moreover, this complicated system containing a CO-removal unit led to low efficiency and reliability. Therefore, developing CO-tolerant anode catalysts is a key priority. The US DOE 2011 targets for fuel cell stack CO tolerance are 500 ppm on steady state (with 2% max air bleed) and 1000 ppm on transient [6].

In a PEMFC, when operating with pure hydrogen at practical current densities, the anode potential is typically less than +0.1 V (vs. RHE (reversible hydrogen electrode)). Under such operating conditions the cell potential is only slightly lower than the cathode potential and the MEA performance essentially reflects the cathode operation. However, when using reformate as a fuel, the CO in the reformate stream binds very strongly to the Pt electrocatalyst sites in the anode catalyst layer, at the typical MEA operating temperature of 80 °C. Even at ppm levels of CO, the CO coverage is above 0.98 [7]. The adsorbed CO prevents the dissociative electrosorption of hydrogen and dramatically lowers the cell potential produced by the MEA, since a much higher anode potential is required to sustain the rate of hydrogen electrooxidation [8]. Poisoning of Pt anode electrocatalysts by CO is deemed to be one of the most significant barriers to be overcome in the development of PEMFC systems.

In addition, CO was found to be a poisoning adsorbate during the oxidation of methanol and other small organic molecules [9]. An important although not unique aspect of the catalysis of methanol oxidation in direct methanol fuel cells (DMFC) is related to the catalysis of CO oxidation. Therefore, methanol and CO oxidation reactions are both discussed in several reviews [10–12].

There are a number of ways to overcome the CO poisoning of electrocatalysts [13–15], namely: (i) advanced reformer design; (ii) use of CO-tolerant catalysts; (iii) oxidant bleeding into the fuel feed stream; (iv) employment of a bilayer (composite) anode structure; (v) higher cell operating temperature; (vi) use of membranes for CO separation; and (vii) pulsing the cell voltage to low values during cell operation, forcing the anode potential to operate for a short time at a potential positive enough to electrochemically oxidize CO to CO_2.

(i) *Advanced reformer design.* Most of the reformers, including the auxiliary processors that are currently available, are capable of producing a CO content of 50 ppm or less after a warm-up period of up to 2 h. To acquire the bleeding oxidant effect by modifying the reformer, many researchers have considered the possibility of designing a new reformer to which auxiliary processors are fitted for clean-up steps, e.g., as shift converters and a selective oxidizer [16–18]. These methods would, however, increase the complexity and cost of the fuel cell system. Even when these additional stages are used, it is difficult to maintain low CO levels

during start-up and transient operations without the addition of an air bleed into the fuel stream [13, 19–24].

(ii) *Use of CO-tolerant catalysts.* Because the use of CO-tolerant electrocatalysts would be more efficient and cause fewer associated problems, this is generally considered the most promising way for solving the CO poisoning problem in PEMFCs. A common approach consists of utilizing a second metal in the Pt-based anode catalyst, able to form oxygenated species (metal-OH) at potentials lower than for pure Pt [18, 25]. Following a bifunctional mechanism, these metal-OH species act as a source of oxygen, required for the oxidation of adsorbed CO to CO_2, liberating active Pt sites on the surface of the catalyst material where the adsorption and oxidation of the gaseous hydrogen takes place [26]. It has been also proposed that CO tolerance can be achieved by an electronic effect [27, 28], which is associated with an energy shift of the Pt 5d electronic states caused by the second element and resulting in a weakening of the Pt–CO interactions.

It has been found that the use of a second element with Pt, such as Ru, Sn, Co, Cr, Fe, Ni, Pd, Os, Mo, Mn, etc., in the form of an alloy or a co-deposit yields significant improvement in the CO-tolerance relative to pure Pt [29–38]. Among these various Pt-based binary systems, the most commonly used catalyst is carbon-supported PtRu alloy (PtRu/C). This material is known to enhance CO tolerance, which can be ascribed to the electronic modification of Pt-Ru in PtRu alloys that decreases the CO binding energy on Pt and also binds OH strongly on the Ru active sites in the PtRu alloys [39]. Within this system, the performance of PEMFCs has been improved for fuel streams containing CO [40–42].

(iii) *Oxidant bleeding into the fuel feed.* Even with PtRu in a well-designed anode layer with the reformate operation there are losses in cell potential that are not recovered. The air bleed technique [8, 43] must be employed to introduce ≤ 2% air into the fuel stream to catalyze the oxidation of CO to CO_2. This recovers the cell potential losses at 100 ppm CO and most of the small loss due to 25% CO_2. Low levels of oxygen or oxygen-evolving compounds [8, 43–46] are bled into the fuel feed to decrease CO poisoning. With this procedure, the levels of CO produced in the reforming reaction can be reduced by reactions such as the water-gas shift (WGS) reaction and the selective oxidation of CO. (Note: CO can also be diminished by the methanation reaction with hydrogen but this is not efficient because it consumes the hydrogen.) Many working groups have reported that oxidant bleeding can be effective. In addition, hydrogen peroxide (H_2O_2) in an anode humidifier has been successfully used to mitigate the level of CO in H_2-rich feed [45, 46]. In this case, however, fuel utilization will certainly be decreased and safety issues must also be considered [47]. During the bleeding of oxidant process, roughly one out of every 400 O_2 molecules participates in the oxidation of CO [48], and the remaining oxygen chemically combusts with hydrogen. This combustion reaction not only lowers the fuel efficiency, but might also accelerate the sintering of catalyst particles, leading over time to a performance decline. In addition, the chemical combustion might also create pinholes in the electrolyte membrane, which could result in cell failure. The increased temperature on the catalyst surface and accelerated membrane failure are drawbacks to this method if moderation is not observed. For this reason, a bilayer anode structure using a

platinum group metal-based gas-phase catalytic oxidation layer between the gas diffusion substrate and the PtRu electrocatalyst layer was adopted to extend the anode lifetime [43]. This moves the heat generation away from the PtRu electrocatalyst layer and the membrane.

(iv) *Employment of a bilayer (composite) anode structure.* In accordance with the fuel selection, a more effective tolerance of CO in a PEMFC can be achieved by modifying the structure of the catalyst, i.e., with a composite or a double-layer. For example, the structure is designed to make the CO react with the CO-active electrocatalyst in advance at a separate layer and have the main hydrogen react at another layer with the traditional Pt electrocatalyst. There is still scope to optimize this type of structure and thus make the method even more effective for the suppression of CO poisoning. Although many attempts have been made in the last few decades to develop Pt-based binary or ternary electrocatalysts for replacing or reducing the platinum in the catalysts of PEMFCs, there has been less effort towards developing CO-tolerant electrodes by modifying their structure. The electrode structure relates to the diffusion process and reaction dynamics. In other words, because the diffusion coefficients of H_2 and CO are different, it is possible to design a special composite electrode structure according to the fuel components. In doing so, the anodes can be made with different electrocatalyst components, contents, and pore distributions. Therefore, this is considered to be a promising alternative approach to decreasing the poisoning of PEMFC anodes [43, 49–51].

Ralph et al. [43] discussed improvements in the reformate (CO and CO_2) tolerance at the anode and in extending the MEA durability. Improvements have been achieved by advances in platinum/ruthenium electrode design, in the application of bilayer anodes for durable air bleed operation. Johnson Matthey and Ballard Power Systems have significantly extended anode lifetimes by introducing a bilayer anode structure, in which a carbon-supported Pt-based catalyst layer is inserted between the PtRu electrocatalyst layer and the anode substrate [52]. It has been shown that the bilayer anode structure achieved a comparable MEA performance to the standard anode when operating both on reformate and on pure hydrogen. More importantly, the bilayer anode did not require an increase in the level of the air bleed beyond 3% to sustain the MEA performance, even after 2000 hours of continuous operation. This minimizes the degree of electrocatalyst sintering and significantly reduces the possibility of membrane pin-holing. Using the bilayer anode has resulted in stable MEA performances over many thousands of hours of continuous operation. For example, for an MEA with a bilayer anode containing 0.35 mg Pt cm^{-2} the reformate performance with a 2% air bleed was stable after in excess of 8000 hours of continuous operation. This bilayer approach may produce the required MEA lifetimes for PEMFC applications that need an air bleed to sustain reformate operation.

Wan and Zhuang [51] proposed a novel layer-wise anode structure to improve the CO-tolerance ability and utilization efficiency of the catalyst. The layer-wise structure consists of an outer and an inner catalyst layer. The outer catalyst layer, acting as a CO barrier, is composed of two nano-Ru layers (0.06 mg cm^{-2}) by the magnetron sputtering deposition method and a $Pt_{50}Ru_{50}$ layer (0.10 mg cm^{-2}) by the screen-printing method on the GDL. The inner catalyst layer providing the hydrogen oxidation reaction is a pure Pt layer (0.07 mg cm^{-2}) prepared by the

direct-printing method on the PEM. The roles of the outer and inner catalyst layers in the improvement of CO-tolerance ability and utilization efficiency of catalyst for the proposed catalyst layer structure were investigated. SEM, X-ray, EDS, and EPMA analysis were used to characterize microstructures, phases, chemical composition, and distributions for the obtained electrocatalyst layers. The hydrogen fuel containing 50 ppm CO + 2% O_2 is continuously fed to the anode side to investigate the dependence of CO-tolerance ability over time for the MEAs, respectively. A combination of two deposited nano-Ru layers with a printed $Pt_{50}Ru_{50}$ layer to form the outer catalyst layer for the anode electrode provides superior CO-tolerance capability to that of conventional and Haug's structures [53] in the presence of 2% O_2 and oxygen-free hydrogen containing 50 ppm CO fuels. In the oxygen-free hydrogen fuel containing 50 ppm CO, the deposited nano-Ru layer functions as a separator and/or for the physical/chemical adsorption of CO from hydrogen. The excess CO completely transforms to CO_2 by the third $Pt_{50}Ru_{50}$ layer at the outer catalyst layer. While in the presence of 2% O_2 hydrogen fuel containing 50 ppm CO, the deposited nano-Ru layer functions as a filter of CO from hydrogen, which reacts with the produced hydroxyl group from oxygen to form CO_2. The excess CO reacts with the hydroxyl group formed from oxygen and water on the surface of the third $Pt_{50}Ru_{50}$ layer of the outer catalyst layer, producing CO_2. The fuel entering the inner catalyst layer is thus free of CO. The inner direct-printed Pt catalyst layer can thus maintain high activity in the hydrogen oxidation reaction. In other words, it is possible by combining two structures to achieve a low noble metal loading MEA with high CO-tolerance capability in both oxygen-free and oxygen-present hydrogen fuels containing 50 ppm CO.

(v) *Higher cell operating temperature.* There is a considerable drive to raise the operating temperatures of the PEMFC to above 100 °C. This would raise the system efficiency and dramatically improve the CO tolerance of Pt-based electrocatalysts. For example, the CO coverage on Pt drops from in excess of 0.98 at 80 °C to ~0.5 at 160 °C [54]. At this temperature a Pt-based anode can function in the presence of 1 to 2% CO rather than with ppm levels of CO, eliminating the need for the PROX reactor. If the temperature can be raised to 160 °C, studies in the phosphoric acid fuel cell (PAFC) with 1 to 2% CO indicate that PtRh and PtNi may offer superior CO tolerance [55, 56]. Indeed, at 200 °C pure Pt is the favored electrocatalyst in the PAFC. At higher temperatures PtRu may not be the electrocatalyst of choice in the PEMFC. There is currently much research [57] aimed at developing membranes capable of proton conduction at 120 to 200 °C.

(vi) *Use of membranes for CO separation.* There is also considerable interest at the present time in the development of membranes designed for purification and separation. One approach has been the development of high-temperature (140 °C) membranes [58]. The CO tolerance of PEMFCs increases with increasing temperature [59]. Therefore, to decrease CO poisoning, it is desirable to develop high-temperature membranes. On the other hand, increasing temperature decreases the life of the membrane and renders maintenance of membrane hydration more difficult. Work on phosphoric acid-doped polybenzimidazole revealed long-term chemical and mechanical stability at high temperature [60]. Nevertheless, there were still problems with membrane cycle-life and hydration. Other membrane

approaches can be used for separating hydrogen from gas mixtures. For example, the palladium membrane has been studied extensively but is still very expensive for use in fuel cells [61].

(vii) *Pulsing cell voltage or current.* It is possible to pulse periodically the load current [62], which reduces the potential on the cell to a value low enough to promote electrooxidation of CO on the surface. In fact, if the cell is kept at constant current in certain conditions it will start oscillations by itself [63]. The problem arises in accommodating both of those techniques into a fuel cell stack. It is most likely that some blend of using a catalyst with high resistance to poisoning and a dynamic cleaning technique could be used in future cells.

The poisonous influence of carbon monoxide on platinum catalyst layers is well researched (e.g., [64–67]). Some reported work and critical reviews on CO tolerance and CO-tolerant catalysts have been published recently by Ralph et al. [43, 68, 69], Urian et al. [70], Ruth et al. [71], and Wee and Lee [15]. Other reviews of PEMFC CO poisoning can be found in the literature [11–13, 72–75].

This review discusses the mechanism of CO tolerance and the development of CO-tolerant catalysts. The development of Pt-based binary/ternary metallic electrocatalysts and Pt-free electrocatalysts is discussed. Useful information is also provided on characterization methods for the understanding of the mechanism of CO tolerance and the evaluation of anode electrocatalysts.

16.2 Mechanisms of CO Tolerance

PEMFC performance degrades when CO is present in the fuel gas; this is referred to as CO "poisoning", a term that may have to be revised, as discussed later in this chapter. Several studies have investigated the deleterious effect of carbon monoxide on platinum catalyst layers (e.g., [64–67]). This results from the attachment of a CO molecule onto the catalyst surface, thereby reducing the surface available for hydrogen reactions. Linear or bridge-bonded CO species are formed on the catalyst surface [64, 67, 76]. Such strong binding has been explained by electron donation from the 5σ carbon monoxide orbital to metal, and subsequent transfer of two electrons from the d metal atomic orbital to the antibinding $2\pi^*$ CO orbital, as shown in Figure 16.1. This electron transfer is known as back-donation.

Despite its importance for low-temperature fuel cells, the exact mechanism of CO oxidation on Pt and the role of co-catalysts are still far from being understood. On Pt(1 1 1), the saturation coverage of CO corresponds to a (2×2)–3CO adlayer with a coverage of $\nu = 0.75$ at low potentials according to STM and FTIR results [77]. Here, the coverage ν is the ratio of CO molecules to Pt-surface atoms. At a potential around 0.4 V, a part of the adsorbate is oxidized, and the adlayer transforms into a lower coverage adlayer with $\nu = 0.68$; Villegas et al. have suggested a $(\sqrt{19}\times\sqrt{19})$R 23.4° structure based on STM results [77]. It is generally accepted that the oxidation of the adlayer proceeds according to a Langmuir-Hinshelwood mechanism. The exact identity of the oxygen species, however, is not really clear. Also, the literature describes contradictory results concerning the

surface diffusion of CO. Whereas fast diffusion should lead to the classical rate equation for a Langmuir–Hinshelwood mechanism as usually treated in textbooks (the rate is proportional to $\Theta(1 - \Theta)$, where Θ is the ratio between coverage and maximum coverage), slow diffusion leads to an oxidation behavior determined by a nucleation and growth mechanism [78–82].

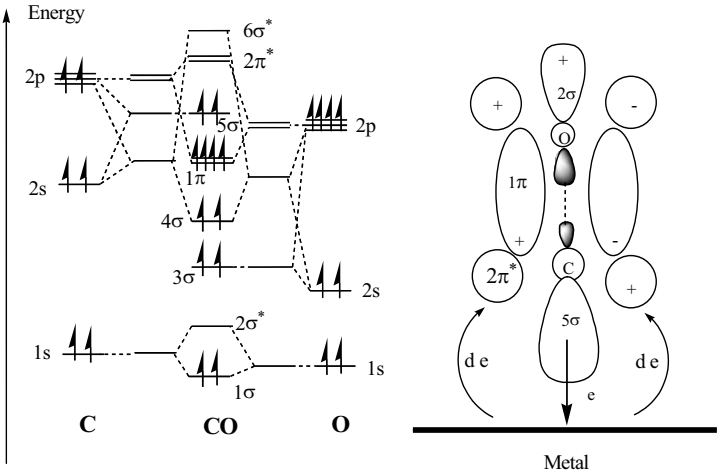

Figure 16.1. The energy level of carbon monoxide molecules, and the formation of metal-carbon monoxide bonding [449]. (Reprinted from Grgur BN, Marković NM, Lucas CA, Ross PN. Electrochemical oxidation of carbon monoxide: from platinum single crystals to low temperature fuel cells catalysis. Part I: carbon monoxide oxidation onto low index platinum single crystals. J Serb Chem Soc 2001;66:785–97. With permission from the Serbian Chemical Society.)

The transition between the high coverage phase and low coverage phase leads to the so-called pre-peak in cyclic voltammetry, which was also observed on polycrystalline Pt and other surfaces (like vicinally stepped Pt(1 1 1) [24, 83–85]), and which is often referred to as a weakly adsorbed state. By recording potential transients during oxidation of the adsorbed CO under galvanostatic conditions, it has been shown that the oxidation of that amount of CO that desorbs during the transition between the two adsorbate states does not follow any of the Langmuir-Hinshelwood-type rate equations [86]. The transients rather suggest an Eley Rideal mechanism. Probably, CO is oxidized at defect sites on the surface, the number of which is constant and to which CO diffuses quickly at high coverage. In contrast, the galvanostatic potential transients during further complete oxidation showed the potential maximum typical for both types of Langmuir-Hinshelwood mechanisms (i.e., fast or slow diffusion) only after oxidation of approximately one tenth of the adsorbate at nearly constant potential.

The promotional effect of ruthenium in improving the CO tolerance of Pt anode catalysts for proton exchange membrane fuel cells (PEMFCs) has long been recognized [87] and carbon-supported PtRu catalysts are currently seen as the best anode catalysts when reformate is the anode feed in such fuel cells [43, 88].

However, there is also an ongoing debate concerning the action of co-catalysts. The mechanism by which the promotion occurs was described by Watanabe and Motoo [89] as bifunctional, with Ru supplying oxygen species at lower potentials that facilitate the removal of adsorbed CO from the active Pt sites (by the activation of water to form OH) as well as decreasing the strength of the Pt–CO bond via a perturbation of electronic properties of the Pt atoms (a ligand effect). It has also been shown that neither of these two effects alone is able to explain the co-catalytic effect of Ru in fuel cell anodes [90]. Considerable effort has gone into further understanding the details of this mechanism and several excellent reviews are available that summarize the findings [12, 91, 92].

In the case of less noble co-catalysts, it is also often assumed that they act according to the bifunctional mechanism. In the case of Mo, this effect seems to be limited to the oxidation of the weakly adsorbed CO [93]. The $Pt_3Sn(hkl)$ alloys have shown a high activity for bulk CO oxidation that is correlated to a weakly adsorbed state of CO, with an onset potential that is lower by approximately 300 mV [34]. Moreover, it was also demonstrated with Sn modifications of Pt single crystal surfaces that a major promoting effect is the shift in the onset potential of the oxidation of the weakly adsorbed state of CO to much lower values and, in addition, that the population of the weakly adsorbed state is drastically increased [24, 83, 94]. A prerequisite for the high CO oxidation activity of Sn/Pt surfaces is a uniform distribution of co-adsorbed Sn, e.g., by step decoration of the Pt(3 3 2) electrode. The oxidation potential of the "strongly adsorbed state", on the other hand, is hardly shifted. It is therefore assumed that contrary to what is generally believed, Sn mainly has an electronic influence on neighboring Pt atoms, changing the binding energy of CO to Pt. On a Pt(1 1 1) electrode, Sn is much less active, and this is due to the formation of 2D islands, which, however, are very mobile in the absence of co-adsorbed CO, as shown in a recent STM study [39]. For the maximum coverage ν (ratio of Sn atoms to surface Pt atoms) of Sn on Pt(1 1 1), a value of 0.33 was postulated. This was only based on a correlation of the oxidation peak charge (presumably OH adsorption on or within the Sn adlayer on Pt(1 1 1)) to the suppression of hydrogen adsorption.

16.2.1 Electrochemistry of Carbon Monoxide and Hydrogen

In order to understand the behavior of a PEMFC in the presence of CO, the electrochemistry of CO and hydrogen on the surface of platinum must be understood. This is because platinum or its alloys are invariably used and needed in low-temperature acid electrolyte fuel cells to facilitate the electrochemical reaction for the production of electric power. The electrochemistry of CO in an acidic environment has been studied extensively [95] and reviewed by Baschuk and Li [96]. CO oxidation and adsorption occurs on the (1 0 0) and (1 1 0) sites of platinum in an acid electrolyte. The adsorption of CO involves CO linearly bonded to platinum, and the adsorption isotherm is that of a Tempkin isotherm, which can be written as [97]:

$$\theta_{CO} = -\frac{\Delta G_o^0}{r} - \frac{RT}{r}\ln H + \frac{RT}{r}\ln\left(\frac{[CO]}{[H_2]}\right) \tag{16.1}$$

The interaction parameter and the free energy of adsorption were found to be functions of temperature, and in addition, the interaction parameter was found to be highly dependent on catalyst structure. Also, this relation was only valid for relatively high temperatures of greater than 130 °C; for low temperatures, such as those encountered in a PEMFC, the coverage appeared to be a function of the anode potential as well as the concentration, in addition to the temperature and catalyst structure.

The oxidation of CO occurs from a voltage range of 0.6–0.9 V, depending on the voltage sweep rate used in the voltammetry experiment [95]. The rate of oxidation of CO at low coverage is rapid while the rate is poisoned by a high coverage of CO. This dependence on coverage could be explained if the electrochemical oxidation of CO involved adjacent surface sites [98].

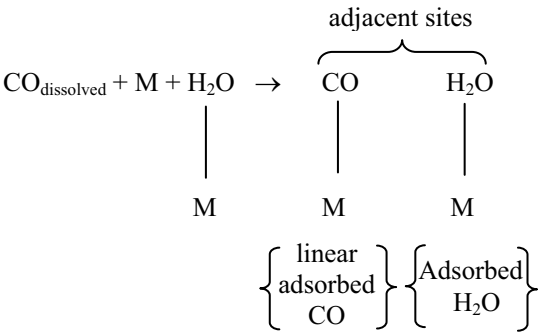

(16.2)

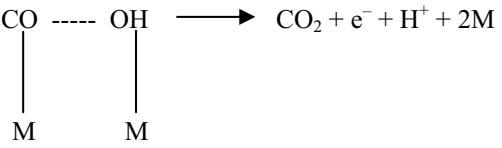

(16.3)

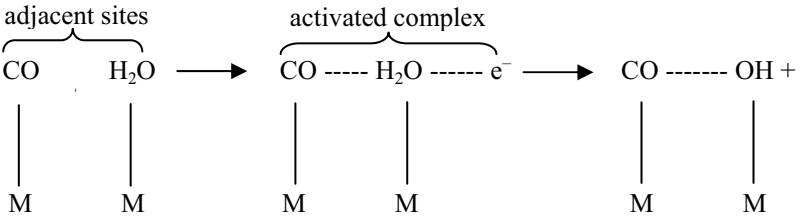

(16.4)

where M is a metal adsorption site. Equation 16.2 is a very rapid adsorption step; in most experimental situations, the rate of CO adsorption is controlled by the diffusion of CO to the metal catalyst surface. This step determines the initial

surface concentration of the reactant pairs. Equation 16.3 is the electron-transfer step, which is rate determining for any fixed concentration of reactant pairs. Equation 16.4 is the final electron transfer reaction and is assumed to be rapid compared to Equation 16.3. This mechanism of CO oxidation can be thought of as CO lowering the energy of activation for the dissociation of water, and is similar to the catalyzed gas-phase oxidation of CO by oxygen.

The oxidation of hydrogen and the effect of CO in an acid environment have also been extensively studied. The mechanism for electrochemical hydrogen oxidation over smooth platinum in an acid electrolyte is the slow dissociation of adsorbed hydrogen molecules to hydrogen atoms, known as the Tafel reaction, followed by the fast electrochemical oxidation of the adsorbed hydrogen atoms, known as the Volmer reaction [99]. This is illustrated below:

$$H_2 + 2M \leftrightarrow 2MH \qquad \text{Tafel} \qquad (16.5)$$

$$2MH \leftrightarrow 2M + 2H^+ + 2e^- \qquad \text{Volmer} \qquad (16.6)$$

It was also discovered that the dissociative chemisorption of hydrogen on platinum was independent of both surface geometry and crystallite size, leading to the result that the exchange current density for the hydrogen reaction was independent of catalyst structure [100].

The mechanism of CO poisoning of the hydrogen oxidation reaction was found to be as follows [100]. CO chemisorbs on the platinum sites to the exclusion of hydrogen. This is possible because CO is more strongly bonded to platinum than is hydrogen, as indicated by a greater potential required for the oxidation of CO than of hydrogen, and a sticking probability of CO on platinum 15 times higher than that of hydrogen on platinum. Also, if the Gibbs free energy of adsorption of hydrogen and CO are compared and it is assumed that the Gibbs free energy of adsorption for CO continues to become more negative as temperature decreases, CO will preferentially adsorb to platinum due to the more negative Gibbs free energy of adsorption. The result is that even a relatively small concentration of CO can result in the complete coverage of the platinum surface, to the exclusion of the hydrogen. In spite of CO preferentially adsorbing on the platinum surface, the rate of hydrogen oxidation on even the few remaining platinum sites is so rapid that it controls the surface potential or free energy of the catalyst. Unfortunately, because this potential is less than the potential needed to oxidize CO, the coverage of CO remains at that dictated by the CO adsorption isotherm. Thus, the mechanism of CO poisoning of hydrogen oxidation is that linearly-bonded CO blocks sites for the dissociative chemisorption of hydrogen, and the current density, or reaction rate, of hydrogen in the presence of CO is reduced and can be written as:

$$i_{H_2/CO} = i_{H_2} (1 - \theta_{CO})^2 \qquad (16.7)$$

Thus, the coverage of CO on the platinum electrode surface becomes a significant parameter in the performance of an electrode. In the experimental studies cited earlier, it was concluded that the coverage of CO was a function of potential as

well as CO partial pressure. Also of interest, CO and hydrogen do not interact during their co-adsorption at temperatures of less than 200 °C. However, it has been noted that the apparent activation energy for hydrogen oxidation increases with increasing CO concentration, indicating an increased difficulty for the hydrogen to oxidize in the presence of CO [97]. This was speculated to be because either CO preferentially adsorbed to the "best" sites for hydrogen oxidation or hydrogen was involved in the CO oxidation process.

Another aspect of CO poisoning that has been studied is termed carbon dioxide (CO_2) poisoning. At CO_2 concentrations in excess of 25%, the voltage losses in the anode are greater than what can be accounted for through the reactant dilution, or the so-called Nernst losses [101]. It was theorized that this was due to CO_2 converting to CO through either the reverse water gas shift reaction:

$$CO_2 + H_2 \rightarrow CO + H_2O \tag{16.8}$$

or by the electroreduction of CO_2:

$$CO_2 + 2H^+ + 2e^- \rightarrow CO + H_2O \tag{16.9}$$

Wilson et al. [101] discovered that the severity of CO_2 poisoning decreased if all of the anode catalyst was tied up within an electroactive structure. Since Equation 16.8 requires only a catalyst site in contact with the gas phase, this indicates that Equation 16.8 is more prevalent than Equation 16.9, which requires a site with good gas, ionic, and electronic access.

Table 16.1. The equilibrium concentration, in ppm, of CO with varying temperature, relative humidity and total pressure. CO concentration for a total pressure of 3 atm is given in parentheses while the values not in parentheses are the result of a total pressure of 1 atm. The initial concentration of dry gas is 25% CO_2 and 75% H_2 [96]. (From Baschuk J, Li X, Carbon monoxide poisoning of proton exchange membrane fuel cells, International Journal of Energy Research, ©2001 John Wiley & Sons Limited. Reproduced with permission.)

Initial relative humidity of H_2O				
Temperature (°C)	**0**	**50**	**80**	**100**
25	1310 (1310)	106 (308)	65.2 (198)	51.5 (159)
50	2590 (2590)	98.0 (315)	56.6 (194)	42.9 (153)
80	4920 (4920)	62.2 (269)	26.0 (152)	15.0 (113)
95	6500 (6500)	35.7 (233)	7.25 (119)	1.44 (82.0)

An increase in temperature will increase the equilibrium concentration of CO, if the initial relative humidity is zero. However, with the initial presence of water vapor in the fuel stream, an increase in temperature will decrease the equilibrium concentration of CO. This is because the partial pressure of water increases at higher temperatures, which drives Equation 16.8 to the left and results in a

decreased CO concentration. An increase in total pressure results in an increased equilibrium concentration of CO due to the larger partial pressures of CO_2 and H_2, which drives Equation 16.8 to the right. The majority of equilibrium concentrations of CO calculated in Table 16.1 are well in excess of the 2–10 ppm CO that a PEMFC can tolerate and thus operation with 25% CO_2 should be impossible. However, the fact that cell operation is possible under these conditions may be explained by the fact that the water gas shift reaction does not proceed rapidly at temperatures experienced by a PEMFC. As a result, the actual concentration of CO may be much less in an operating PEMFC than the equilibrium value shown in Table 16.1. This may also explain why the effect of this CO_2 poisoning is minimal if CO is already present, as the effect of CO is much greater than that of the CO_2 poisoning [74]. Thus, the production of CO from CO_2 was found to be kinetically limited and the effect was negligible unless no CO was initially present in the fuel gas and the concentration of CO_2 was high (say, 25% or higher).

16.2.2 Characteristics of PEMFC CO Poisoning

The polarization of a PEMFC in the presence of CO yields interesting results. Oetjen et al. [102] examined the effect of CO on a PEMFC performance. The cell operating temperature was 80 °C and CO concentrations of 25, 50, 100, and 250 ppm were used in the fuel gas. It was found that for hydrogen and 25 ppm CO, the cell polarization curve looked similar to the curve without CO, only with a more negative slope. However, for CO concentrations greater than 100 ppm, the polarization curve had two distinct slopes. The lower slope was explained by the adsorption and oxidation kinetics of hydrogen and CO at the anode. At increasing current densities, the potential of the anode increased to values at which adsorbed CO could be oxidized to CO_2, thus leading to higher reaction rates for hydrogen adsorption and oxidation. The poisoning of a PEMFC is illustrated in Figure 16.2. It was also found that the poisoning effect takes a significant amount of time to reach steady state, as illustrated in Figure 16.3. The CO poisoning could be reversed by operation at open circuit voltage with pure hydrogen for 2–3 h. Therefore, the CO poisoning effect must be taken as a transient phenomenon in the operation of PEMFCs used in transportation applications. Similar PEMFC performance data with CO in the fuel gas can be found in the literature [101, 103, 104].

Zawodzinski et al. [105] compared their PEMFC poisoning data with others' and found discrepancies in the amount of CO that could be tolerated. It was surmised that these discrepancies may have been due to different flow rates. Lower flow rates allow better CO tolerance via the oxidation of CO by oxygen crossover from the cathode to the anode, thus freeing up sites for the hydrogen oxidation reaction. This conjecture may be confirmed by an estimate of the amount of oxygen crossover from the cathode.

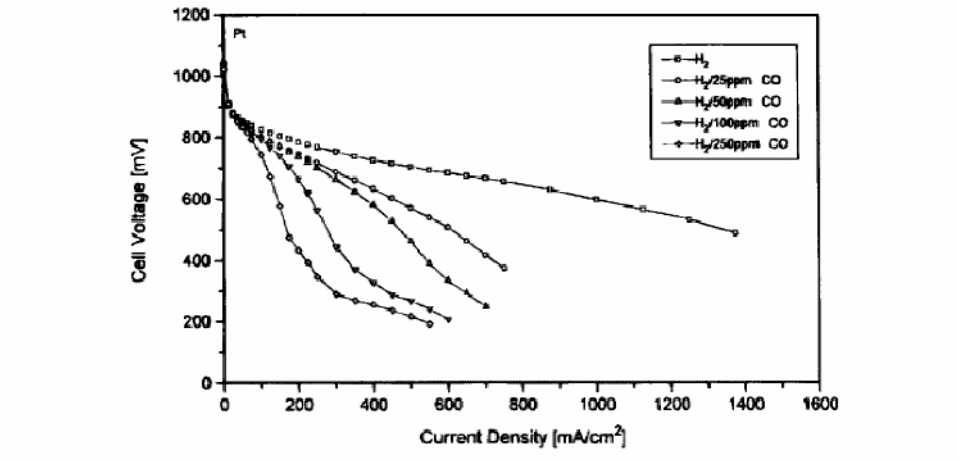

Figure 16.2. Illustration of the effect of CO on a PEMFC [102]. (Reproduced by permission of ECS—The Electrochemical Society, from Oetjen H-F, Schmidt VM, Stimming U, Trila F. Performance data of a proton exchange membrane fuel cell using H_2/CO as fuel gas.)

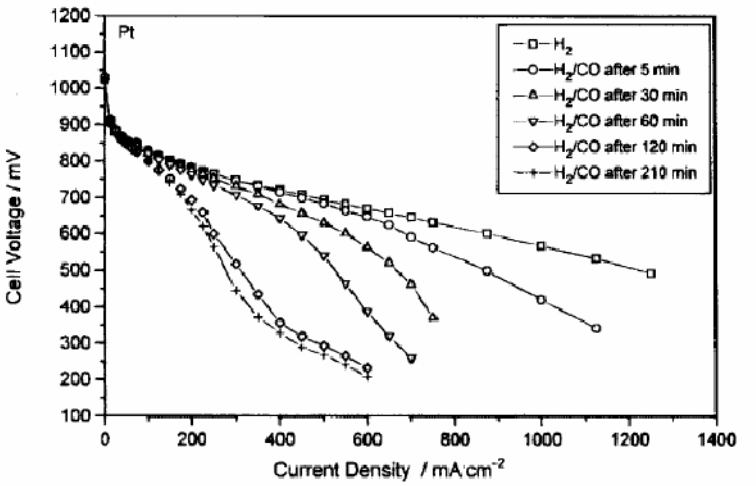

Figure 16.3. Illustration of the transient nature of the CO poisoning of a PEMFC. CO concentration is 100 ppm [102]. (Reproduced by permission of ECS—The Electrochemical Society, from Oetjen H-F, Schmidt VM, Stimming U, Trila F. Performance data of a proton exchange membrane fuel cell using H_2/CO as fuel gas.)

16.2.3 Bifunctional Mechanism of CO Tolerance

Despite the wealth of research in this area, the reasons for the effectiveness of Pt-Ru over other alloys are still hotly debated. Two widely accepted mechanisms for the oxidation of CO from the Pt-Ru surface exist [31, 106–109]: (1) the

"bifunctional" mechanism and (2) the direct mechanism, enabled by the ligand or electronic effect.

To remove CO_{ads} from the surface it is necessary to generate some oxygenated species that can react with CO_{ads} to produce CO_2 and release some free sites on Pt surfaces for the hydrogen oxidation reaction. The mechanism for the oxidative removal of the CO_{ads} from platinum anodes has been a topic of intense investigation for the past 40 years. The overall reaction for removing CO_{ads} is

$$CO_{ads} + H_2O = CO_2 + 2H^+ + 2e \qquad E_{o\ 25\ °C} = -0.10\ \text{V (vs. NHE)} \qquad (16.10)$$

The mechanism of hydrogen oxidation in the H_2/CO mixtures on platinum has been given by Equations 16.2–16.6.

Hydrogen oxidation reaction occurs on the free sites liberated during the time between CO_{ads} oxidative removal, Equation 16.4, and CO re-adsorption from solution, Equation 16.2. At the low potential (E < ~0.6 V) the rate constant of CO_b re-adsorption is much higher than the rate constant for CO_{ads} oxidation, and in practical terms only an infinitely small number of platinum sites could be liberated for H_2 oxidation.

The hydrogen oxidation reaction reaches maximum at the same potential where CO_{ads} is oxidized by Pt-OH (coverage with CO_{ads} in that potential region tends to zero). According to this, it is necessary to provide a supply of OH species to adjunct platinum atoms covered by CO_{ads} using some other metal that does not adsorb CO. This is known as a bifunctional catalyst. Schematic representation of such a catalyst is given in Figure 16.4.

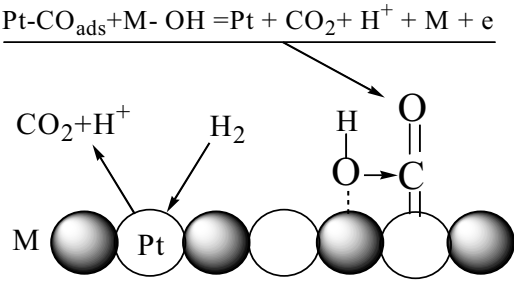

Figure 16.4. Bifunctional catalyst (schematic representation)

Based on early work by Watanabe and Motoo [89] (originally on the enhanced oxidation of CO and methanol at Pt electrodes with various oxygen-adsorbing adatoms [34, 39, 81–83, 90, 93, 94]), a bifunctional mechanism involving water activation by Ru (Equation 16.11) and subsequent CO electrooxidation on a neighboring Pt atom (Equation 16.12) has been postulated by a number of groups [20, 102, 103, 110–112].

$$Ru + H_2O = Ru\text{–}OH + H^+ + e^- \qquad (16.11)$$

$$Pt–CO + Ru–OH = CO_2 + H^+ + e^- + Pt + Ru \quad (16.12)$$

It should be noted that Ru-OH means simply oxygen-containing surface species at the Ru surface; the exact nature of this species is still unknown.

To investigate the mechanism of CO tolerance by PtRu, half-cell studies in H_2SO_4 at 80 °C with PEMFC anode structures containing Nafion were performed using pure CO as the reactant. The half-cell outlet gas was analyzed using in-line mass spectrometry for evidence of CO_2 – to examine PtRu for CO electrooxidation activity (Equation 16.12). The results indicated that CO electrooxidation was occurring on PtRu at above +0.25 V (vs. RHE). This is some 0.2 V less anodic than required for pure Pt electrocatalysts and reflects the greater ability of the Ru to adsorb water (Equation 16.11), as compared with Pt. In the cyclic voltammograms measured in H_2SO_4 at 25 °C, the promotional effect from PtRu is also reflected in a lower peak potential for CO electrooxidation at the electrodes: PtRu (+0.5 V (vs. RHE)) compared with Pt (+0.8 V (vs. RHE)). Both the half-cell and the cyclic voltammetry studies confirmed that at anode potentials above +0.25 V (vs. RHE) the improved CO tolerance of PtRu is due to the enhanced electrocatalysis of CO electrooxidation to CO_2 (Equations 16.11 and 16.12).

This mechanism has been adopted as the explanation of CO-tolerant H_2 oxidation on other Pt-M alloy catalysts. Although practically all transition metals are oxidized in acid solutions, the fact is that only a few metals alloyed with platinum show certain activity for oxidation of H_2/CO mixtures, as such metals have to be able to provide OH at low potential (e.g., near the hydrogen reversible potential). Research has been conducted on both Pt–M bimetallic nanocrystals such as Pt-Ru, Pt-Sn, and Pt-Mo [20, 21, 35, 113] and M-decorated Pt single crystals involving Ru [16–20, 26, 44–47, 70, 81, 106–108, 114–122, 123–128], Mo [24, 70, 126–128, 129–131], Sn [26 , 29–31, 125] and other transition metals [42, 114, 129, 130]. The bifunctional mechanism is generally acknowledged as the dominant effect for single-crystal Pt decorated by other metals, particularly for Ru on Pt(111) [46, 106–108, 124].

16.2.4 Direct Mechanism of CO Tolerance (Ligand or Electronic Effect)

The bifunctional mechanism does not take into account a possible change in the CO binding energy on Pt induced by Ru (often referred to as an electronic effect), nor does it directly describe the effect of CO and OH competitive adsorption on the Ru. The origin of such an effect has not yet been completely understood. On the one hand, according to the *d*-band shift model of Hammer and Norskov [131], it was proposed that the addition of a second element, by donating electron density, provides modification of the electronic interactions between Pt and the CO adsorbate. Such a “ligand effect” [118, 132–136] results in a decrease of the Pt–CO bond strength and yields facile CO_{ads} electrooxidation, either directly by OH deposited on the Pt surface, or by enhancing Pt–H_2O activation and thereby allowing the reaction of OH and CO directly on the Pt. The ligand model proposes that ruthenium modifies the electronic properties of platinum, weakening the Pt–CO bond and thereby lowering the CO electrooxidation potential.

The electronic effect has been suggested to provide increased tolerance to CO in reformate systems, presumably by weakening the Pt–CO bond and decreasing the CO coverage, thereby increasing the anode efficiency by leaving more surface sites free for H adsorption at low potential [31]. Additionally, the ligand effect has been shown to have a large effect on Pt atoms near Ru islands for Ru/Pt(111), but Pt atoms far from these islands are minimally affected [116]. The externally exposed Ru islands are known to be in some stage of oxidation in an aqueous electrode (i.e., RuO_nH_m) at nearly all potentials [127]. Recent experiments using well-defined PtSn and PtMo electrodes [119, 120, 127, 128] have shown that both surfaces are better CO oxidation catalysts than PtRu, even though both may not be particularly useful as practical CO-tolerant hydrogen or methanol oxidation catalysts. This enhanced performance compared with PtRu was ascribed to a lack of adsorption of CO on either Sn or Mo, leaving more adsorption sites for oxygen-containing species.

The consequences of the ligand effect and the bifunctional mechanism for CO oxidation on Pt/Ru have been debated extensively in the literature. The emerging consensus seems to be that the ligand effect is less important than the bifunctional mechanism [106, 107, 138–142]. Some authors have attempted to quantitatively determine the relevance of the ligand effect as compared to the bifunctional mechanism, with Masel, Wieckowski, and coworkers concluding that about 20% of the enhancement in CO oxidation afforded by Ru deposition can be attributed to the ligand effect, while the remaining 80% of the enhancement is due to the bifunctional mechanism [106, 107].

16.2.5 Surface Science Study and Modeling of CO-tolerance Mechanism

CO adsorption and oxidation have been studied for many years, but a greater understanding was achieved by the development of *ex situ* and *in situ* spectroscopic and microscopic methods for application in electrochemistry [9, 143–146], together with the use of well-defined nanocrystalline electrode surfaces [147]. The opportunity to study *in situ* electrooxidation of carbon monoxide [148–157] under fuel cell reaction conditions has brought significant progress in understanding interfacial electrochemistry on metallic surfaces. In combination with conventional electrochemical methods these techniques have been used to find connections between the microscopic surface structures and the macroscopic kinetic rates of the reactions.

Pt-Ru alloy [158–160] or Ru modified Pt surfaces [161] are known to be prominently effective catalysts for methanol oxidation. Watanabe and Motoo [87] introduced a “bifunctional mechanism” into electrochemical interfaces in that Ru in Pt-Ru alloy surfaces supplies OH moieties to promote CO oxidation on neighboring Pt surfaces. In this context, it is crucial to elucidate water or hydroxide that are anticipated to adsorb on Ru in the alloy or modified Pt electrode surfaces. Nevertheless, there have been substantial uncertainties on this point because of experimental constraints in vibrational spectroscopy relevant for this purpose, e.g., poor sensitivity or uncompensated interruption by bulk solution species in IRAS (infrared reflection absorption spectroscopy). Watanabe and co-workers recently reported that water molecules were detected on the Pt-Ru alloy surfaces, a finding

dissimilar to those for Pt surfaces, using ATR-IR spectroscopy [108]. It seems, however, that the surface morphology of their Pt [160] and Pt-Ru alloy films [108] prepared with a sputtering method was not optimized to obtain fairly large enhancement for the IR absorption from adsorbates. Possibly, the enhancement factor of such Pt films was not sufficiently large to detect rather weak water bands, as absorbance of the O–H stretch is about 1/18 compared to on-top CO. In contrast, Pt films prepared by electroless plating give much larger IR absorption for adsorbates by a factor of > 10 [161–163]. Concerning the bifunctional mechanism, Friedrich et al. reported on the Ru-modified Pt(1 1 1) surface that (1) an Ru island with 2–5 nm size and monoatomic height is formed by electrochemical deposition, of which coverage is feasibly controlled by the deposition potentials, and (2) the CO oxidation peak is shifted to more negative potentials by ~120–130 mV due to a cooperative mechanism between Pt and Ru involving CO surface mobility [112, 164, 165]. At this stage, it appeared necessary to characterize water and CO adsorbed on various alloy or modified Pt surfaces, using ATR-SEIRA spectroscopy to provide information on the role of Ru in their catalytic activity. Consequently, it was found using ATR-SEIRA spectroscopy that (1) preferentially adsorbed CO on the Ru surface was oxidized up to ~+0.3 V, (2) it induced marked adsorption of water on the empty Ru surface, which could accelerate the following CO oxidation on the adjacent Pt surface, compatible with the bifunctional mechanism, and (3) diffusion of surface species from Ru to Pt was indicated in a dilute CH_3OH solution. Highly sensitive ATR-SEIRA spectroscopy was used by Futamata and Luo [166] to elucidate water, CO, and electrolyte anions adsorbed on the Ru-modified Pt film electrode. CO on Ru domains was oxidized below ~+0.3 V, followed by pronounced water adsorption. Since the oxidation potential of CO on the Pt domain was significantly reduced compared to that on bare Pt, these water molecules on Ru obviously prompted CO oxidation on the adjacent Pt surface, consistent with the bifunctional mechanism. Diffusion of adsorbate from Ru to Pt surfaces was indicated in dilute CH_3OH solution by spectral changes with potential.

In order to understand the mechanism of CO and methanol electrooxidation on binary platinum alloys catalysts, much work is needed on the surface structure (including its electronic aspects) and its relationship with the reactivity. Adsorbed carbon monoxide exhibits a surface-sensitive behavior, which influences the vibrational frequencies of the C–O band. Consequently, *in situ* Fourier transform infrared (FTIR) spectroscopy appears to be a useful technique for studying CO interaction with the surface. CO tolerance of carbon-supported $Pt_{80}Ru_{20}$, $Pt_{80}Os_{20}$, and $Pt_{85}Co_{15}$ electrocatalysts has been studied by García et al. [167] in 0.1 M perchloric acid solution, applying cyclic voltammetry and *in situ* FTIR spectroscopy. It was shown that FTIR spectra can be acquired during CO oxidation at these technical materials in an electrochemical cell, yielding valuable information on the reactivity and allowing predictions on their behavior in a polymer electrolyte membrane fuel cell (PEMFC). Linear adsorbed CO is the main adsorbate, but small amounts of bridge-bonded CO are also formed. Moreover, COH species seem also to be present for $Pt_{80}Os_{20}$ and $Pt_{85}Co_{15}$. All bimetallic alloys are able to oxidize adsorbed CO at lower potentials than platinum, and a shift of about 0.20 V has been determined. From the FTIR spectra, fundamental

information can be obtained on the CO adsorption energies and metal properties of these systems.

The electronic effect may be inferred from XPS measurements of the Pt(111)/Ru system [168] and X-ray absorption spectroscopy (XAS) measurements of Pt/Ru alloy nanoparticles [29], which have indicated a transfer of electron density from Pt to Ru. The electrocatalytic activity for oxidation in the presence of 100 ppm CO has been investigated by Watanabe et al. [169] using XPS and FTIR, on a series of binary Pt alloy electrocatalysts with non-precious metals of various compositions. At these CO-tolerant electrodes, the equilibrium coverage of CO was suppressed to values less than ~0.6. Based on X-ray photoelectron spectroscopy (XPS) data, it was found that the surfaces of all non-precious metal alloys are composed of a thin Pt layer with an electronic structure different from that of pure Pt, indicating an increased 5d vacancy of Pt in the layers of the CO-tolerant alloys. The CO coverage, particularly with multi-bonding, was lowered due to decreased electron donation from the Pt band to the $2\pi^*$ orbital of CO. A weakening of bond strength between the Pt skin layer and CO was also indicated by *in situ* FTIR, suggesting that the H_2 oxidation sites are not blocked by CO due to its enhanced mobility. Thus, the mechanism of CO tolerance described above at the Pt skin on alloy surfaces was proposed as a "detoxification mechanism".

XPS and FTIR spectroscopy have also been used by Tillman et al. [170] to study the co-adsorption of CO with Sn on Pt(1 1 1). It was concluded that Sn exerts an electronic influence on CO molecules adsorbed in its neighborhood. This influence leads to the disappearance of the band at 1780 cm^{-1} indicative of the (2×2)–3CO adlayer at low potentials and to a shift of CO from the strongly adsorbed state to the weakly adsorbed state. Alternatively, the disappearance of the 1780 cm^{-1} band might also be explained by a disturbed order in the neighborhood of the Sn islands. Such an effect is observed for CO adsorbed at unmodified stepped surfaces, but it does not lead to a shift to the weakly adsorbed state. In addition, there also seems to be an effect according to the bifunctional mechanism, which is active only for the weakly adsorbed state but extends over all the surface, including that part of the adsorbate that is not electronically influenced by Sn. Similar to the case of Mo, this effect does not work for the strongly adsorbed CO.

In situ XAS measurements, including both X-ray absorption near edge spectroscopy (XANES) and extended X-ray absorption fine structure (EXAFS) at the PtL_3 and RuK edges, have been used by Scott et al. [171] on three different carbon-supported PtRu electrocatalysts in an electrochemical cell in 1 M $HClO_4$ with 0.3 M methanol. The CO and OH adsorbate coverage on Pt and Ru were determined as a function of the applied potential via the novel delta XANES technique, and the particle morphology was determined from EXAFS and a modeling technique. Both the bifunctional and direct CO oxidation mechanisms, the latter enhanced by electronic ligand effects, were evident for all three electrocatalysts; however, the dominant mechanism depended critically on the particle size and morphology. Both the Ru island size and overall cluster size had a very large effect on the CO oxidation mechanism and activation of water, with the bifunctional mechanism dominating for more monodispersed Ru islands, and the direct surface ligand effect dominating in the presence of larger Ru islands.

Stamenković et al. [172] reviewed the research of *in situ* CO oxidation on well characterized $Pt_3Sn(hkl)$ surfaces. Bimetallic single crystals $Pt_3Sn(110)$ and $Pt_3Sn(111)$ have been characterized for *in situ* CO oxidation. Following UHV characterization, crystals were transferred into the electrochemical environment where surface electrochemistry of adsorbed CO was studied *in situ* by infrared spectroscopy. Changes in band morphology and vibrational properties – splitting of the band and increase in the frequency mode – were found on $Pt_3Sn(hkl)$ and correlated to Pt(hkl) surfaces. Continuous oxidative removal of adsorbed CO starts as low as $E < 0.1$ V, which is an important property for CO-tolerant catalysts. In addition to electronic effects, other factors, such as surface structure and intermolecular repulsion between adsorbed species, are responsible for the high catalytic activity of $Pt_3Sn(hkl)$ alloys.

Electrochemical nuclear magnetic resonance (EC-NMR) spectroscopy has emerged as one useful probe with which to investigate the surface electronic properties of catalyst nanoparticles [173, 174]. ^{13}C EC-NMR of adsorbed CO is particularly informative since it can be used to deduce both the electronic properties of the nanoparticle surfaces as well as the nature of CO bonding with the transition metal [116, 175–177]. This provides a powerful method to correlate the surface electronic alterations with catalytic activity variations and yields a firm basis for rational synthesis of bimetallic nanoparticle catalysts with improved activities in fuel cells. NMR studies on Pt nanoparticles modified by spontaneous deposition of Ru have demonstrated changes in the metal–CO bonding that result from Ru modification. On CO-covered Pt/Ru nanoparticles, ^{13}C NMR spectra (Figure 16.5) show the presence of two broad peaks. Each of these spectra can be deconvoluted into two Gaussians, whose peak areas have the same ratio as Pt and Ru on the Pt/Ru surface, in excellent agreement with the CO-stripping data. Thus, EC-NMR discriminates between the two populations: Pt/Ru–CO and Pt–CO, as has previously been shown by using infrared methods [109, 119, 178]. On the other hand, the NMR spectrum of ^{13}CO adsorbed on Ru-black also shows only one peak, centered at a much lower chemical shift compared to the Pt/Ru samples.

Unlike CO adsorbed onto supported Ru nanoparticles, CO adsorbed on Ru-black showed a large isotropic shift and a symmetric broadening of the NMR spectrum. In all these catalysts, the spin-lattice relaxation time (T1) has followed the Korringa behavior characteristic of metallic systems [179]. Thus, CO adsorbed on Pt/Ru catalysts attains metallic properties due to the mixing of CO molecular orbitals with the conduction electron states of the transition metal. This observation strongly suggests that the electronic influence of Ru on surface Pt atoms is only a local effect, and Pt atoms situated away from Ru sites retain their original electronic band structure properties.

Results of CO temperature programmed desorption (TPD) measurements on Ru-modified Pt single crystals have demonstrated a weaker Pt–CO bond than on pure Pt surfaces [107, 117, 180], again pointing toward a decreased availability of Pt d electrons for forming the Pt–CO bond [181]. The decreased availability of d electrons may be understood as a consequence of the lowering of the d band center, as described in the Norskov model [182]. Similar CO TPD results were obtained on the inverted Ru(0001)/Pt surface, on which the ligand effect and the strain effect were deconvoluted through elegant experiments with varied Pt deposit thicknesses

[183]. The deconvolution of the two effects has also been accomplished through computational work [184, 185]. The effect of PtRu surface alloy formation on hydrogen adsorption/desorption and of CO co-adsorption on hydrogen adsorption on a bimetallic PtRu surface was investigated by TPD, using a PtRu surface alloy (40% Pt surface atoms) as an example [186].

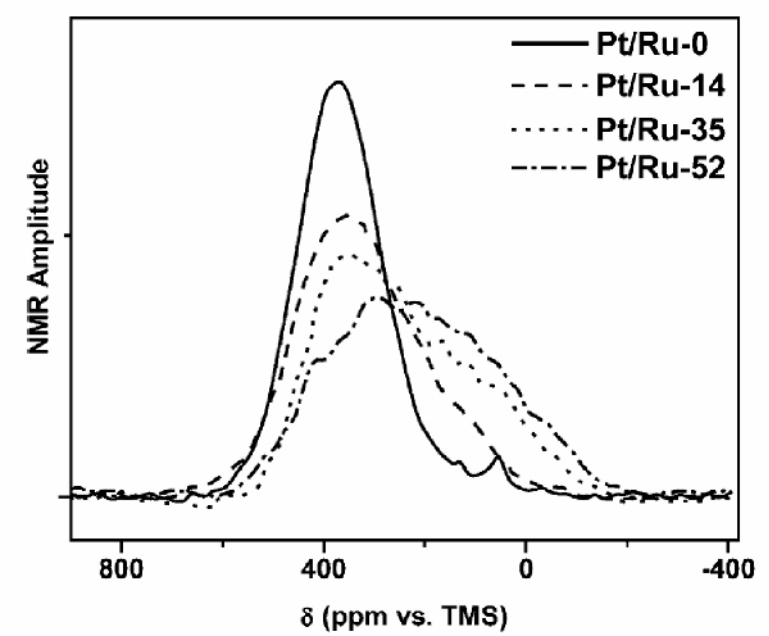

Figure 16.5. 13C NMR spectra of adsorbed CO on Pt and Pt/Ru catalysts [116]. (Reprinted with permission from J Am Chem Soc 2002;124:468–73. Copyright 2002 American Chemical Society.)

The concentration and distribution of the Pt surface atoms were determined by high-resolution scanning tunneling microscopy (STM), which provides further information for the mechanistic interpretation of the results and the underlying physical effects.

Electrochemical impedance spectroscopy (EIS) technique has been used for the experimental assessment of CO tolerance on different Pt-alloy catalysts and at different temperatures [187]. Hsing et al. [187] proposed that the critical potential at which pseudo-inductive behavior occurs could be used as a criterion for the evaluation of CO tolerance. A mathematical impedance model based on two state-variables (Pt-H and Pt-CO) was also developed to elucidate the reaction kinetics and mechanism of the H_2/CO oxidation on a Pt/C catalyst [188]. In fact, this study has given better insight into explicitly understanding the impedance patterns and the quantitative assessment of the effect of applied potentials upon the oxidation reaction kinetics in a broad range of applied potentials. Nevertheless, with the consideration of only two adsorbed species, Pt-H and Pt-CO, the impedance model based on two state-variables was not able to explain the experimental observation

of reversing impedance patterns in the II and III quadrants at high potentials. The model with two state-variables assumes that the water molecules are responsible for the electrooxidation of CO species. However, this is not the case in the high potential region, where the possibility of the dissociation of water molecules is more pronounced and consequently, OH species can be generated. The neglect of this aspect in the two state-variables model is the probable reason for its inability to explain the reversed impedance pattern. An impedance model based on three state-variables (Pt-CO, Pt-H, and Pt-OH) has been proposed by Wang and Hsing [189] for the kinetics investigation of H_2/CO electrooxidation on Pt/C and its alloys (PtRu/C and PtSn/C). The simulation results of Pt/C in a high potential range exhibit unusual reversal behavior of the impedance pattern in the II and III quadrants. This behavior reveals the change of the rate determining step from CO oxidation to CO adsorption. The experimental impedance results of the alloy PtRu/C are in agreement with the simulation studies, and suggest that the enhanced CO oxidation observed on the alloy can be well explained by the promoted OH_{ads} generation on the Ru surface at low potential. Meanwhile, a different reaction mechanism has been elucidated for the PtSn/C. It has been concluded that the promoted OH generation is the primary reason for enhanced activity towards CO oxidation on the PtRu/C. The high activity of the PtSn/C system towards H_2/CO oxidation is due to the combination of the promoted OH generation, exclusion of CO on Sn sites, and minimization of CO adsorption caused by the intermetallic bonding.

Based on CO thermal desorption data obtained on PtRu surface alloy model surfaces, Buatier de Mongeot et al. [135] also suggested that the improved CO tolerance is at least partly caused by a significant reduction in CO adsorption energy on these PtRu catalysts compared to CO adsorption on platinum. Similar results and conclusions were reached in recent density functional theory calculations [27], which showed a significant reduction in the CO adsorption energy on both Ru(0 0 0 1) surfaces covered by a pseudomorphic Pt monolayer and substitutional Pt surface atoms in a Ru(0 0 0 1) substrate, as compared to CO adsorption on Pt(1 1 1) [27, 135, 189, 190] or comparable cluster geometries [191]. CO adsorption and CO removal, however, are only part of the reactions going on in a reformate-operated PEMFC. The current determining step is the electrooxidation of hydrogen (hydrogen oxidation reaction – HOR), which for most platinum metal and platinum alloy electrodes is largely determined by the respective steady-state hydrogen coverage. Two important questions to be answered are therefore (i) how much are hydrogen adsorption and the H_{ad} steady state coverage under reaction conditions affected by the presence of co-adsorbed CO, and (ii) what is the influence of PtRu alloy formation on hydrogen adsorption and H/CO co-adsorption? Quantitative data on the influence of the CO coverage on the HOR rate are scarce [99, 192–194]. Recently, Jusys et al. reported a nonlinear relation between CO coverage and HOR rate, with smaller effects in the low CO coverage regime for the HOR on carbon-supported Pt catalysts [195]. For PtRu no such data exist. Electrocatalytic measurements showed no measurable effect of PtRu alloy formation on the HOR activity; this was tentatively attributed to the very high activity of the remaining, accessible Pt surface atoms, which are sufficiently active that possible differences in the activity are masked by transport limitations [111].

Likewise, little is known about the energetics and kinetics of hydrogen adsorption on bimetallic PtRu surfaces at the solid-vacuum interface, or about the influence of co-adsorbed CO on these properties. Diemant et al. [185] have shown that hydrogen (deuterium) adsorption on a bimetallic PtRu layer, which is pseudomorphic on a Ru(0 0 0 1) substrate, is considerably weaker than on an unmodified Pt(1 1 1) or Ru(0 0 0 1) surface. Following the d band model introduced by Nørskov and coworkers, this reduction in metal–H bond strength is attributed to a strain-induced modification of the electronic properties of Pt-rich adsorption ensembles. Co-adsorption of CO leads to a further weakening of hydrogen adsorption. This is explained by a CO-induced displacement of the adsorbed hydrogen from strongly binding Ru-rich ensembles to less strongly binding Pt-rich ensembles. Even a 100 K adsorption temperature post exposure to CO causes a partial displacement of adsorbed hydrogen. At elevated temperatures and pressures, as are present in a fuel cell, these effects will result in a severe reduction of the steady-state hydrogen coverage. Further improvement of the CO tolerance of PEMFC anode catalysts by the use of platinum alloys will be limited by the reduction in hydrogen electrooxidation activity due to a reduction in the steady-state hydrogen coverage, which is caused by the same electronic effects responsible for the reduction of the steady state CO_{ad} coverage.

Quantum chemical calculations offer the opportunity to probe details of catalytic chemistry that are difficult to obtain from experiments, and they should be employed not only for understanding the mechanism in detail, but also at the screening level of catalyst design. Shubina and Koper [184] described the results of quantum chemical calculations of CO and OH interacting with a variety of bimetallic surfaces, in order to assess from the computational viewpoint the molecular nature of the bifunctional mechanism and the electronic effects involved. They considered in some detail the results of density-functional calculations of CO and OH adsorption on PtRu, PtMo, PtSn, and a number of Pt-modified transition metals such as Rh and Ir. The advantage of using quantum-chemical calculations is that they give direct information on the binding energetics of the different species, which are relatively difficult to extract from electrochemical measurements. Moreover, calculations permit one to establish the quantum chemical nature of the surface bond and the different factors involved, and how these might be related to measurable properties of chemisorbates such as their vibrational characteristics. In this way, quantum-chemical calculations provide invaluable information to complement and correctly interpret experimental data, even if the calculated systems considered may appear rather idealized compared with the experimental catalysts. Concerning the PtRu alloy, they found that mixing of Pt with Ru weakens the binding of both CO and OH to the Pt surface sites. By contrast, the CO and OH binding gets stronger as Pt is mixed in. The surface with the weakest CO binding energy in their calculation is Pt_{ML}-Ru(0001). Interestingly, a similar surface was recently found to have good CO tolerant properties [109]. Also, there is no apparent correlation between the binding energy of CO and the internal C-O and Me-C stretching frequency on the different PtRu surfaces. According to the calculations, the PtMo and PtSn systems seem to be better CO oxidation catalysts than PtRu. On PtMo, CO does not have a strong preference for either site, whereas OH has a clear preference for Mo. On PtSn, CO

interacts only with Pt, and OH (or oxygen) interacts preferentially with Sn. If CO tolerance is related to good hydrogen oxidation properties, a low CO coverage may be sufficient. For such systems, Pt overlayer systems seem quite promising The CO binding energy of these systems is primarily determined by Pt-Pt distance in the overlayer. Contracted overlayers lead to low CO bonding energies, expanded overlayers to high CO bonding energies.

The adsorption properties of CO on Pt_3Sn were investigated by Gűlmen et al. [196] using quantum mechanical calculations. The (111), (110), and (001) surfaces of Pt_3Sn were generated with all possible bulk terminations, and on these terminations all types of active sites were determined. The adsorption energies and the geometries of the CO molecule at those sites were found. Those results were compared with the results obtained from the adsorption of CO on similar sites of Pt(111), Pt(110) and Pt(001) surfaces. The comparison reveals that adsorption of CO is stronger on Pt surfaces; this may be the reason why catalysts with Pt_3Sn phase do not suffer from CO poisoning in experimental works. With the aim of understanding in detail the interactions between CO and the metal adsorption sites, the local density of states (LDOS) profiles were produced for atop-Pt adsorption, for both the carbon end of CO for its adsorbed and free states, and the Pt atom of the binding site. The study showed that: (i) inclusion of a Sn atom at the adsorption site structure causes a dramatic decrease in stability, which limits the number of possible CO adsorption sites on the Pt surface, (ii) the presence of Sn causes angles different from 180° for M–C–O orientation, (iii) the presence of Sn in the neighborhood of Pt on which CO is adsorbed causes superposition of the $5\sigma/1\pi$ derived-state peaks at the carbon end of CO and changes in the adsorption energy of CO, (iv) Sn present beneath the adsorption site strengthens the CO adsorption, whereas neighboring Sn on the surface weakens it for all Pt_3Sn surfaces tested, and (v) the most stable site for CO adsorption is the atop-Pt site of the mixed atom termination of $Pt_3Sn(110)$.

16.3 Development of CO-tolerant Catalysts

Because the use of CO-tolerant electrocatalysts would be more efficient and cause fewer associated problems, it is generally considered the most promising way for solving the CO poisoning problem in PEMFCs. It is well established that binary systems of CO-tolerant electrocatalysts, with Pt as one of the components, can exhibit a substantial resistance to the presence of CO in the fuel stream. It has been found that the use of a second element with Pt, such as Ru, Sn, Ge, Co, Cr, Fe, Ni, Pd, Os, Mo, Mn, etc., in the form of an alloy or a co-deposit yields significant improvement in the CO-tolerance relative to pure Pt [20, 21, 34, 35, 67, 89, 110, 111, 197–208]. Among these various Pt-based binary systems, PtRu/C is still regarded as the most efficient anode electrocatalyst for both reformate and methanol fuel, due to its electronic or bifunctional effects in reducing CO poisoning [209–211]. Superior CO-tolerance has been evidenced for alloyed PtRu materials [13, 14, 102, 212, 213] or Ru-decorated Pt electrocatalysts [112, 164, 165, 214–222]. Therefore, the development of CO-tolerant electrocatalysts is still concentrated on Pt or PtRu-based bimetallic catalyst systems. Some reported work

and critical reviews on this topic have been published recently by Ralph [43, 68, 69] and Urian et al. [70].

Ternary catalyst systems, typically based on a PtRu alloy, have also been investigated and their performance has been compared with that of pure Pt/C or PtRu/C [129, 223–227]. Specifically, PtRu alloys with Ni, Pd, Co, Rh, Ir, Mn, Cr, W, Zr, and Nb have been investigated. Nevertheless, there remain associated problems with the preparation method and the enhancement of electrochemical performance.

Many papers in recent years have presented details of new preparation methods and the performance of Pt-based electrocatalysts such as PtSn/C, PtMo/C, PtRuMo/C, PtRu-HxMoO$_3$/C, and PtRu/(carbon nanotubes). In addition, efforts to develop Pt-free electrocatalysts such as PdAu/C have been undertaken.

Watanabe et al. [226] recently classified the Pt alloys studied into 3 groups with respect to their CO tolerance. The first group of alloys exhibits excellent stability for H_2 oxidation in the presence of 100 ppm CO, the second exhibits stability for 1 h and the third exhibits no CO tolerance, i.e., they are comparable to pure Pt. The first contains PtFe alloys such as $Pt_{95}Fe_5$, $Pt_{85}Fe_{15}$, $Pt_{56}Fe_{44}$, and $Pt_{40}Fe_{60}$, PtNi alloys such as $Pt_{76}Ni_{24}$ and $Pt_{56}Ni_{44}$, PtCo alloys such as $Pt_{82}Co_{18}$ and $Pt_{57}Co_{43}$, PtMo alloys such as $Pt_{67}Mo_{33}$ and $Pt_{55}Mo_{45}$, and the conventional PtRu alloys such as $Pt_{93}Ru_7$, $Pt_{57}Ru_{43}$, $Pt_{50}Ru_{50}$, and $Pt_{35}Ru_{65}$, where the numbers after an element symbol are the concentration of the element expressed in atom%. The second group includes PtMn alloys such as $Pt_{80}Mn_{20}$ and $Pt_{48}Mn_{52}$, PtSn alloys such as $Pt_{78}Sn_{22}$ and $Pt_{79}Sn_{51}$, PtAg alloys such as $Pt_{87}Ag_{13}$ and $Pt_{54}Ag_{46}$, and PtZn alloys such as $Pt_{70}Zn_{30}$ and $Pt_{52}Zn_{416.}$ The third group contains $Pt_{80}Cr_{20}$, $Pt_{52}Cr_{48}$, $Pt_{85}Cu_{15}$, $Pt_{70}Ge_{30}$, $Pt_{40}Ge_{60}$, $Pt_{90}Nb_{10,}$ $Pt_{55}Nb_{45}$, $Pt_{65}Pd_{35}$, $Pt_{66}In_{34}$, $Pt_{76}Sb_{24}$, $Pt_{48}Sb_{52}$, $Pt_{80}W_{20}$, $Pt_{50}W_{50}$, $Pt_{81}Au_{19}$, $Pt_{57}Au_{43}$, $Pt_{64}Pb_{33}$, and $Pt_{65}Bi_{35}$.

Figure 16.6 shows examples of saturated CO coverage on Pt and the alloys after H_2 oxidation for a prolonged period in the presence of 100 ppm CO. The CO coverage (θ_{CO}) on all of the CO-tolerant alloys is suppressed to values less than 0.6, while the other groups of alloys and pure Pt are almost completely covered with CO [228]. In the case of PtFe alloys, for example, the addition of only 5% Fe to Pt reduces the saturated θ_{CO} to less than 0.3, resulting in the same activity level as those of other compositions or combinations.

It should be noted that the non-noble alloying metal has to be stable in the severe environment of the catalyst layer, where a major component is a strong perfluorosulfonic acidic. Fuel cell operation may produce changes in the catalyst crystallinity, particle surface composition, and the oxidation state of M, which consequently may decrease the CO tolerance [229]. Ishikawa et al. [230], by using relativistic density-functional calculations, found that the alloying metals should be those that possess low-activation energies for H_2O dissociation and for the CO_{ads} + OH_{ads} → $COOH_{ads}$ reaction. Once $COOH_{ads}$ is formed, it rapidly forms $CO_{2,ads}$ (+H_{ads}) because of its decomposition. Based on energetic predictions emphasizing water activation, it was predicted that the most suitable alloying metals for the CO electrooxidation are Mo, W, and Os, with Ru close behind. Among the several possibilities of binary alloys, PtRu has shown the most promising performance for the hydrogen oxidation reaction in the presence of CO [67, 111]. However, the low natural abundance of Ru is a drawback of this catalyst for practical uses, and for

this reason alternative approaches have been sought, some of them with recent promising results [43, 169], that will be reviewed here.

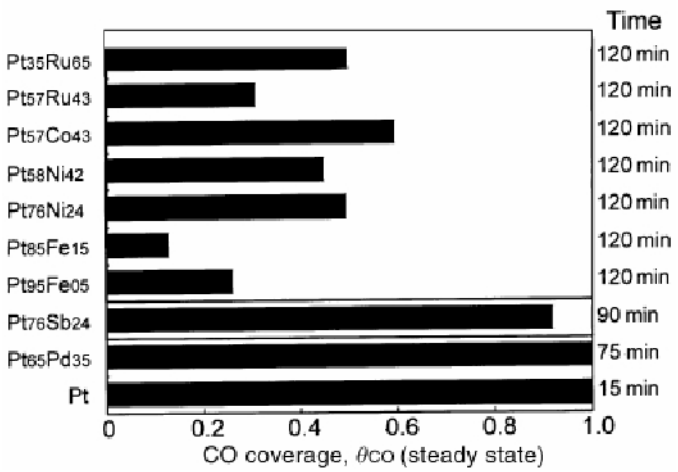

Figure 16.6. Equilibrium coverage of CO on the alloy electrodes in 0.1 M $HClO_4$ saturated with 100 ppm balance gas. Alloy compositions are shown on the left-hand side. Potential for CO adsorption: 50 mV vs. RHE, rotation rate of electrodes during the CO adsorption: 1500 rpm [169]. (Igarashi H, Fujino T, Zhu Y, Uchida H, Watanabe M. CO tolerance of Pt alloy electrocatalysts for polymer electrolyte fuel cells and the detoxification mechanism. Phys Chem Chem Phys. 2001;3:306–14. Reproduced by permission of The Royal Society of Chemistry.)

16.3.1 PtRu Binary System

16.3.1.1 PtRu Catalysts

The most commonly used anode electrocatalyst in PEMFCs is the platinum-ruthenium binary catalyst (PtRu). Based on early work by Watanabe and Motoo [89] (on methanol electrooxidation), a bifunctional mechanism involving water activation by Ru (Equation 16.11) and subsequent CO electrooxidation on a neighboring Pt atom (Equation 16.12) has been postulated by a number of groups [20, 102, 103, 110–112]. In fact, this system evidently enhances CO tolerance and decreases the CO binding energy on platinum due to its electronic or bimetallic effects. It has been proposed that the addition of ruthenium to platinum can improve CO tolerance through either a ligand effect [157] or through a bifunctional mechanism [133], and possibly a combination of the two.

It is well documented [102, 103, 118, 231–233] that in the PEMFC at 80 °C PtRu alloys are much more tolerant to CO poisoning than pure Pt electrocatalysts. This has made them the electrocatalysts of choice for reformate operation. For example, Figure 16.7 shows the large improvement in CO tolerance for an MEA with an anode based on a $Pt_{50}Ru_{50}$ alloy electrocatalyst prepared as 20 wt% Pt, 10 wt% Ru supported on Vulcan XC72R. The cell potentials are significantly higher at all current densities compared with the MEA based on pure Pt, for operation with hydrogen containing 10, 40, and 100 ppm CO. This improved CO tolerance

has resulted in much effort to optimize the PtRu electrocatalyst for reformate operation.

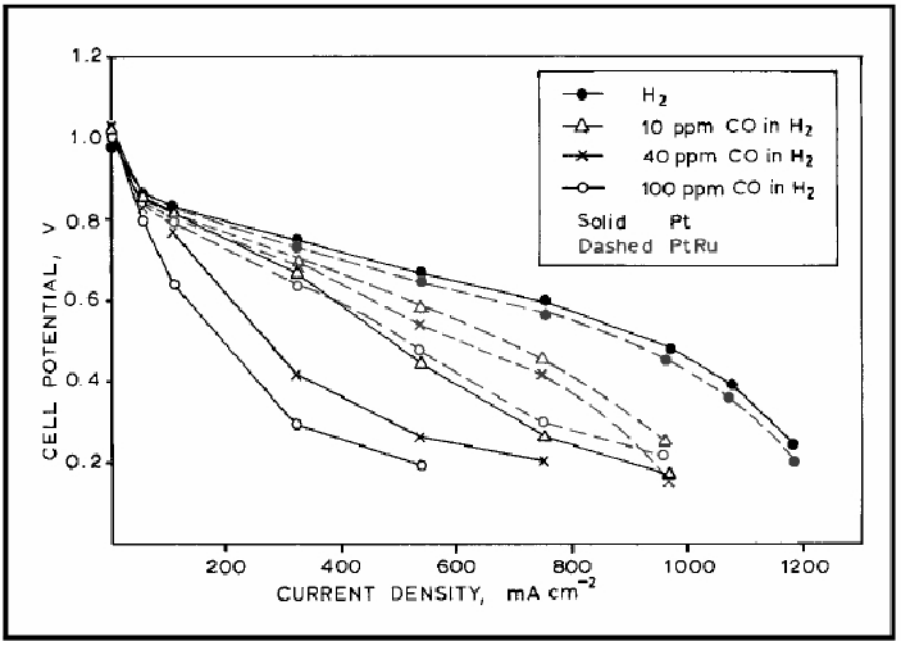

Figure 16.7. Progressive poisoning from 10, 40, and 100 ppm CO on pure Pt and $Pt_{50}Ru_{50}$ alloy anodes. Increased CO tolerance is shown by the $Pt_{50}Ru_{50}$ alloy anodes. The anodes are prepared from 20 wt% Pt on Vulcan XC72R or 20 wt% Pt, 10 wt% Ru on Vulcan XC72R at a loading of 0.25 mg Pt cm^{-2}. The cathode uses 40 wt% Pt/Vulcan XC72R at a loading of 0.6 mg Pt cm^{-2}. The MEAs are based on catalyzed substrates bonded to Nafion NE-115 membrane. The Ballard Mark 5E single cell is operated at 80 °C, 308/308 kPa, 1.3/2 stoichiometry with full internal membrane humidification [43]. (Reprinted from Ralph TR, Hogarth MP. Catalysis for low temperature fuel cells, part II: the anode challenges, Plat Met Rev 2002;46(3):117–35. With permission from Platinum Metals Review.)

16.3.1.2 Effect of PtRu Composition

The HOR performance of PtRu alloys in the presence of CO has been studied extensively [20, 209] and it has been shown that the HOR overpotential for CO-containing hydrogen decreases as the ruthenium content increases, reaching a minimum around the 1:1 (atomic ratio) composition.

Using a 20 wt% Pt, 10 wt% Ru/Vulcan XC72R electrocatalyst, the effect of alloy formulation on CO tolerance was examined by Johnson Matthey [43], both as fully alloyed and as completely unalloyed materials, with a nominal composition of $Pt_{50}Ru_{50}$. The unalloyed $Pt_{50}Ru_{50}$ was prepared by depositing Ru onto a pre-reduced Pt electrocatalyst. XRD confirmed that there was no alloying from the Pt lattice spacing of 0.392 nm, which is equivalent to pure Pt. In addition, there was no significant crystalline Ru, suggesting the Ru was present as amorphous Ru oxide. The peak potential for CO electrooxidation (Equation 16.10) at the unalloyed $Pt_{50}Ru_{50}$ occurred at +0.44 V (vs. RHE), close to the +0.37 (vs. RHE) for

the $Pt_{50}Ru_{50}$ alloy and much lower than the +0.58 V (vs. RHE) for the pure Pt electrocatalyst. With hydrogen containing 100 ppm CO as reactant the specific activity for hydrogen electrooxidation was measured. At +0.010 V (vs. RHE) the specific activity increased from 8 mA cm^{-2} Pt for pure Pt to 25 mA cm^{-2} PtRu for the unalloyed $Pt_{50}Ru_{50}$ and to 60 mA cm^{-2} PtRu for the $Pt_{50}Ru_{50}$ alloy. This suggests that the alloying process, which incorporates the Ru into the Pt lattice (and reduces the Pt lattice spacing), is important for improving the CO tolerance. Besides enhancing the intimate contact between the Pt and the Ru, extended X-ray absorption fine structure (EXAFS) analysis has shown that alloying removes electron density from the Pt [29]. Both these effects are capable of promoting a lower CO coverage on Pt and increasing the hydrogen electrooxidation activity of the anode.

A possible consequence of these findings is that low Ru contents might not show such high CO tolerance in the PEMFC. The Ru content in a fully alloyed 20 wt% Pt, Ru/Vulcan XC72R electrocatalyst was lowered from $Pt_{50}Ru_{50}$ to the mined ratio of $Pt_{70}Ru_{30}$, and then examined in the PEMFC. The XRD lattice spacing of 0.390 nm confirmed a $Pt_{70}Ru_{30}$ alloy was formed. For hydrogen containing 10, 40, and 100 ppm CO, MEAs prepared with $Pt_{70}Ru_{30}$ matched the performances in Figure 16.7 for the $Pt_{50}Ru_{50}$ electrocatalyst at an identical anode loading of 0.25 mg Pt cm^{-2}. This confirmed that at an atomic ratio of $Pt_{70}Ru_{30}$ there is sufficient Ru incorporated into the Pt lattice to adequately modify the CO tolerance of Pt. These findings were in agreement with the fundamental kinetic work of Gasteiger et al. [110], who used 1000 ppm CO in hydrogen and bulk, planar $Pt_{50}Ru_{50}$ and $Pt_{90}Ru_{10}$ alloys. The findings also agree with the more applied results in the PEMFC of Iwase and Kawatsu [103] for alloys of composition $Pt_{85}Ru_{15}$ to $Pt_{15}Ru_{85}$, all based on 20 wt% Pt, 10 wt% Ru/Vulcan XC72R electrocatalysts. They found that the CO tolerance was significantly lower only at Ru contents below $Pt_{80}Ru_{20}$ or above $Pt_{20}Ru_{80}$. However, there have also been a few reports of lower CO tolerance at lower Ru levels, including $Pt_{70}Ru_{30}$ [102]. This highlights the importance of the manufacturing route for the degree of PtRu alloying and for the nature of the electrocatalyst surface. This variability probably accounts for the significant spread in CO tolerances reported for PtRu anode electrocatalysts [234].

Stevens et al. [235] prepared $Pt_{1-x}Ru_x$ random alloy samples via dc magnetron sputtering. The alloys were deposited through shadow masks onto 3M nanostructured thin-film catalyst support for testing in a 64-electrode PEMFC. Electron microprobe data confirmed that linear composition gradients covering almost the whole binary range were prepared. The phases present were examined with XRD. All samples were found to have the Pt fcc structure at high Pt content. At high Ru content, only hexagonal close-packed (HCP) Ru was seen. Electron microprobe measurements on catalyst electrodes after fuel cell testing showed that the Ru-based alloys were stable to corrosion. Alloying Pt with intermediate levels of Ru led to lower CO-stripping onset potentials, implying improved CO tolerance. Hydrogen oxidation polarization curves were measured for the alloy gradients to determine overpotentials as a function of composition, with a reformate fuel containing up to 50 ppm CO. The $Pt_{1-x}Ru_x$ composition spreads all showed lower overpotentials at intermediate M content with 50 ppm CO (approximate as-sputtered ranges: Ru: $0.2 < x < 0.9$), implying that these binary catalysts would be

more CO-tolerant than Pt alone. An overpotential of approximately 200 mV was required for the Ru-containing samples before the surface became clean enough to support high current densities, consistent with the CO-stripping voltammetry results.

16.3.1.3 Effect of PtRu Particle Size

The optimum particle size for methanol oxidation has been the subject of several investigations and the values vary with the preparation procedure, the conditions of the reaction, and the metals present in the catalyst. It has been found that the optimum specific activity for Pt was achieved with particle sizes of 3 nm [236]. Other reports [239, 240] conclude that the specific activity declines below 4.5 nm. Particles below 5.0 nm have enough coordination sites to produce strong Pt–OH bonds, leading to high coverage with this species. Mukerjee and McBreen have studied the role of the geometric parameters and the changes in the electronic structure due to specific adsorbates, such as hydrogen and oxygenated species (OH and CO), on methanol oxidation [239]. They found by X-ray absorption spectroscopy that, for particle sizes of carbon-supported Pt clusters below 5.0 nm, there is a strong adsorption of H, OH, and C1-compounds such as CO. On these small particles, H adsorption is strong enough to induce restructuring and morphological changes in Pt clusters at negative potentials. Moreover, the strong adsorption of OH for potentials more positive than 0.8 V inhibits the reduction of oxygen, and the combined effect of strongly adsorbed CO and OH impedes the oxidation of methanol.

16.3.1.4 Stability of PtRu Catalysts and the Impact on Oxygen Reduction Reaction Activity

Fuel cell operation may produce changes in the catalyst crystallinity, particle surface composition, and the oxidation state of M, which consequently may decrease the CO tolerance [229]. Knights et al. [240] investigated several of the key mechanisms attributed to fuel cell power loss over extended periods of time and provided an overview of those operating conditions that influence durability. The authors claimed that by enhancing the water retention at the anode side in combination with advanced electrocatalyst designs, the degradation of PtRu via the dissolution of noble metals could be avoided. However, most PtRu materials were found to be prone to preferential leaching of Ru, especially in the presence of methanol [241–243], thereby entailing undesired changes in the composition and, consequently, in the activity of the electrocatalyst [243]. Earlier reports have proposed that the onset potential of Ru oxidation can be somewhere between 0.2 and 0.4 V vs. RHE [12, 289, 217, 243]. It was observed [244] that a large amount of Ru leaves by the dissolution of the thermodynamically instable (oxide) phases, which can largely be removed by washing. At the same time, the PtRu alloy matrix seems less prone to leach Ru. Focusing on the mechanism behind Pt and Ru corrosion, Chen et al. [242] demonstrated through potential cycling of the anode in a DMFC that dissolution of the anode electrocatalyst contributes to a lower catalytic activity for methanol electrooxidation. A study by Piela et al. [245] showed that the impact of Ru dissolution on fuel cell performance is complicated by Ru crossover from the anode to the cathode side. Because the mobility and

transport of metal ions in PEMs are well documented [246–248], it is reasonable to evaluate the indirect effects of Ru corrosion and mobility in terms of overall PEMFC performance, especially because the concentration of the leached Ru is expected to exceed trace levels [243, 245]. Ruthenium crossover in DMFCs was recently discovered by the Los Alamos Group [245]. In their pioneering work, X-ray fluorescence and CO-stripping data evidenced the transport of Ru across the PEM and its deposition on the Pt cathode, respectively, under various DMFC operating conditions. Such a series of events with Ru was also confirmed in single-cell experiments [243], in which the DMFC was operated in the mass transport-limited region under massive methanol crossover. Interestingly, no accumulation of Ru in the Nafion membrane could be detected by energy dispersive X-ray spectroscopy (EDX). Rather, dissolved Ru species were assumed to travel across the PEM and fill the drained voids in the cathode electrocatalyst layer. In those pores, Ru^{n+} concentration is predicted to reach the several moles per liter level [249]. Ru contamination can impair oxygen reduction activity more severely, as was evidenced by the corresponding rotating disk electrode study. Unlike the observed progressive decrease in surface oxide coverage on Pt with increasing Ru^{n+} contamination, oxygen reduction seems to occur at a minimum activity level beyond a certain Ru coverage on Pt. Such a lower limit of ORR activity beyond a threshold Ru^{n+} concentration was attributed to the ability of Ru adatoms to reduce molecular oxygen at sufficiently high overpotential [250, 251].

Ru leaching from PtRu fuel cell anode electrocatalysts can have a dramatic impact on the activity of a Pt/C oxygen-reducing cathode. Even from highly diluted Ru-containing electrolytes (micromolar concentration range), Ru deposits instantly onto Pt and remains stable on its surface in the electrode potential window of the ORR. Rotating disk electrode data [244] showed that the rate of oxygen reduction can decrease by a factor of eight, which can translate to a ~160 mV overpotential penalization in galvanostatic conditions. Polarization curves recorded for fuel cells with clean and Ru-contaminated Pt cathodes suggest that Ru contamination plays a crucial role in the unrecoverable performance degradation of PEMFCs. Because a typically ten-times larger Pt loading in fuel cell cathodes is not expected to compensate for the suspected several orders of magnitude higher Ru^{n+} concentration in the voids of the cathode electrode layer [245], those data stress that Ru contamination can indeed play a major role in the performance degradation of PEMFCs and especially of DMFCs. Unless highly stable PtRu anode electrocatalysts are developed, the problem of Ru crossover and contamination at the cathode should be addressed by either novel fuel cell designs such as laminar-flow fuel cells [252, 253], in which crossover is reduced using less Ru-permeable membranes, or by more Ru-tolerant ORR electrocatalysts in PEMFCs.

16.3.2 PtMo Binary System

Under reformate-feed conditions, carbon-supported PtRu alloys are widely used as reasonably reformate-tolerant anode catalysts [254–257]. However, the CO tolerance of PtRu is still unsatisfactory for the higher CO concentrations expected at system start-up or during changes in load. Moreover, the limited availability of

Ru may become a significant problem before stationary PEMFC systems can be placed on the market. Many Pt-based catalysts have thus been proposed as alternatives to PtRu. Based on the ‘‘bifunctional mechanism’’ in CO removal, along with anodic hydrogen oxidation, the search for oxophilic components [198] has been the main trend in the development of alternative CO-tolerant electrocatalysts for the PEMFC. Those with the most successful and cost-effective combinations so far have been Pt_3Mo and Pt_4Mo [21–23, 258]. Recent theoretical and experimental studies suggest that Pt-Mo combinations could be not only much cheaper, but even more efficient catalysts for CO oxidation than PtRu [21–23, 230, 258]. Bimetallic PtMo alloy catalysts have thus attracted considerable attention for their high catalytic activity in H_2 oxidation with CO/H_2 feed [22, 23, 70, 126, 127, 204, 225, 259–263]. Such enhanced performance in contrast with PtRu was ascribed to (1) the lack of adsorption of CO on Mo, leaving more adsorption sites for oxygen-containing species that are acting as CO oxidation reagents within the frame of such a bifunctional mechanism, or (2) changes in Pt–Pt atomic distance, which modifies the Pt–CO adsorption energy [230].

Grgur et al. [22, 23] reported the electrochemical oxidation of H_2, CO, and CO/H_2 on well-characterized $Pt_{70}Mo_{30}$ bulk alloy or carbon-supported PtMo (3:1 or 4:1) catalysts in sulfuric acid solution. Their work suggested a similar bifunctional mechanism with Ru in the role of Mo in PtMo alloy: an increase in free Pt sites by the oxidative removal of adsorbed CO. Mukerjee et al. [70, 127, 204] showed two- to three-fold enhancement of the CO tolerance of PtMo in a PEM fuel cell compared to that of PtRu, which was ascribed to the onset of CO oxidation at very low potentials (~100 mV). The PtMo (atomic ratio = 5:1) electrocatalyst also displays a lower variation in overpotential losses than the PtRu counterpart [126, 204, 263]. Recently, the high CO tolerance of PtMo catalysts has also been reported by Santiago et al. [262, 263]. The catalytic activity of Mo/C for the water-gas shift (WGS) reaction was observed using a fixed-bed catalytic reactor, and they concluded that the CO tolerance of PtMo is due to lowering of the CO concentration in the gas channel inside the electrode through the chemical reaction catalyzed by Mo-species. With regard to the PtMo alloy, Mo atoms have been reported to have oxygen-containing ligands even at H_2 potentials, which were responsible for the excellent CO tolerance [23, 260]. This notion was supported by the results for Mo K-edge XANES spectra, which showed that Mo was present as hydrated oxides with a valence state of +IV at 0 V [260].

A $Pt_{75}Mo_{25}$ alloy was prepared [43] as 20 wt% Pt, 3 wt% Mo by sequentially depositing Pt oxide and Mo oxide followed by thermal reduction at high temperature. Half-cell measurements in H_2SO_4 at 80 °C using Nafion-containing electrodes were performed to determine the specific activity for hydrogen electrooxidation in the presence of 100 ppm CO. It was shown that for the Pt_3Mo alloy electrode with pure CO, there is considerable specific activity for CO electrooxidation starting from anode potentials of +0.05 V (vs. RHE). Mass spectrometry of the exhaust gas confirmed that the electrooxidation current was due to product CO_2 formation. This indicated that at anode potentials below +0.2 V (vs. RHE) (needed for efficient PEMFC operation), the CO tolerance of the PtMo electrocatalyst comes from promoting CO electrooxidation (Equation 16.10). The low electrode potentials required for CO electrooxidation were also evident in the

cyclic voltammograms. For the Pt_3Mo alloy electrode a broad oxidation current starting at +0.15 V (vs. RHE) is complicated by Mo surface redox reactions [264]. These results are in direct contrast to those from both the pure Pt and the PtRu alloy electrodes. There is no detectable specific activity for CO electrooxidation below +0.2 V (vs. RHE) and no product CO_2 was detected in the half-cell exhaust gas. There was no electrooxidation activity measured at these low electrode potentials for either the PtRu alloy or the pure Pt electrodes in the cyclic voltammograms. Greatly improved CO tolerance for hydrogen containing from 40 to 100 ppm CO has been confirmed using MEAs containing $Pt_{50}Mo_{50}$ catalysts [43]. $Pt_{67}Mo_{33}$ alloy showed almost the same polarization properties for H_2 oxidation in the presence and absence of 100 ppm CO, while H_2 was hardly observed on pure Pt after 2 h CO adsorption [169]. CO poisoning of H_2 oxidation was not observed on this PtMo alloy at all. However, as the CO concentration is reduced, the benefit due to the $Pt_{75}Mo_{25}$ alloy electrocatalyst is also reduced, until at 10 ppm CO the PtRu alloy electrocatalyst is the more CO-tolerant. The difference in reaction order for the $Pt_{75}Mo_{25}$ and the PtRu alloys is perhaps indicative of the distinct mechanisms of CO-tolerance operating at the electrocatalysts.

A much larger issue than the MEA performance at low ppm levels of CO was found for the $Pt_{75}Mo_{25}$ alloy. When operating on hydrogen with 25% CO_2, the $Pt_{75}Mo_{25}$ alloy showed poor CO_2 tolerance [43]. Poor CO_2 tolerance of the PtMo system reflects an increased ability of the electrocatalyst to promote the electroreduction of CO_2 (Equation 16.9). This produces much higher coverage of the "Pt–CO" poison. The source of the CO tolerance shown by the PtMo electrocatalyst, namely its ability to electrooxidize CO (Equation 16.10) also results in an ability to catalyze the reverse electroreduction reaction (Equation 16.9). PtMo alloy catalysts have been reported to be more susceptible to poisoning by CO_2 compared to PtRu [70, 127, 260, 265]. A performance evaluation on CO(100 ppm)/H_2 and CO_2(25%)/H_2 showed that the voltage loss with PtMo (7:1) catalyst caused by 25% CO_2 is much greater than that with PtRu, while PtMo shows better performance than PtRu on CO(100 ppm)/H_2 [260]. Systematic evaluation of the CO_2 tolerance of PtMo with various atomic ratios showed that variation of the PtMo atomic composition affects the tolerance to CO_2, and a similar voltage loss on CO_2/H_2 was observed for PtMo(1:1)/C and PtRu(1:1)/C [70]. Recently, Mukerjee et al. [127] reported no significant additional voltage loss for a PtMo(1:1) anode upon the addition of 21% CO_2 compared to the cell voltage on CO(100 ppm)/H_2. These reports suggest that the CO_2 tolerance of PtMo alloy catalysts is highly influenced by the catalyst composition and/or the method of catalyst preparation.

In 2007, $Pt_{1-x}Mo_x$ binary composition spreads were deposited via dc magnetron sputtering through shadow masks onto 3M nanostructured thin-film catalyst support by Stevens et al. [235]. Electron microprobe data confirmed that linear composition gradients covering almost the whole binary range were prepared. The phases present were examined with XRD. All samples were found to have the Pt fcc structure at high Pt content. The body-centered cubic (bcc) Mo phase was also formed for compositions containing greater than 35 atom% Mo, dominating at high Mo content. Electron microprobe measurements on catalyst electrodes after fuel

cell testing showed some loss of Mo in $Pt_{1-x}Mo_x$ alloys containing > 40 atom% Mo. Hydrogen oxidation measurement results obtained from testing with CO-free reformate suggest that $Pt_{1-x}Mo_x$ at high Mo levels may be binary alloys that are able to catalyze the RWGS reaction. RWGS CO poisons the platinum surface, requiring larger overpotentials for a given current density. CO-stripping voltammetry measurements indicated that alloying Pt with intermediate levels of Mo led to lower CO-stripping onset potentials, implying improved CO tolerance. The $Pt_{1-x}Mo_x$ composition spreads all showed lower overpotentials at intermediate M content with 50 ppm CO (approximate as-sputtered ranges: Mo: $0.4 < x < 0.7$), implying that the binary catalysts would be more CO-tolerant than Pt alone. Mo gave lower overpotentials (for x in $Pt_{1-x}Mo_x$ ~0.5 as-sputtered) than Ru and Sn, especially at low current densities.

The relative magnitude of the electrooxidation of CO and the electroreduction of CO_2 will depend strongly on the concentrations of each reactant and on the PEMFC operating conditions. At present, for operation below 100 °C, the reformate streams usually contain much more CO_2 than CO. As a consequence, for full reformate operation with hydrogen containing both 25% CO_2 and 40 ppm CO, the PtRu alloy is much more tolerant than the $Pt_{75}Mo_{25}$ alloy [43]. Thus, today, with typical reformate feeds that contain CO_2, PtRu remains the electrocatalyst of choice for PEMFC operation below 100 °C. Based on those results, Ralph et al. [43] pointed out that the search for alternative electrocatalysts to provide improved CO tolerance by electrooxidizing CO at low anode potentials may be fundamentally flawed for current PEMFC stack operating conditions. They suggested that membrane purification [266] could be adopted to reduce CO_2 to ppm levels. Using membrane purification would allow PtMo to show a clear benefit over PtRu electrocatalysts at CO concentrations greater than 10 ppm.

16.3.3 PtSn Binary System

Evaluation of CO oxidation on PtSn electrocatalyst systems has been investigated in earlier work [26, 34, 267–274]. It was demonstrated that bimetallic PtSn catalysts with an oxide support display superior catalytic activity for CO oxidation [35, 275–278]. In 2000, Crabb et al. [267] applied a PtSn/C anode electrocatalyst, prepared by a surface organometallic chemistry method, in a PEMFC. Their preparation method involved a selective means of adding a second metal to the surface of another. This produced a controlled surface reaction between an organometallic species of the second metal (tetrabutyl- or tetraethyl-tin) with a pre-reduced monometallic platinum metal catalyst. The PtSn/C prepared by this method gave enhanced activity that resulted in a large decrease in the onset potential of CO oxidation compared with that for Pt/C. It was claimed that this enhancement was caused by the addition of Sn to the Pt/C-suppressed chemisorption of both the hydrogen and the carbon monoxide. Furthermore, in using this method, only a small amount of Sn was required to decrease the onset potential of CO oxidation. Analysis with TEM, EDX, and XPS provided evidence of a bimetallic effect, as the Pt and Sn appeared together on the support and the catalysts consisted mainly of metallic platinum in close association with tin oxide after exposure to air.

The Pt_3Sn alloy has been found to be a more effective CO electrooxidation catalyst than pure Pt and thus more active for hydrogen oxidation in the presence of CO than pure Pt, with the activity strongly dependent on the surface orientation. The (111) face, in particular, is very active for CO electrooxidation [279]. In addition to electronic effects, other factors, such as surface structure and intermolecular repulsion between adsorbed species are responsible for the high catalytic activity of Pt_3Sn(hkl) alloys. This enhanced CO tolerance has also been used to improve DMFC performance [280]. A Pt_3Sn/C catalyst was synthesized by Lim et al. [281] via borohydride reduction and hydrothermal treatment for the anode electrode of a low-temperature fuel cell. In the TEM image, the PtSn nanoparticles were uniformly well-dispersed on the carbon support with an average particle size of around 2.4 nm. Good distribution of the Pt_3Sn/C nanoparticles is known to be an important factor in catalytic activity. The oxidation of CO on the Pt_3Sn/C catalyst occurred at a lower potential than that on the commercial catalysts. It appeared that Sn has the ability to promote the oxidation of adsorbed CO at low potentials. The removal of the CO adsorbed onto Pt proceeded via its reaction with OH adsorbed onto the Sn or Sn oxide sites formed by the dissociative adsorption of water.

It has been shown that at low Sn contents, the Pt_3Sn phase is easier to form, and an increase in the Sn content will prompt the main alloy structure to change to the PtSn phase. As for CO-stripping over the PtSn/C catalyst, it had already been indicated that oxidation of the CO adsorbed on Pt sites is promoted by the adjacent Sn atoms in the Pt_3Sn alloy [282]. Despite reports that Sn can supply the OH to improve the oxidation of CO_{ad}, it has been proposed that the electroactivity of PtSn/C catalyst is proportional to the amount of Pt_3Sn phase present, without any contribution for CO oxidation derived from the PtSn phase, Pt/SnO_2 clusters, or other structures [271]. Stevens et al. [235] prepared $Pt_{1-x}Sn_x$ binary composition spreads via dc magnetron sputtering through shadow masks onto 3M nanostructured thin-film catalyst support. All samples were found to have the Pt fcc structure at high Pt content. At high Sn content, only tetragonal Sn was seen. Electron microprobe measurements on catalyst electrodes after fuel cell testing showed some loss of Sn in $Pt_{1-x}Sn_x$ alloys containing > 80 atom% Sn. The HOR overpotentials for the $Pt_{1-x}Sn_x$ samples increased significantly for compositions at intermediate metal levels (Sn > 40 atom%), implying that the alloying elements significantly degraded the HOR capability of Pt. CO-stripping voltammetry measurements indicated that alloying Pt with intermediate levels of Sn led to lower CO-stripping onset potentials, implying improved CO tolerance. The $Pt_{1-x}Sn_x$ composition spreads all showed lower overpotentials at intermediate M content with 50 ppm CO (approximate as-sputtered ranges: Sn: $0.1 < x < 0.4$), implying that binary catalysts would be more CO-tolerant than Pt alone.

16.3.4 PtM (M = Fe, Co, Ni, Ta, Rh, Pd) Binary Systems

PtFe alloys such as $Pt_{95}Fe_5$, $Pt_{85}Fe_{15}$, $Pt_{56}Fe_{44}$, and $Pt_{40}Fe_{60}$, PtCo alloys such as $Pt_{82}Co_{18}$, and $Pt_{57}Co_{43}$, and PtNi alloys such as $Pt_{76}Ni_{24}$, and $Pt_{56}Ni_{44}$ are within the same group as PtRu and PtMo that exhibits excellent stability for the activity of H_2 oxidation in the presence of 100 ppm CO, in comparison with pure Pt, as classified

by Watanabe et al. [169]. They studied the cyclic voltammograms on Pt and Pt-Fe alloy surfaces. From the cyclic voltammograms in the solution saturated with and without CO, it is clear that the blank anodic current on the Pt skin of the Pt-Fe alloy electrode commences to increase at about 0.6 V, which is ~0.2 V less positive than that of the pure Pt and shows a larger current at more positive potentials in comparison with the blank cyclic voltammograms on the pure Pt. This result infers that the Pt skin surface on the alloy has a larger affinity, or oxidizing property, to water molecules than the bulk pure Pt. On the alloy electrode with the saturated CO adlayer, the anodic current for CO oxidation begins to increase at about 0.6 V, corresponding to the onset of the water molecule oxidation or the adsorption of OH species, and shows only one anodic peak at 0.73 V without any shoulder peak. On the other hand, the oxidation of the adsorbed CO on pure Pt starts at a potential less positive than 0.55 V and shows a peak at ~0.7 V via a small pre-shoulder. The shoulder current and the less positive onset potential can be ascribed to carboxyl radicals formed on the pure Pt surface [160, 283]. Despite almost the same total CO adlayer coverage on the Pt skin and the pure Pt, the electric charge (per real Pt surface area) for the CO adlayer oxidation on the Pt skin layer is larger than that of the pure Pt; this indicates that the former adlayer involves CO species with a larger number of electrons per Pt site, associated with the oxidation reaction not as a carboxyl radical or bridge-bonded CO but as linear CO.

Cobalt is used to promote CO oxidation in reformers [284, 285], suggesting PtCo alloys may be useful catalysts for H_2 oxidation in the presence of CO. PtCo alloys have been proposed as improved methanol oxidation catalysts [286] because cobalt may assist with CO removal (CO is an intermediate in methanol electrooxidation) through a mechanism analogous to the PtRu bifunctional mechanism. PtCo alloys have also been studied as improved ORR catalysts [200, 287, 288]. In addition to their improved ORR kinetics, these alloys have been shown to be more tolerant to methanol crossover in direct methanol fuel cells (DMFCs), again possibly through improved CO removal kinetics [289]. However, Stevens et al. [235] observed no impact on CO-stripping with the addition of cobalt to Pt, and explained this as due to surface cobalt dissolving away.

Tantalum is resistant to corrosion because it forms a passivation layer under all practical conditions. In a study of $Pt_{1-x}Ta_x$ alloys, it was shown that all of the tantalum was retained across the whole $Pt_{1-x}Ta_x$ binary range after exposure to 0.5 M H_2SO_4 at 80 °C for 1 week [290]. This means that if a PtTa catalyst composition with improved performance is developed, it is likely that the composition will give stable performance over time. There are few reports in the literature on the use of PtTa alloys in PEMFC applications. The most relevant work, completed by Papageorgopoulos et al. [210], involved a study of alloys of platinum with molybdenum, niobium, and tantalum. In this study it was shown that Pt_6Ta was more active than pure platinum for hydrogen oxidation in the presence of CO. Stevens et al. [235] prepared $Pt_{1-x}Ta_x$ binary composition spreads via dc magnetron sputtering through shadow masks onto 3M nanostructured thin-film catalyst supports. A nanocrystalline/amorphous PtTa phase formed for compositions containing at least 30 atom% Ta and the fcc phase was no longer observed. Electron microprobe measurements on catalyst electrodes after fuel cell testing showed that the Ta-based alloys were stable to corrosion. The HOR overpotentials

for the $Pt_{1-x}Ta_x$ samples increased significantly for compositions at intermediate metal levels (> 50 atom%), implying that the alloying elements significantly degraded the HOR capability of Pt. CO-stripping voltammetry measurements indicated that alloying Pt with intermediate levels of Ta may lead to lower CO-stripping onset potentials, implying improved CO tolerance.

Gómez et al. [291] studied rhodium adlayers on Pt(1 1 1) substrates prepared by electrodeposition from dilute Rh^{3+} acidic solutions. For the electrooxidation of CO, the experimental behavior cannot be described as a linear combination of the behavior of Pt and Rh regions: there is a sizable shift of the voltammetric CO oxidation curve toward less positive values. In addition, two different voltammetric contributions are distinguishable, reaching to split voltammetric peaks. A bifunctional mechanism as proposed by Watanabe and Motoo [89] would be applicable in this case. Rhodium adatoms would adsorb OH, which would react with CO molecules adsorbed both at the center of the islands and at the platinum sites in the vicinity of the Rh islands. This would correspond to the first peak in the CO voltammetric stripping wave. The second (at more positive potentials) would correspond to the oxidation of CO adsorbed on Pt sites and needing to diffuse to the island edges in order to combine with adsorbed OH. The periphery of the islands would contain the bifunctional catalytic centers. The reaction in the center of the islands is especially slow probably because of a high adsorption energy for both CO and OH, which leads to a much higher real energy of activation. In any case, the adsorptive and catalytic activity of the adlayers differ from those of the bulk Pt(1 1 1) and Rh(1 1 1) electrodes. The existence of strain in the film, together with a diminution in the coordination number for adatoms at the edges of the islands, are considered to be at the origin of the observed behavior.

The PtPd bimetallic system also exhibits a high resistance against CO poisoning from the oxidation of formic acid [292–294]. Stonehart [295, 296] proposed PtPd alloys as suitable electrocatalysts in phosphoric acid fuel cells for hydrogen oxidation. According to his study, the alloys were more tolerant than platinum alone, were resistant to sintering, and could be prepared with a very high surface area. An extensive examination of the PtPd alloy system showed that a minimum in hydrogen polarization, for constant current density, was obtained at 50–50 atom% levels [296]. However, PtPd alloys have given an inferior performance of Pt in a PEMFC [103]. The potential use of carbon-supported $PtPd_y$ electrocatalysts (where y = 1–6) as CO-tolerant anodes for PEMFC applications has been investigated by Papageorgopoulos et al. [297]. Since exploratory experiments conducted in their lab in the past revealed extremely poor performance for PtPd catalysts with up to 50 atom% Pd, only Pd-rich electrocatalysts, supported on high surface area carbon and doped with Nafion, have been prepared. Cyclic voltammetry experiments at 80 °C, the operating temperature of the PEMFC, reveal that upon CO saturation, a lower fraction of surface sites is poisoned in the case of $PtPd_y$ as compared to Pt, resulting in higher amounts of adsorbed hydrogen. By increasing the Pd content, this effect becomes more pronounced. Fuel cell tests demonstrated that the need for reasonable hydrogen oxidation currents, with and without CO, necessitates the presence of Pt in the catalyst. As a type of CO-tolerant PEMFC anode catalyst, $PtPd_y$ catalysts exhibit enhanced CO tolerance compared to Pt under operating conditions, with

$PtPd_4$ providing the best results. More importantly, improved performance compared to PtRu is demonstrated with 100 ppm or more of CO in the fuel stream.

16.3.5 PtRuM (M = Mo, Sn, W, Cr, Zr, Nb, Ag, Au, Rh, Os, and Ta) Ternary Systems

Of all the platinum alloys tested, platinum-ruthenium alloys, typically around the 1:1 composition, are the only ones to have been introduced commercially. However, even the PtRu catalyst still suffers a loss of 25 and 40% in the maximum power density obtained when the H_2 feed contains 25 and 100 ppm CO, respectively [102], although injection of 4.5% O_2 in the fuel stream was found to restore the performance with 100 ppm CO to that of pure hydrogen [8]. Other elements such as Mo [126, 204, 263] and Sn [35] when alloyed with platinum have also shown some promise in terms of improving CO tolerance, possibly performing better than the platinum-ruthenium alloys. They have not as yet been introduced into commercial applications, probably because PEMFC catalysts need to perform well under a variety of operating conditions for long periods of time with minimal degradation in performance. Non-noble elements such as Mo and Sn have the potential to corrode during operation, which may impact long-term stability. In addition, although these alloys are more CO-tolerant than pure Pt, the HOR overpotentials in the presence of CO are still very high relative to the overpotentials of the HOR in a CO-free gas feed.

It is likely that further improvements in CO tolerance will only be found in more complex (e.g., ternary, quaternary, etc.) alloy systems. The range of compositions that can be studied in such systems is enormous and realistically can only be mapped well through the use of high throughput materials science methods. Several CO-tolerant Pt-containing anodes exist, such as Pt/Ru/Sn [225], Pt/Ru/W [225], Pt/Ru/Mo [225], Pt/Ru/Os [233], and Pt/Ru/Pd [298, 299]. There is interest in determining whether there would be any synergistic effects if both elements were incorporated into Pt, with Mo increasing the rate of CO removal at low current densities, leading to low overpotentials at low to moderate current densities with Ru providing high current capability at higher overpotentials. Pt-based ternary electrocatalysts, such as PtRuMo (Mo 10 wt%), do give better performance than those of PtRu/C in the presence of CO.

In 2002, Papageorgopoulos et al. [210] investigated the effect on CO tolerance of including a metal M (M = Mo, Nb, and Ta) in Pt/C and PtRu/C. This was undertaken by comparing the cyclic voltammetry data and cell performance of the modified catalysts with those of traditional Pt/C and PtRu/C catalysts [210]. The new catalysts were binary PtM/C and ternary PtRuM/C (Vulcan XC72) systems, with a 20 wt% metal loading. The results showed that the inclusion of 10 at% Mo in PtRu – $Pt_9Ru_9Mo_2$ – produced an electrocatalyst with higher activity in the presence of CO than PtRu/C. Two earlier sets of studies prompted these experiments. One was work demonstrating that PtMo/C gave an up to three-fold enhancement in performance with H_2 (100 ppm CO)/O_2 compared with PtRu/C in the absence of CO_2 in the fuel [23, 204, 300]. The other research [224, 225] had reported the improved behavior of PtRu binary catalysts with the incorporation of a third metal, such as Cr, Zr, or Nb.

In another report, Pinheiro and co-workers [301] studied a number of PtRuMo catalysts and found that $Pt_{70}Ru_{20}Mo_{10}$ was a more effective fuel oxidation catalyst than PtRu for DMFCs. At low Mo content, $Pt_xRu_yMo_z$ (e.g., $Pt_{70}Ru_{26}Mo_4$) dispersed as nanoparticles in a conducting polymer matrix was found to give higher methanol oxidation current densities at 400 mV and in full DMFC fuel cell testing than PtRu alone [224]. These reports were all consistent with the finding that relatively low Mo levels can improve either CO tolerance or methanol oxidation performance relative to PtRu alone. In order to study this composition space in more detail, Stevens et al. [302] prepared a $(Pt_{1-x}Ru_x)_{1-y}Mo_y$ ($0 < x < 1$, $0 < y < 0.3$) ternary composition spread catalyst array and tested the HOR capabilities of 64 discrete catalyst compositions across this phase space in a 64-electrode proton exchange membrane fuel cell. The film was found to be reasonably stable when exposed to acid at 80 °C. The ratio of Ru to Pt across the composition spread was unchanged after a sample film was exposed to acid at 80 °C for one week, implying minimal Ru dissolution. There was evidence for some loss of Mo at the high Mo end of the composition spread during acid testing, most likely indicative of loss of Mo from the surface. CO-stripping voltammetry results showed that the addition of Ru to Pt led to a reduction in the onset potential for CO-stripping, coupled with an increase in CO-stripping area. The results also showed that the addition of Mo to Pt led to a reduction in both CO-stripping onset potential and CO-stripping area. These results were consistent with those obtained on equivalent binary composition spreads reported in an earlier paper. The addition of both Ru and Mo to Pt led to a combination of these trends. All compositions, with the exception of those containing high Ru content, showed good hydrogen oxidation catalytic activities. At low Ru content, the overpotential for hydrogen oxidation in the presence of 10 and 50 ppm CO at moderate current densities was very large (400 mV), highlighting the impact of poor CO tolerance on catalytic activity for Pt. As either the Mo or Ru content increased, the HOR overpotential measured under simulated reformate decreased. Optimum performance at 500 mA/cm^2 was recorded on channels containing both Ru and Mo, e.g., $Pt_{0.40}Ru_{0.35}Mo_{0.25}$, in addition to Pt. Air bleed was beneficial for electrodes with low Mo content, where it helped slow down the rate of CO poisoning as the potential was swept to lower values. Air bleed was found to have very little impact on hydrogen oxidation in the presence of CO for electrodes containing moderate to high (within the range prepared) Mo content. Electrodes in the optimum performance region performed at least as well with no air bleed as electrodes with minimal Mo content performed with air bleeds. These results all suggest that compositions around $Pt_{0.40}Ru_{0.35}Mo_{0.25}$ are worth examining further as candidates for the anode in improved CO-tolerant fuel cells.

Well-dispersed ternary PtRuSn catalysts of various atomic ratios (60:30:10, 60:20:20, and 60:10:30) were deposited onto carbon using a modified alcohol-reduction process by Wu et al. [303]. The alloy phase structure and surface morphology for each variation of the PtRuSn/C catalysts were determined by XRD and HR-TEM. In order to evaluate the contributions of Ru and Sn in the different stages of ethanol oxidation, electrochemical oxidations of adsorbed CO, ethanol, acetaldehyde, and acetic acid were performed on each PtRuSn/C catalyst. The results indicated that the Ru-rich PtRuSn/C catalyst (60:30:10) exhibited the lowest

onset potential for the electrooxidations of adsorbed CO, which may be partially attributed to it having the highest Ru content and also to the abundant Pt_3Sn structures in the catalyst, which was confirm by XRD analysis. On the other hand, the amount of Ru or Sn alloyed with Pt usually is smaller than nominally predicted, because some of these atoms are present as amorphous species on the catalyst surface, most likely as oxides [283]. So, as expected, Sn will exist in part as SnO_2 surrounding Pt alloy, which was confirmed by the XRD pattern at the 2θ value of 33.1 and 52.1 in the Sn-rich PtRuSn/C catalyst (60:10:30).

Venkataraman et al. [304] investigated four ternary catalysts, Pt-Ru-Ag, Pt-Ru-Au, Pt-Ru-Rh, and Pt-Ru-W_2C, as anode electrocatalysts for the oxidation of hydrogen containing carbon monoxide. These third components were selected as co-catalysts that help in CO oxidation and/or which reduce CO adsorption on Pt. The catalysts were either alloys or intimate admixtures of the components. Alloying non-adsorbing or weakly adsorbing components can modify the nature of the adsorbed CO by modifying the electronic structure (filling of d orbitals) as observed with PtSn alloys [305], and by introducing a steric or ensemble effect as observed with PdAg alloys [306]. The nature of CO adsorption on Pt and Pd was modified from bridged to linearly-bonded CO by the addition of Sn and Ag, respectively. Tungsten carbide has good stability in acid solutions and has electronic properties similar to platinum. Tungsten carbide has also been found to be a good CO-tolerant catalyst in a phosphoric acid fuel running on unprocessed methanol reformate gas [307]. Gold has been found to lend CO tolerance to Pd. Rhodium is a very good catalyst for hydrogen electrooxidation and has been found to enhance the activity of Pt in a PtRh [56] alloy catalyst. The Pt-Ru-W_2C (1:1:0.4 molar ratio) oxidizes CO at a lower potential (~200 mV), and the polarization for oxidation of hydrogen-containing CO was lower than the widely used PtRu (1:1 molar ratio) catalyst. At low polarization, the Pt-Ru-W_2C catalyst showed twice the activity of the PtRu catalyst when the oxidation currents were normalized to the Pt area. W_2C appears to aid in the oxidation of CO. X-ray diffraction and CO-stripping voltammetric studies indicate that the presence of a third component reduces the amount of Ru alloyed with Pt in the catalyst and increases the potential at which CO oxidation occurs. The anode polarization was found to be higher than that of PtRu for all ternary catalysts other than Pt-Ru-W_2C.

Though these ternary catalysts still suffer anode polarization losses in the presence of CO, optimization of the composition and structure of the catalyst and use of new components could lead to further improvements in CO tolerance.

16.3.6 The Pt, PtRu-MO_x (M = Mo, W, and V) System

It has been mentioned previously that bimetallic PtMo alloy catalysts have attracted considerable attention as alternatives to PtRu for their high catalytic activity in H_2 oxidation with CO/H_2 feed [22, 23, 70, 127, 204, 225, 259–263]. With regard to the PtMo alloy, Mo atoms have been reported to have oxygen-containing ligands even at H_2 potentials, which were responsible for the excellent CO tolerance [23, 204]. This notion was supported by the results for Mo K-edge XANES spectra, which showed that Mo was present as hydrated oxides with a valence state of +IV at 0 V [204]. It has been reported that carbon-supported nano-

sized Pt/Mo-oxide heterogeneous catalyst has improved CO tolerance [308, 309]. In Pt/MoO_x catalyst, both Pt and MoO_x nanoparticles were dispersed on the support surface, and therefore Mo would be present as a stable oxide form under PEMFC conditions. A performance evaluation of CO(100 ppm)/H_2 showed that the CO tolerance of Pt/MoO_x was nearly comparable to that of alloy catalysts [127, 225], and the role played in CO tolerance by O_2 that has crossed over from the cathode was discussed [309]. While the oxygen that permeates from the cathode mitigates CO poisoning to some extent, the CO tolerance of Pt/MoO_x is most likely to be dominated by intrinsic mechanisms such as bifunctional CO removal and/or the WGS reaction. CO tolerance of these non alloy-type anode catalysts is due to the interaction between Pt and metal oxides affected by the nature of the Pt catalyst [310]. Therefore, it is important to examine the nature of the intrinsic CO tolerance of Pt/MoO_x catalysts for the further development of catalysts. Ioroi et al. [311] prepared carbon-supported Pt/Mo-oxide catalysts, and the reformate tolerances of Pt/MoO_x/C and conventional PtRu/C anodes were examined to clarify the features and differences between these catalysts. Fuel cell performance was evaluated under various reformate compositions and operating conditions, and the CO concentrations at the anode outlet were analyzed simultaneously using on-line gas chromatography. Pt/MoO_x showed better CO tolerance than PtRu with CO(80 ppm)/H_2 mixtures, especially at higher fuel utilization conditions, which was mainly due to the higher catalytic activity of Pt/MoO_x for the water-gas shift (WGS) reaction and electrooxidation of CO. In contrast, the CO_2 tolerance of Pt/MoO_x was much worse than that of PtRu with a CO_2(20%)/H_2 mixture. The results of voltammetry indicated that the coverage of adsorbates generated by CO_2 reduction on Pt/MoO_x was higher than that on PtRu, and therefore, the electrooxidation of H_2 is partly inhibited on Pt/MoO_x in the presence of 20% CO_2. With CO(80 ppm)/CO_2(20%)/H_2, the voltage losses of Pt/MoO_x and PtRu were almost equal to the sum of the losses with each contaminant component. The behavior of the CO concentration at the anode outlet is essentially the same as in the case of CO(80 ppm)/H_2. Although the adsorbate coverage on Pt/MoO_x increases in the presence of 20% CO_2, CO molecules in the gas phase could still adsorb on Pt through an adsorbate "hole" to promote WGS or electrooxidation reactions, which leads to a reduction in the CO concentration under CO/CO_2/H_2 feeding conditions.

The Pt-WO_x system has been the subject of several research studies and in sulfuric acid a co-catalytic activity for oxidation of H_2/CO is shown by tungsten, although the effect is not as strong as that for ruthenium [199, 225, 312, 313]. At the potential of a PEMFC anode, tungsten is supposed to be active as a redox catalyst which is present in an oxidized state and written as WO_{3-x}. The co-catalytic activity is supposed to be due to a rapid change of the oxidation state of W, involving the postulated redox couples W(VI)/W(IV) [314] or W(VI)/W(V) [312]. These redox activities render the tungsten sites active for either the dissociative adsorption of water or the oxidation of adsorbed hydrogen. In 2003, based on the results of previous papers [199, 315–318] that showed the addition of Mo or W (especially for PtRu/WO_3/C [317]) could enhance the CO tolerance of catalysts, Hou et al. [319] prepared new composite catalysts of PtRu–H_xMO_3/C (M = Mo and W) by dispersing PtRu particles in a composite support composed of

colloidal H_xMO_3 (M = W or Mo) and Vulcan XC72. These authors investigated the performance of the catalyst by comparing its electrochemical behavior with that of PtRu/C. The contents of the noble metals in all the catalysts were 20 wt% Pt and 10 wt% Ru, and the content of H_xMO_3 in PtRu–H_xMO_3/C was 20 wt%. It was found that the noble metals in both PtRu/C and PtRu–H_xMO_3/C were uniformly and highly dispersed on the supports, and there were no obvious differences when a composite support was used instead of the carbon support. Both H_xWO_3 and H_xMoO_3 existed in an amorphous form, and provided sufficient interfaces between the noble metals and the transition metal oxides in the catalysts. Such a structure promises a better CO tolerance than PtRu/C by lowering the starting potential for CO oxidation and by improving the H_2 oxidation when active sites on the noble metals are blocked by CO. In single-cell performance tests of all the catalysts, operated with H_2/50 ppm CO and H_2/100 ppm CO, those with PtRu–H_xMoO_3/C electrodes were better than those with PtRu/C. These results were attributed to the presence of sufficient interfaces between the noble metals and transition metal oxides in the catalysts and to the bifunctional effects of CO electrooxidation reactions strengthened by the existence of active water that is bonded on the transition metal oxides.

CO_{ads} cannot spillover the carbon substrate, which implies that contact between the co-elements is necessary to improve the CO_{ads} tolerance. Maillard et al. [320] thus adopted another tactic in which the interface between the electrocatalyst and the substrate provides new electrocatalytic sites. This is the case of tungsten bronzes H_xWO_y-supported Pt electrocatalysts in which the (electro)catalytic activity is provided by metallic platinum and the Brönsted acid function by WO_x. Pt-WO_x/C composite materials elaborated via a two-step impregnation-electrochemical reduction method have been characterized and tested by Maillard et al. [320] for the electrooxidation of CO/H_2 mixtures. TEM and EDS measurements revealed that WO_x imperfectly covered the C particles. Nanometer-sized or agglomerated Pt particles were found on the WO_x/C surface. XRD measurements revealed the absence of diffraction peaks characteristic of crystalline WO_x and could indicate that this material is amorphous. No evidence of alloying between the Pt and W was observed. WO_x/C evidenced stability in acidic medium (1M H_2SO_4) within the time scale of their experiments (1 day) and survived extensive potential sweeping up to 1.4 V vs. RHE. The H de-intercalation from WO_x is clearly visible in cyclic voltammograms at 0.1 V vs. RHE, H intercalation into WO_x being hidden by the electrochemical features associated with Vulcan XC72R. Pt nanoparticles have been electrodeposited onto this material. The results suggested that WO_x very slightly modifies the electronic density of the Pt nanoparticles. A significant improvement toward the electrooxidation of a CO_{ads} monolayer was observed for the composite material compared to pure Pt/C electrocatalyst, which is evidenced by a new electrooxidation peak at 0.55 V vs. RHE ($v = 0.02\ Vs^{-1}$). As the electrical charge below this electrooxidation peak is sweep-rate-dependent, it is probably associated with the electrooxidation of CO_{ads} on Pt sites at the interface with the WO_x/C support. Potentiostatic measurements revealed that Pt-WO_x/C materials presented comparable CO tolerance to 20 wt% PtRu/C at short times ($t < 3000$ s). Significant degradation of the electrocatalytic performances is evidenced at longer times. A likely reason for this is the lower

equilibrium CO_{ads} coverage observed with perfect PtRu alloys. Comparison of these data with the literature suggests that the best CO_{ads} tolerance with Pt-WO_x materials is achieved when the interaction between Pt and WO_x materials is maximized.

Pereira et al. [321] investigated the anodes with Pt-WO_x/C and phosphotungstic acid (PTA)-impregnated Pt/C electrocatalysts. The choice of phosphotungstic acid is based upon its high protonic activity, suitable oxygen affinity properties [322, 323], and previously demonstrated positive action on CO oxidation with Pt-Ru/C catalysts [324]. Heteropolyacids (like PWA, PMoA, SiWA, etc.) containing these oxides were selected by Gatto et al. [325] for the development of CO-tolerant electrodes. Different electrodes were prepared by using a spray technique for both diffusive and catalytic layers. The catalytic layer was obtained using a 30 wt% Pt/Vulcan as an electrocatalyst mixed with a Nafion solution for the standard electrode (SE). CO-tolerant electrodes were prepared by adding different weight percentages (6–15%) of phosphomolybdic acid (PMoA) to SE, and for all the prepared electrodes, the Pt loading was maintained as a constant at 0.5 mg cm^{-2}. By feeding the fuel cell with H_2–CO/air, an improvement in the cell performance proportional to the increase of the percentage of PMoA was observed. The best value was reached by using a percentage of inorganic compounds in the range of 12–15 wt%. A short time test (160 h) was carried out at 80 °C in H_2–CO/air with an average power density of 220 $mWcm^{-2}$, confirming the stability of the system. The right compromise between the Pt catalyst and the heteropolyacid ratio could be a helpful tool in limiting Pt poisoning. Quite a high performance was achieved for the PEMFC fed with H_2 + 100 ppm CO and with anodes containing 0.4 mg $PtWO_x$ cm^{-2}, and also for those with 0.4 mg Pt cm^{-2} impregnated with ~1 mg PTA cm^{-2}. However, a decay of the single cell performance with time was observed, and this was attributed to an increase of the membrane resistance due to the polymer degradation promoted by the crossover of the tungsten species throughout the membrane.

16.3.7 Ru-modified Pt Catalysts and Pt-modified Ru Catalysts

In recent years, investigation of the mechanism of promotion as well as the search for more active or less expensive PtRu catalysts has turned to the study of Ru modified Pt and/or Pt modified Ru catalysts. Spendelow et al. have recently reviewed the results of such studies [12]. Although not all of the catalysts produced by the modification of carbon-supported Pt particles by Ru exhibit performances in a fuel cell environment that are any better than that of the best conventionally prepared PtRu/C catalysts, they and Ru-modified single crystal Pt surfaces have proved useful in providing a more detailed understanding of the bifunctional mechanism. In particular, Herrero et al. [326] showed that OH adsorption on Ru sites on a Pt(1 1 0) surface could be identified as active in the bifunctional mechanism (their study was of methanol oxidation, enhancement of which is thought also to occur via the bifunctional mechanism). Evidence of a local electronic modification of Pt atoms near Ru atoms on a modified surface has also been provided by such studies [107, 112, 168, 180]. The relative contributions of water activation and the electronic perturbation of Pt have been debated in the

literature, with the consensus being that most of the enhancement may be attributed to water activation at the Ru sites [106, 107, 132].

Modification of Pt nanoparticles by Ru has been accomplished using a variety of Ru pre-cursors [217, 220, 327–329]. The spontaneous deposition from acidic aqueous solutions of $RuCl_3$ [217, 220, 327] has been shown to result in the formation of ruthenium oxides on the surface of the Pt, which after subsequent reduction form metallic Ru islands [217]. Fachini et al. showed that $Ru_3(CO)_9(CH_3CN)_3$ in dichloromethane could be used [328]. The adsorbed Ru species was reduced by treatment with H_2. Most recently it has been shown that $Ru(C_5H_5)_2$ in heptane can be reacted with the reduced Pt/C surface and subsequently treated with H_2 to selectively deposit Ru on the Pt and not the C support [329]. The resulting catalyst was shown, using XRD and EXAFS, to consist of a ruthenium oxide decorated surface, which upon electrochemical reduction formed a metallic PtRu surface alloy. The results obtained in this study further inform the understanding of the role of Ru in promoting the oxidation of CO at PtRu alloy surfaces, by providing direct evidence of the presence of both Ru^{3+} and Ru^{4+} species at the surface of PtRu catalyst particles in the potential region in which CO oxidation occurs.

Ru-modified Pt surfaces can be prepared in a variety of ways, all starting with a pure Pt surface that is subsequently modified by Ru deposition from a gas phase, an aqueous phase, or a non-aqueous liquid phase. A variety of methods have been used to deposit Ru submonolayers on Pt surfaces, including wet electroless deposition (either spontaneous deposition [215, 330] or forced deposition [178, 232]), electrodeposition [326, 331–333], vacuum deposition by evaporation [334, 335] or chemical vapor deposition [107, 117], and deposition from a variety of organic and inorganic Ru precursors dissolved in non-aqueous solvents [328, 329, 336]. Studies on Pt single crystals have verified that the deposition results in the growth of three-dimensional Ru islands (Volmer-Weber growth) [116, 335, 338], as would be expected based on the higher surface energy of Ru compared with Pt (reference [338] and references therein). The method of Ru deposition influences the resulting surface structure, with consequences for electrocatalysis.

In agreement with previous observations on PtRu alloy surfaces [18, 20, 67, 339], ruthenium-modified Pt surfaces exhibit a substantial electrocatalytic enhancement toward the oxidation of adsorbed CO, demonstrated by the shift of the CO oxidation peak to more negative values [112, 116, 180]. FTIR spectra on the CO-covered electrodes indicate that the electrocatalytic activity of the Ru-modified Pt(111) for CO oxidation is slightly higher than that of a 50:50 Pt/Ru alloy [116].

A new method based on spontaneous deposition of Pt on Ru has recently been demonstrated for Pt [340] and Pd [341] deposition on a Ru(0001) single crystal surface, which involves a reduction of H_2PtCl_6 coupled with the oxide formation on Ru [340]. A selective Pt deposition on Ru (no deposition on carbon) is attainable without the application of an external potential [342]. Spontaneous deposition of Pt on Ru nanoparticles can be used to control the Pt cluster size and to tune the electronic and catalytic properties of PtRu catalysts. In addition, this approach facilitates a considerable reduction of Pt loadings by depositing Pt at the surface of Ru nanoparticles rather than having Pt throughout the PtRu

nanoparticles. Brankovic et al. [109] used this new method for the preparation of PtRu and similar bimetallic electrocatalysts. It involves a spontaneous deposition of Pt submonolayers on metallic Ru nanoparticles, which yields electrocatalysts with a considerably lower Pt loading and higher CO tolerance than the commercial PtRu alloy electrocatalysts. The method offers a unique possibility to place the Pt atoms onto the surface of Ru nanoparticles, which very likely makes almost all of them available for hydrogen oxidation, in contrast to the PtRu alloy catalysts that have Pt throughout the nanoparticles. Thus, an ultimate reduction of Pt loading can be achieved. It also facilitates a fine-tuning of the electrocatalyst's activity and selectivity by changing the coverage (the cluster size) of Pt for optimal performance under required CO tolerance levels.

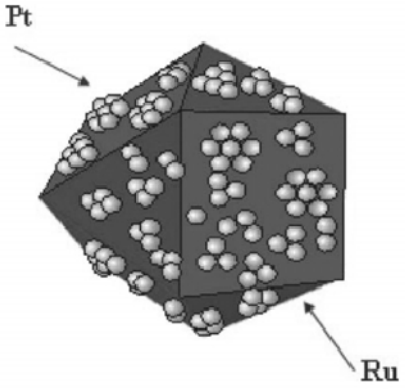

Figure 16.8. A cubo-octahedral particle model for the electrocatalyst, consisting of the Ru particle with two-dimensional Pt islands on its surface [343]. (Reprinted from Electrochimica Acta, 49(22–23), Sasaki K, Wang J.X, Balasubramanian M, McBreen J, Uribe F and Adzic R.R, Ultra-low platinum content fuel cell anode electrocatalyst with a long-term performance stability, 3873–7, ©2004, with permission from Elsevier.)

An active anode electrocatalyst, consisting of 1/8 of a monolayer of Pt on a surface of carbon-supported Ru nanoparticles, has been shown to exhibit excellent long-term performance stability in an operating fuel cell [343]. Figure 16.8 depicts a proposed structural model for the active electrocatalyst; it shows a cubo-octahedral model of the Ru particle with two-dimensional islands of Pt on its surface. The electrocatalyst has reduced susceptibility to poisoning by CO, in addition to the strong segregation of the Pt atoms on the Ru substrate that determines this characteristic. Kinetic parameters were determined by electrochemical techniques using thin-film rotating disk electrodes. X-ray absorption spectroscopy near edge structure was used to determine the *d*-band vacancies of a Pt submonolayer on a surface of carbon-supported Ru nanoparticles, and to relate it to the bonding strength of CO. XANES, electrochemical and gas-phase experimental data, and DFT calculations suggest there is a favorable electronic effect that reduces CO adsorption energy in a Pt submonolayer on a Ru catalyst, compared to pure Pt and PtRu alloys. In addition to the high activity for H_2 oxidation and CO tolerance, the strong segregation of Pt from the Ru substrate

is a key factor that ensures this catalyst's stability. Such segregation can be predicted using simple thermodynamic considerations of surface tensions, the enthalpy of mixing and the atomic radii of the two metals [344], and recent DFT calculations [345]. The latter show that a Pt overlayer on a Ru substrate represents a very strongly segregated system, in agreement with the observed stability of the catalytic activity of the PtRu [345] over 1000 h at 80 °C.

16.3.8 PtRu on Functionalized Carbon and Carbon Nanotube Systems

Because the size and structure of nanoparticles have a significant effect on catalytic reactions, well-controlled nanostructures are essential for creating efficient catalysts. In general, this is achieved by supporting the noble metal on a high-surface-area carbon support, such as Vulcan XC72, which maximizes the specific surface area of the noble metal and therefore its activity per unit weight. With respect to the electrocatalyst, an alternative approach to enhance the catalyst performance could be the search for suitable active supporting materials for Pt or Pt-M alloy [346]. In order to improve metallic dispersion it would be advantageous to utilize large surface carriers displaying a high number of anchoring sites. Thus, increasing the amount of surface functional groups of the support without decreasing its surface area would increase the dispersion of the metallic function. In a similar vein, small particles would be more active than large ones, since their surface area would be maximized. However, it must be taken into account that for small particles, strong interaction with the support may play a key role in their catalytic behavior. As well, it must be considered that the high Miller index crystal faces expose surface irregularities such as kinks and steps. Such defects may increase the intrinsic activity of a metal [347]. In spite of the large body of information concerning the CO oxidation reaction on Pt and carbon-supported Pt catalysts, there is a lack of studies dealing with the effect of the support nature in such processes.

Acid treatment can improve the performance of the carbon-supported activated catalysts [348]. Usually, additional treatments of the support are essential to remove (partially) any surface contaminant. Such contaminants are known to decrease the surface area of the deposited Pt [301]. There is no clear relationship between the amount of oxide surface groups in the carbon and the amount of anchored metal. Recently, a series of PtRu electrocatalysts supported over modified carbon displayed better performances than the commercial ones that have been reported [349]. Chemical modification of carbon Vulcan XC72R for fuel cell applications has been undertaken by de la Fuente et al. [350], with the aim of optimizing the anchoring of metallic particles. Treated carbons were used as carriers for the deposition of Pt nanoparticles and used as electrocatalysts. The influence of the carbon treatment as well as that of the Pt nanoparticles generation and their deposition route have been studied. Carbon modification by chemical treatment leads to an enhancement of the amount of surface oxygen groups. However, neither larger amount of Pt nor better Pt dispersion was observed during the preparation of Pt/C samples. Final particle size depended on the strength of the reducing agent, although the actual nature of the reducing agent has to be taken carefully into account. The ability of Pt/C samples towards CO oxidation depended

to a larger extent on the nature of the support than on the nature of the Pt particles, although both aspects should be taken into account. A single CO-stripping peak was observed over samples prepared on treated carbons, due to the homogenization of the sample surface after the treatment. CO mobility over actual electrocatalysts formulations, i.e., carbon-supported Pt, is low, resulting in broad or double CO-stripping peaks, depending on the support treatment.

Being a new form of carbon materials [351], carbon nanotubes (CNTs) have been a main focus of many current research efforts since recent development in large-scale syntheses of the material has significantly increased their availability [352, 353]. Due to their unique structure, high surface area, low resistance, and high stability, CNTs are considered promising supporting materials for electrocatalysts in PEMFC technology [279, 354–360]. A number of earlier investigations have shown that Pt deposited on CNTs can exhibit high activity for methanol electrooxidation as well as oxygen electro-reduction [279, 355–534]. But a pretreatment of the CNT support in oxidative mineral acid was always found to be beneficial for a homogeneous metal deposition and thus better for catalytic performance [279, 355, 356, 361–363]. Oxidative pretreatment can affect the density of surface functional groups, which could be necessary for better metal deposition and metal-support interaction [279]. The characteristics of nanosized Pt electrocatalyst deposited on carbon nanotubes (CNTs) were studied by Li et al. [364] with CO-stripping voltammogram and chronoamperometry measurements. The CNTs were pretreated by oxidation in HNO_3, mixed HNO_3+H_2SO_4, and H_2SO_4+$K_2Cr_2O_7$ solutions, respectively, to enable surface modification. Well-homogenized Pt particles (average size: ~3 nm) were loaded onto the pretreated CNT samples by a modified colloidal method. The morphology, crystallinity, and surface properties of CNTs were modified by pretreatments with oxidative mineral acids. In particular, pretreatment of the as-received CNTs with mixed HNO_3+H_2SO_4 acids produced material CNTs-II having fairly large mesoporosity at pore sizes larger than 10 nm, higher concentration of surface functional groups, and good graphitic crystallinity. The CO-stripping cyclic voltammetric measurements showed that the Pt/CNT catalysts are more tolerant to CO poisoning, since the CO electrooxidation peak potentials over these Pt/CNT catalysts are 40–160 mV lower than that over the conventional Pt/XC72 catalyst. Moreover, they found that the pretreatment of CNTs in mixed HNO_3+H_2SO_4 solution was very beneficial for the performance enhancement of Pt/CNT electrocatalyst; the catalyst obtained as such gave the lowest peak potential and the highest catalytic activity for the electrooxidation of CO. Larger amounts of oxygen-containing functional groups, a higher percentage of mesopores, and higher graphitic crystallinity of the pretreated CNTs were considered crucial for performance enhancement, e.g., by strengthening the interaction between Pt nanoparticles and the CNT support and enhancing the mass diffusion in the electrochemical reaction.

In 2005, Gonzalez and co-workers [365] reported the performance of PtRu catalysts supported on carbon nanotubes [366, 367] for H_2 + 100 ppm CO. Their results were similar to those of PtRu on Vulcan XC72, with an overpotential of 100 mV at 1 Acm^{-2} in a PEMFC. By contrast, a direct methanol fuel cell gave power densities and activity levels that exceeded those obtained with PtRu/Vulcan XC.

16.3.9 PtAu Binary System

Typically, gold is considered to be a poor choice as a fuel cell electrocatalyst. However, gold would be a stable alloying element, although still expensive. PtAu alloys have been studied as potential DMFC catalysts and have shown methanol oxidation activity [368] for specific structures. Gold catalysts are also effective for removing CO from H_2 gas streams in reformers [369].

$Pt_{1-x}Au_x$ binary catalysts prepared by Stevens et al. [235] were found to have the Pt fcc structure across the whole composition range. Electron microprobe measurements on catalyst electrodes after fuel cell testing showed that the Au-based alloys were stable to corrosion. The HOR overpotentials for the $Pt_{1-x}Au_x$ samples increased significantly for compositions at intermediate metal levels (Au > 50 atom%), implying that the alloying elements significantly degraded the HOR capability of Pt. The results obtained from testing with CO-free reformate suggest that $Pt_{1-x}Au_x$ may be binary alloys that are able to catalyze the RWGS reaction. RWGS CO poisons the platinum surface, requiring larger overpotentials for a given current density. CO-stripping voltammetry measurements indicated that the addition of Au to platinum led to an increase in the CO-stripping onset potential. With ~75 atom% Au, a CO-stripping peak could no longer be seen. The peak may have shifted to higher potentials, meaning that the CO binds even more strongly to the Pt and results in a catalyst that is even less CO-tolerant than Pt. The lack of a CO-stripping peak may also mean that little or no CO binds to gold and/or that the presence of gold minimizes the amount of CO that binds to Pt. It is unclear from these data, therefore, whether the addition of gold is beneficial to Pt in terms of improving CO tolerance. The results of hydrogen oxidation polarization curves with a reformate fuel containing up to 50 ppm CO showed that $Pt_{1-x}Au_x$ binary does not improve CO tolerance. There was no HOR activity up to 400 mV vs. H_2, regardless of composition prepared. This implies that the addition of Au to Pt does not improve CO tolerance in any way; in fact, it is quite possible that $Pt_{1-x}Au_x$ alloys require even higher potentials to remove adsorbed CO.

16.3.10 Pt-free Systems

Although not to the same extent as Pt, palladium is another noble metal of high catalytic activity, which is used in some industrially relevant reactions [370]. Pd is a very good electrocatalyst for organic fuel electrooxidation [371] and has the remarkable ability to store and release substantial amounts of hydrogen [372]. While voltammetry studies have indicated stronger CO bonding on Pd [373] as predicted [27], another study [374] showed that the release of hydrogen occluded in palladium may provide a viable route for lowering the surface concentration of adsorbed CO.

In Pt-free electrocatalysts, the surfaces of PdAu/C electrocatalysts are less strongly poisoned by CO than those of PtRu at temperatures of 60 °C. In 2001, Schmidt et al. [65] reported the CO tolerance of PdAu/C (Vulcan XC72) that was prepared via bimetallic colloidal precursors. This work was based on an earlier study by Fishman [375] in which PdAu-black alloys provided a highly active medium for the hydrogen oxidation reaction and a second metal (Au) produced

surfaces that did not adsorb CO under the operating conditions of a phosphoric acid fuel cell (PAFC). In addition, much lower CO adsorption energies on different poly- and single-crystalline PdAu surfaces, compared with pure Pd or pure Pt surfaces, were found from ultrahigh vacuum (UHV) studies [376]. At low overpotentials, these were more free active surface sites for hydrogen oxidation on PdAu than on PtRu at room temperature. Furthermore, at an elevated temperature of 60 °C, the surface of the PdAu/C appears to be less strongly poisoned by CO than that of PtRu/C, which gives rise to a larger concentration of free active Pd sites for H_2 oxidation. The superior activity of PdAu compared with PtRu/C was shown by CO/H_2 oxidation measurements at fuel-cell-relevant anode potentials (0.50–0.10 V). However, these results were obtained at temperatures below 60 ◦ C and further improvements, such as optimizing the PdAu/C with respect to particle size, alloy homogeneity, and stoichiometry are required.

A Pt/SnO_2 anode catalyst has been developed for PEMFC using CO-contaminated H_2 [310, 377]. The Pd/C and Pt/C anodes modified with SnO_2 nanoparticles for the PEMFC were investigated by Takeguchi et al. [379] using pure and 500 ppm CO-contaminated H_2 as fuel gas. Modification of the Pd/C anode with SnO_2 nanoparticles enhanced the cell performance in pure H_2, while modification of the Pt/C anode somewhat lowered the performance. Since Pd/SnO_2 and Pt/SnO_2 were known to be active for the low-temperature oxidation of CO, avoidance of CO poisoning of Pt-group metals was expected [379]. The effect of SnO_2 addition on the performances of the cell with the Pd anode in CO-contaminated H_2 was examined. The SnO_2 addition to the anode somewhat decreases the electrochemical activity in pure H_2, but clearly increases the CO tolerance of the anode catalysts. It was revealed by CO pulse titration that the SnO_2-containing catalysts adsorbed CO more weakly than the other catalysts without SnO_2 nanoparticles. This phenomenon was derived from the interaction between Pt or Pd atoms and SnO_2 nanoparticles, since these catalysts mixed with carbon did not exhibit intermetallic compounds. The cell voltage with the $Pd/SnO_2/C$ anode in 500 ppm CO-contaminated H_2 was 0.41 V at a current density of 0.2 A/cm^2, while that in pure H_2 was 0.59 V. The $Pd/SnO_2/C$ anode exhibited good tolerance to CO poisoning, since the anode adsorbed CO more weakly. Neither electrochemical oxidation of CO nor a shift reaction contributed to the CO tolerance of the $Pd/SnO_2/C$ anode.

16.4 Preparation of CO-tolerant Catalysts

The first step in the development of an anode catalyst is preparation. Several approaches have been used for the production of catalysts, both supported and unsupported. It is generally agreed that preparation has an important influence on catalyst performance [380]. Several techniques have been used to prepare the catalysts, such as colloidal chemistry methods [381–385], the impregnation method [386–390], and the reverse micelles method [391, 392]. Although the colloidal chemistry methods and the reverse micelles method produce very promising results, they are very complex compared to the impregnation method. The

application of these methods is still hindered by the complex colloid synthesis or catalyst preparation, which leads to non-competitive catalyst prices.

Reduction of the metallic ions from their salts with sulfite [209], borohydride [383], formaldehyde [393], hydrazine [394], or formic acid [395] has been proposed, resulting in catalysts with such diverse physical characteristics that direct comparison of their electrochemical performances is a rather difficult task. In the case of bimetallic catalysts, the reduction of both metals can be done simultaneously or one after the other, as was described for Pt-Ru/C [396] and Pt–Co/C [397].

Catalysts can also be prepared by melting, arc-melting in an argon atmosphere, ion-beam implantation, etc., followed by heat treatment for homogenization. In some cases due to strong segregations during the heat treatment, surface composition can differ from bulk composition. An example of this is PtMo alloy. The bulk composition of the alloy was 66 mol% Pt and 33 mol% Mo (Pt_2Mo). But after UHV annealing treatment at 970 K for 30 min, the resulting surface concentration of Mo was 23 mol%, and after Ar ion (0.5 keV) spattering, 30 mol%,

It is known that the use of well-defined substrates (single-crystal electrodes) allows a more detailed understanding of the action mechanism of the two types of surface atoms. There are two main potential ways of preparing these surfaces. First, one could think of preparing single crystals of alloys with different compositions and cut them to obtain alloy surfaces with different orientations. Second, one of the components would be deposited (either reversibly or irreversibly) onto a single crystal of the other component. The first approach, only partially explored in electrochemical environments [37, 40, 202, 398–400], suffers from several drawbacks. Only some binary systems have solubility in the whole range of composition (total miscibility) and segregation can easily occur during the experiment, especially in the course of electrode pretreatment (i.e., during the flame-annealing procedure). On the other hand, the second procedure allows separation of the pretreatment of the electrode from the preparation of the bimetallic surface. Also, a whole range of coverage is attainable in most cases. However, adatoms of elements with high cohesive energy show a strong tendency to form islands, or even three-dimensional clusters or nanoparticles, at the surface, it not being possible to obtain bimetallic surfaces with a random distribution of both types of atoms (two-dimensional substitutional alloys). Goméz et al. [291] explored the deposition and electrocatalytic activity of a number of adatoms on platinum single-crystal electrodes, focusing especially on irreversibly adsorbed adatoms. Two main types of adatoms have been investigated: those of elements of the p-block in the periodic table (see, for example, Refs. [401–405]) and those of platinum-group metals (see, for example, Refs. [406–411]). The first are characterized by low cohesive energy and electronegativities that are rather different from that of platinum, which leads to the formation of ordered open structures composed of isolated adatoms at a relatively low coverage. High cohesive energies and electronegativities similar to that of the platinum substrate characterize the second group of adatoms (platinum-group metals). Many of the corresponding bimetallic surfaces possess intrinsic adsorption and electrocatalytic properties, in some instances distinct from those of the corresponding bulk substrate electrodes. Effects from the underlying substrate on the surface states as

well as the generation of new bimetallic sites at the edges of the islands are two of the factors explaining this particular behavior. Among the noble well-ordered bimetallic surfaces formed by Pt and another element, great attention has been devoted to Pd/Pt(1 1 1) [400, 406, 407, 410–415] and Ru/Pt(1 1 1) [46, 122, 215], and to a lesser extent to Pd/Pt(1 0 0) [292, 407, 416], Rh/Pt(1 1 1) [408, 412, 417], and Ru/Pt(1 0 0) [215, 337]. Some work has been devoted to Os/Pt(1 1 1) [330], Rh/Pt(1 0 0) [409, 418], Pt/Rh(1 0 0) [418], Pt/Au(1 1 1) [419, 420], and Pt/Ru(0 0 0 1) [340]. One of the systems only partially explored is that of Rh adlayers on Pt(1 1 1). The preparation and characterization of these adlayers was presented a number of years ago [408, 412, 417].

Table 16.2. Physical characterization of PtRu alloy electrocatalysts [43]. (Reprinted from Ralph TR, Hogarth MP. Catalysis for low temperature fuel cells, part II: the anode challenges, Plat Met Rev 2002;46(3):117–35, 2002. With permission from Platinum Metals Review.)

Electrocatalyst	XRD crystallite size, nm	Calculated metal area m^2g^{-1} PtRu	CO chemisorption, metal area, m^2g^{-1} PtRu	XRD lattice parameter, nm
67 wt% Pt, 33 wt% Ru (unsupported)	2.9	114	77	0.388
40 wt% Pt, 20 wt% Ru supported on XC72R	2.5	131	104	0.388
20 wt% Pt, 10 wt% Ru supported on XC72R	1.9	150	139	0.388

For industrial-scale manufacture of PtRu alloy electrocatalysts, Johnson Matthey use an aqueous slurry route with chemical reduction to form the metal alloy particles [421]. Table 16.2 shows physical characterization data of an unsupported $Pt_{0.5}Ru_{0.5}$ alloy black electrocatalyst and two high metal loaded $Pt_{0.5}Ru_{0.5}$ alloys supported on Vulcan XC72R carbon black at 40 wt% Pt, 20 wt% Ru, and at 20 wt% Pt, 10 wt% Ru. Particularly interesting is the high metal dispersion of all of the electrocatalysts, especially at high metal loadings. The X-ray diffraction (XRD) crystallite sizes are 2.9 nm (PtRu black), 2.5 nm (40 wt% Pt, 20 wt% Ru), and 1.9 nm (20 wt% Pt, 10 wt% Ru). These are much lower than the corresponding values of 5.8 nm (Pt black), 4.5 nm (60 wt% Pt), and 2.8 nm (30 wt% Pt) for the corresponding pure Pt electrocatalysts. The high degree of PtRu dispersion is most probably a reflection of the surface characteristics of the materials. Although the $Pt_{0.5}Ru_{0.5}$ electrocatalysts were well alloyed, the contraction in the lattice parameter shown in Table 16.2 suggests all were slightly

Pt-rich (that is, $Pt_{0.59}Ru_{0.41}$). The lack of any crystalline Ru-rich phases in the XRDs suggests that the unalloyed Ru is present as an amorphous phase. Cyclic voltammetry and X-ray photoelectron spectroscopy (XPS) studies indicated that the surface of the electrocatalysts were rich in amorphous Ru oxide. This amorphous Ru oxide may play an important role in the co-deposition of the PtRu particles and in reducing the degree of sintering during the electrocatalyst manufacturing process. Many research efforts have been devoted to improving the catalytic performance of PtRu/C by increasing the catalyst dispersion [360, 422–430], and optimizing the atomic ratio [431–436] and surface state of PtRu [118, 218, 321, 437–439]. Although there have been many debates over the optimal composition ratio in the PtRu/C alloy catalyst, the 1:1 atomic ratio of Pt and Ru was widely employed.

Previously, it was known that a simple way to produce the alloy catalyst of the desired composition, in a wet-chemistry based method, is to match the ratio of metallic precursor concentrations to the target value. However, Kim et al. [424] recently showed that the synthesis parameters can significantly affect the yield of Pt and Ru loadings, and consequently the composition of Pt and Ru. In recent years, there has been considerable interest in the development of colloidal methods to prepare Pt-based fuel cell catalysts with narrow particle size distribution and homogeneous catalyst dispersion [422, 360, 426–428, 440, 441]. The investigation of Li et al. [442] focused on the effect of the synthesis conditions of a surfactant-stabilized colloidal method [441] upon the loss of Pt and Ru loadings and thus upon the Pt:Ru ratio in the resultant catalysts. Well-dispersed PtRu/C catalysts were prepared by supporting surfactant-stabilized PtRu hydrosol on carbon, followed by heat treatment at elevated temperature. The effect of the synthesis conditions and the heat treatment on the composition and electrocatalytic properties of PtRu/C towards methanol oxidation was systematically investigated. It was found that the pH environment and the reaction temperature could greatly affect the yields of Pt and/or Ru loadings, resulting in a final PtRu composition far from the expected nominal value. Moreover, after a post-heat-treatment process, the electrocatalytic activity of PtRu colloidal catalysts can be much improved, the enhancement of which can largely be explained by the improved alloy formation and removal of surfactant from the catalyst as demonstrated by the XRD and XPS analyses, respectively.

Early studies revealed that rare earth oxides could interact with the noble metals to prepare catalysts of an unusual and unexpectedly high degree of dispersion and stabilization [443]. An efficient impregnation-reduction method, which is easy to control and does not need protective reagents and thermal treatments, was applied to synthesize uniform PtRu spherical nanoparticles with small size [448]. At the same time, Nd_2O_3 was introduced as a dispersing reagent during the preparation step to control the crystallite growth of noble metals and enhance the degree of dispersion of the catalysts. TEM, XRD, and the CO-stripping voltammetry experiment results showed that noble metal particles of the PtRu/C catalysts are highly dispersed uniformly on the support and have similar morphology, and that the PtRu/C catalysts prepared adding Nd_2O_3 have smaller particle size and higher degree of dispersion of the PtRu particles than the PtRu/C catalyst prepared without adding Nd_2O_3. Well-dispersed catalysts with an average

particle size of about 2 nm were achieved. The electrochemically active surface area of the different PtRu/C catalysts was determined by the CO_{ad} stripping voltammetry experiment. The effect of Nd_2O_3 on the degree of dispersion of the noble metal and the reasons for the higher catalytic activity of the best in-house prepared PtRu/C catalyst were discussed. This preparation method also has other advantages, such as no need for protective reagents or thermal treatments, simple preparation procedure, and good reproducibility.

A carbon-supported PtRu/C catalyst (PtRu-2/C) was prepared by a simple reversal of the order of mixing in catalyst preparation [445]: adding the metal precursor salts to a carbon slurry of $NaBH_4$ instead of adding $NaBH_4$ to a carbon slurry of the metal precursor salts (PtRu-1/C), as is more commonly done. These modifications in the preparation method resulted in catalysts of different attributes. The improved performance did not come from smaller particle size and/or a higher state of metal dispersion, since PtRu-2/C had neither. It has been reported that homogeneous PtRu alloys are far less reactive than bulk mixtures of Pt metal, Pt hydrous oxides, hydrous and dehydrated RuO_2 [446, 447]. The enhanced activity was attributed to the presence of the mixed (electronic and ionic) conductor, hydrous ruthenium oxide [448]. The presence of mixed phases in PtRu-2/C and a single phase in PtRu-1/C was evident from CO-stripping voltammetry. In addition to PtRu, the mixed phases in PtRu-2/C have been identified as Pt(0) (based on a typical CO-stripping peak at 0.54 V and the well-defined hydrogen adsorption/desorption region), and platinum and ruthenium oxides (from XPS analyses). The lower cell resistance for PtRu-2/C relative to PtRu-1/C also suggests the existence of more electronically conducting components, presumably the mixed conductor hydrous ruthenium oxide.

Although as described above these alloy systems have been studied by a number of research groups, it is difficult to directly compare one system to another because of differences between sample preparation methods and experimental techniques. Such multielement comparisons do not appear routinely in the literature because the amount of work involved in sample preparation and testing using traditional “one at a time” methods is prohibitive. Thus, a paper published by Stevens et al. [235] demonstrated the usefulness of composition spread preparation and analysis techniques for fuel cell catalyst research. Furthermore, performance measurements of $Pt_{1-x}M_x$ composition were used to identify more complex ternary or quaternary composition for future studies.

16.5 Conclusions

An overview of the mechanism of CO tolerance and the development of CO-tolerant catalysts, including Pt-based binary/ternary metallic electrocatalysts and Pt-free electrocatalysts, was presented. For many PEMFC applications, fuel containing CO other than pure H_2 is the most practical choice. The use of CO-tolerant electrocatalysts is generally considered the most promising way for solving the CO poisoning problem in PEMFCs. CO-tolerant catalysts are thus still being investigated by numerous research groups and will be for many years. CO-tolerant anodes usually contain a PtRu alloy as the state-of-the-art catalyst. The mechanism

of CO oxidation and the CO tolerance of PtRu catalysts with well-defined surfaces has been investigated and clarified.

Although an electrocatalytic enhancement afforded by the addition of Ru to Pt catalysts is universally recognized, the exact mechanism of enhancement is still the subject of some debate. It is widely agreed that the bifunctional mechanism of Ru enhancement is a significant factor, and most authors agree that this is more important than any electronic (ligand) effects. Still, it seems that the ligand effect plays at least a small role. The relative effect of the two mechanisms depends on both the surface structure and the reaction being studied.

Based on the bifunctional mechanism of CO tolerance, it is necessary to find a metal that can provide OH at as low a potential as possible (e.g., near the hydrogen reversible potential). Although PtRu is widely used as a reasonably reformate-tolerant anode catalyst, its CO tolerance is still unsatisfactory for the higher CO concentrations expected at system start-up or during changes in load. Moreover, the limited availability of Ru may become a significant problem before stationary PEMFC systems can be placed on the market. A wide range of Pt alloys has been examined in an attempt to modify the CO and hydrogen electrosorption properties of Pt – to reduce the CO coverage and increase the rate of hydrogen electrooxidation. It was shown that below 100 °C none of the Pt alloys was superior to PtRu but that the CO tolerance of PtRh approached that of PtRu. There are many bimetallic catalysts. Among them, PtRu, PtSn, and PtMo are the best CO-tolerant catalysts. Pt-Fe, Pt-Ni, and Pt-Co alloys have been found to exhibit excellent CO tolerance in H_2 oxidation, similar to that of the PtRu alloy. PtRuW and PtRuMo showed an improved CO tolerance over Pt and PtRu catalysts in the presence of 50–100 ppm of CO. It should be noted that practically all transition metals are oxidized in acid solutions. Non-precious metals such as Fe or Mo will be leached out, at least from the surface, and a Pt skin layer is formed, in contrast to the precious metal Ru in the PtRu alloy.

Although attempts to find a more active catalyst than Pt/Ru have been ongoing for decades, the Pt/Ru systems still shows the best activity and stability for oxidation reactions relevant to anodes in direct methanol and reformate-fed fuel cells. Despite extensive study of Pt/Ru surfaces, many unanswered questions remain. The ideal distribution of Ru in or on Pt-based electrocatalysts is also a subject of debate. Another area of debate focuses on the question of the ideal oxidation state of Ru in Pt/Ru catalysts. Thus, there is reason to hope that further study and optimization of the Pt/Ru system may yield even more active electrocatalysts. Ru leaching from PtRu fuel cell anode electrocatalysts has a dramatic impact on the activity of a Pt/C oxygen-reducing cathode, and thus has a major role in the performance degradation of PEMFCs, particularly of DMFCs. Unless highly stable PtRu anode electrocatalysts are developed, the problem of Ru crossover and contamination at the cathode should be addressed by novel fuel cell designs where crossover is omitted, by less Ru-permeable membranes, or by more Ru-tolerant ORR electrocatalysts in PEMFCs.

There is a considerable drive to raise the operating temperatures of the PEMFC to above 100 °C. This would raise the system efficiency and dramatically improve the CO tolerance of Pt-based electrocatalysts. If the temperature can be raised to 160 °C, studies in the phosphoric acid fuel cell (PAFC) with 1 to 2% CO indicate

that PtRh and PtNi may offer superior CO tolerance. Indeed, at 200 °C pure Pt is the favored electrocatalyst in the PAFC. At higher temperatures PtRu may not be the electrocatalyst of choice in the PEMFC. There is currently much research aimed at developing membranes capable of proton conduction at 120 to 200 °C.

PEMFC research directed towards the development of CO-tolerant anode electrocatalysts will furthermore be well suited to direct alcohol fuel cells, particularly direct methanol fuel cells. Success in the arenas of cost and complexity reduction rely on continued advances in materials development and fabrication routes, and are essential for realizing the market and environmental potential of fuel cells. In the next couple of years it is likely that much research and development will still focus on reducing the costs of existing fuel cell stack materials and increasing the durability of available components. This means that innovative materials scientists and engineers can still have a major impact on the commercialization of fuel cell technology. The challenge is to design, and process economically, materials that would allow PEMFC stacks and associated reformers to operate at elevated temperatures (over 120 °C). Material scientists and engineers have the opportunity to overcome these challenges and to ensure that fuel cells become a commercial success.

Acknowledgements

The author would like to acknowledge support from the R&D and Product Development Departments of Ballard Power Systems.

References

1. Trimm DL, Önsan ZI. Onboard fuel conversion for hydrogen-fuel-cell-driven vehicles. Catal Rev 2001;43:31–84.
2. Herman RG, Klier K, Simmons GW, Finn BP, Bulko JB, Kobylinski TP. Catalytic synthesis of methanol from CO/H_2: I. Phase composition, electronic properties, and activities of the $Cu/ZnO/M_2O_3$ catalysts. J Catal 1979;56:407–29.
3. Gadgil MM, Sasikala R, Kulshreshtha SK. CO oxidation over Pd/SnO_2 catalyst. J Mol Catal 1994;87:297–309.
4. Haruta M, Tsubota S, Kobayashi T, Kageyama H, Genet KJ, Delmon B. Low-temperature oxidation of CO over gold supported on TiO_2, α-Fe_2O_3, and Co_3O_4. J Catal 1993;144:175–92.
5. Echigo M, Shinke N, Takami S, Higashiguchi S, Hirai K, Tabata T. Development of residential PEFC cogeneration systems: Ru catalyst for CO preferential oxidation in reformed gas. Catal Today 2003;84:209–15.
6. US Department of Energy. Fuel cell. In: DOE multi-year research, development and demonstration plan: planned program activities for 2005–2015. Available on: http://www1.eere.energy.gov/hydrogenandfuelcells/mypp/pdfs/fuel_cells.pdf.
7. Ralph TR, Hards GA, Thompsett D, Gascoyne JM. Fuel cell seminar extended abstracts; 1994 Nov 28–Dec. 1; San Diego, CA: p. 199.
8. Gottesfeld S, Pafford J. A new approach to the problem of carbon monoxide poisoning in fuel cells operating at low temperatures. J Electrochem Soc 1988;135:2651–2.

9. Beden B, Lamy C, Bewick A, Kumimatsu K. Electrosorption of methanol on a platinum electrode. IR spectroscopic evidence for adsorbed CO species. J Electroanal Chem 1981;121:343–7.
10. Crown A, Kim H, Lu GQ, de Moraes IR, Rice C, Wieckowski A. Research toward designing high activity catalysts for fuel cells: structure and reactivity. J New Mat Electrochem Systems 2000;3:275–84.
11. Iwasita T. Methanol and CO electrooxidation. In: Vielstich W, Gasteiger HA, Lamm A, editors. Handbook of fuel cells – fundamentals, technology and applications, Vol 2. New York: John Wiley & Sons, 2003: 603–24.
12. Spendelow JS, Babu PK, Wieckowski A. Electrocatalytic oxidation of carbon monoxide and methanol on platinum surfaces decorated with ruthenium. Curr Opin Solid State Mater Sci 2005;9:37–416.
13. Adams WA, Blair J, Bullock KR, Gardner CL. Enhancement of the performance and reliability of CO poisoned PEM fuel cells. J Power Sources 2005;145:55–61.
14. Iorio T, Yasuda K, Siroma Z, Fujiwara N, Miyazaki Y. Enhanced CO-tolerance of carbon-supported platinum and molybdenum oxide anode catalyst. J Electrochem Soc A 2003;150:A1225–30.
15. Wee JH, Lee KY. Overview of the development of CO-tolerant anode electrocatalysts for proton-exchange membrane fuel cells. J Power Sources 2005;157:128–35.
16. Kuk ST, Wieckowski A. Methanol electrooxidation on platinum spontaneously deposited on unsupported and carbon-supported ruthenium nanoparticles. J Power Sources 2005;141:1–7.
17. Spendelow JS, Lu GQ, Kenis PJA, Wieckowski A. Electrooxidation of adsorbed CO on Pt(1 1 1) and Pt(1 1 1)/Ru in alkaline media and comparison with results from acidic media. J Electroanal Chem 2004;568:215–24.
18. Lin WF, Iwasita T, Vielstich W. Catalysis of CO electrooxidation at Pt, Ru, and PtRu alloy. An in situ FTIR study. J Phys Chem B 1999;103:3250–3257.
19. McGovern MS, Waszczuk P, Wieckowski A. Stability of carbon monoxide adsorbed on nanoparticle Pt and Pt/Ru electrodes in sulfuric acid media. Electrochim Acta 2006;51:1194–8.
20. Gasteiger HA, Markovic N, Ross PN Jr, Cairns EJ. Co electrooxidation on well-characterized Pt-Ru Alloys. J Phys Chem 1994;98:617–625.
21. Grgur BN, Zhuang G, Marković NM, Ross PN Jr. Electrooxidation of H_2/CO mixtures on a well-characterized $Pt_{75}Mo_{25}$ alloy surface. J Phys Chem B 1997;101:3910–3.
22. Grgur BN, Marković NM, Ross PN Jr. Electrooxidation of H_2, CO, and H_2/CO mixtures on a well-characterized $Pt_{70}Mo_{30}$ bulk alloy electrode. J Phys Chem B 1998;102:2494–501.
23. Grgur BN, Marković NM, Ross PN. The electro-oxidation of H_2 and H_2/CO mixtures on carbon-supported Pt_xMo_y alloy catalysts. J Electrochem Soc 1999;146:1613–9.
24. Massong H, Wang H, Samjeske G, Baltruschat, H. The co-catalytic effect of Sn, Ru and Mo decorating steps of Pt(111) vicinal electrode surfaces on the oxidation of CO. Electrochim Acta 2000;46:701–7.
25. Pozio A, Giorgi L, Antolini E, Passalacqua E. Electroxidation of H_2 on Pt/C Pt–Ru/C and Pt–Mo/C anodes for polymer electrolyte fuel cell. Electrochim Acta 2000;46:555–61.
26. Lee SJ, Mukerjee S, Ticianelli EA, McBreen L. Electrocatalysis of CO tolerance in hydrogen oxidation reaction in PEM fuel cells. Electrochim Acta 1999;44:3283–93.
27. Christoffersen E, Liu P, Ruban A, Skriver HL, Norskov JK. Anode materials for low-temperature fuel cells: a density functional theory study. J Catal 2001;199:123–31.
28. Giorgi L, Pozio A, Bracchini C, Giorgi R, Turtu S. H_2 and H_2/CO oxidation mechanism on Pt/C, Ru/C and Pt–Ru/C electrocatalysts. J Appl Electrochem 2001;31:325–34.

29. McBreen J, Mukerjee S. In-situ X-ray-absorption studies of a Pt-Ru electrocatalyst. J Electrochem Soc 1995;142:3399–404.
30. Mukerjee S, McBreen J. An in situ X-ray absorption spectroscopy investigation of the effect of Sn additions to carbon-supported Pt electrocatalysts: Part I. J Electrochem Soc 1999;146:600–6.
31. Koper MTM. Electrocatalysis on bimetallic and alloy surfaces. Surf Sci 2004;548:1–3.
32. Gallagher ME, Lucas CA, Stamenkovic V, Marković NM, Ross PN. Surface structure and relaxation at the Pt_3Sn(1 1 1)/electrolyte interface. Surf Sci 2003;544:L729–34.
33. Morimoto Y, Yeager EB. Comparison of methanol oxidations on Pt, PtRu and PtSn electrodes. J Electroanal Chem 1998;444:95–100.
34. Wang K, Gasteiger HA, Marković NM, Ross PN Jr. On the reaction pathway for methanol and carbon monoxide electrooxidation on Pt-Sn alloy versus Pt-Ru alloy surfaces. Electrochim Acta 1996;41:2587–93.
35. Gasteiger HA, Marković NM, Ross PN Jr. Electrooxidation of CO and H_2/CO mixtures on a well-characterized Pt_3Sn electrode surface. J Phys Chem 1995;99:8945–9.
36. Paffett MT, Gebhard SC, Windham RG, Koel BE. Chemisorption of carbon monoxide, hydrogen, and oxygen on ordered tin/platinum(111) surface alloys. J Phys Chem 1990;94:6831–9.
37. Haner AN, Ross PN. Electrochemical oxidation of methanol on tin-modified platinum single-crystal surfaces. J Phys Chem 1991;95:3740–6.
38. Marković NM, Widelov A, Ross PN, Monteiro OR, Brown IG. Electrooxidation of CO and CO/H_2 mixtures on a Pt-Sn catalyst prepared by an implantation method. Catal Lett 1997;43:161–6.
39. Xiao X-Y, Tillmann S, Baltruschat H. Scanning tunneling microscopy of Sn coadsorbed with Cu and CO on Pt(111) electrodes. Phys Chem Chem Phys 2002;4:4044–50.
40. Stamenkovic VR, Arenz M, Lucas CA, Gallagher ME, Ross PN, Marković NM. Surface chemistry on bimetallic alloy surfaces: adsorption of anions and oxidation of CO on Pt_3Sn(111). J Am Chem Soc 2003;125:2736–45.
41. Hayden BE, Rendall ME, South O. Electro-oxidation of carbon monoxide on well-ordered Pt(111)/Sn surface alloys. J Am Chem Soc 2003;125:7738–42.
42. Arenz M, Stamenkovic V, Ross PN, Marković NM. Preferential oxidation of carbon monoxide adsorbed on Pd submonolayer films deposited on Pt(1 0 0). Electrochem Commun 2003;5:809–13.
43. Ralph TR, Hogarth MP. Catalysis for low temperature fuel cells, part II: the anode challenges. Platinum Metals Rev Vol No pp 2002;46(3):117–135.
44. Waszczuk P, Wieckowski A, Zelenay P, Gottesfeld S, Coutanceau C, Leger JM, et al. Adsorption of CO poison on fuel cell nanoparticle electrodes from methanol solutions: a radioactive labeling study. J Electroanal Chem 2001;511:55–64.
45. Lu GQ, White JO, Wieckowski A. Vibrational analysis of chemisorbed CO on the Pt(1 1 1)/Ru bimetallic electrode. Surf Sci 2004;564:131–40.
46. Lu GQ, Waszczuk P, Wieckowski A. Oxidation of CO adsorbed from CO saturated solutions on the Pt(111)/Ru electrode. J Electroanal Chem 2002;532:49–55.
47. Brankovic SR, Marinkovic NS, Wang JX, Adzic RR. Carbon monoxide oxidation on bare and Pt-modified Ru(1010) and Ru(0001) single crystal electrodes. J Electroanal Chem 2002;532:57–60.
48. Bellows RJ, Marucchi-Soos E, Reynolds RP. The mechanism of CO mitigation in proton exchange membrane fuel cells using dilute H_2O_2 in the anode humidifier. Electrochem Solid State Lett 1998;1:69–70.
49. Lindstrom RW, inventor; Protech Co., assignee. Electrocatalytic gas diffusion electrode employing thin carbon cloth layer. US Patent US4647359. 1987 Mar 3.

50. Yu H, Hou Z, Yi B, Lin Z. Composite anode for CO tolerance proton exchange membrane fuel cells. J Power Sources 2002;105:52–57.
51. Wan C-H, Zhuang Q-H. Novel layer wise anode structure with improved CO-tolerance capability for PEM fuel cell. Electrochim Acta 2007;52:4111–23.
52. Wilkinson DP, Voss HH, Prater KB, Hards GA, Ralph TR, Thompsett D, inventors; Johnson Matthey PLC, Ballard Power Systems, assignees. Electrode. US Patent US5795669. 1998 Aug 18.
53. Haug A, White RE, Weidner JW, Huang W, Shi S, Rana N, et al. Using sputter deposition to increase CO tolerance in a proton-exchange membrane fuel cell. J Electrochem Soc 2002;149:A868–72.
54. Wilkinson DP, Thompsett D. In: Proceedings of the second international symposium on new materials for fuel cell and modern battery systems. Savadogo O, Roberge PR, editors. Montreal, Canada: Les edition de l'Ecole Polytechnique de Montreal, 1997: 266.
55. McKee DW, Pak MS. Electrocatalysts for hydrogen/carbon monoxide fuel cell anodes. J Electrochem Soc 1969;116:516–20.
56. Ross PN, Kinoshita K, Scarpellino AJ, Stonehart P. Electrocatalysis on binary alloys: I. Oxidation of molecular hydrogen on supported Pt−Rh alloys. J Electroanal Chem 1975;59:177–89.
57. Hogarth M, Glipa X. High temperature membranes for solid polymer fuel cells. Report issued by Johnson Matthey Technology Centre to the ETSU on behalf of the Department of Trade and Industry as ETSU F/02/00189/REP; DTI/Pub URN 01/893; 2001.
58. Hogarth WHJ, Diniz da Costa JC, Lu GQ. Solid acid membranes for high temperature (at 140 °C) proton exchange membrane fuel cells. J Power Sources 2005;142:223–37.
59. Springer TE, Rockward T, Zawodzinski TA, Gottesfeld S. Model for polymer electrolyte fuel cell operation on reformate feed: effects of CO, H_2 dilution, and high fuel utilization. J Electrochem Soc 2001;148:A11–23.
60. Benicewicz BC. In: Advances in materials for PEM fuel cell systems. Polymer Division, American Chemical Society; Asilomar, California; 2003 February 23–27.
61. Kikuchi E. Membrane reactor application to hydrogen production. Catal Today 2000;56:97–101.
62. Thomason AH, Lalk TR, Appleby AJ. Effect of current pulsing and "self-oxidation" on the CO tolerance of a PEM fuel cell. J Power Sources 2004;135:204–11.
63. Zhang J, Datta R. Sustained potential oscillations in proton exchange membrane fuel cells with PtRu as anode catalyst. J Electrochem Soc 2002;149:1423–31.
64. Beden B, Bewick A, Kunimatsu K, Lamy C. Infrared study of adsorbed species on electrodes: adsorption of carbon monoxide on Pt, Rh and Au. J Electroanal Chem 1982;142:345–56.
65. Schmidt TJ, Jusys Z, Gasteiger HA, Behm RJ, Endruschat H, Boennemann U. On the CO tolerance of novel colloidal PdAu/carbon electrocatalysts. J Electroanal Chem 2001;501:132–40.
66. Bhatia KK, Wang C-Y. Transient carbon monoxide poisoning of a polymer electrolyte fuel cell operating on diluted hydrogen feed. Electrochim Acta 2004;49:2333–41.
67. Kabbabi A, Faure R, Durand R, Beden B, Hahn F, Leger JM, et al. In situ FTIRS study of the electrocatalytic oxidation of carbon monoxide and methanol at platinum–ruthenium bulk alloy electrodes. J Electroanal Chem 1998;444:41–53.
68. Ralph TR, Hogarth MP. Catalysis for low temperature fuel cells part I the cathode challenges. Platinum Met Rev 2002;46:3–14.
69. Ralph TR, Hogarth MP. Catalysis for low temperature fuel cells part III the challenges for the direct methanol fuel cell. Platinum Met Rev 2002;46:146.

70. Urian RC, Gulla AF, Mukerjee S. Electrocatalysis of reformate tolerance in proton exchange membranes fuel cells: Part I. J Electroanal Chem 2003;554–555:307–24.
71. Ruth K, Vogt M, Zuber R. Development of CO-tolerant catalysts. In: Vielstich W, Gasteiger HA, Lamm A, editors. Handbook of fuel cells – fundamentals, technology and applications, Vol 3. New York: John Wiley & Sons, 2003: 489–96.
72. Watkins DS. Research, development and demonstration of solid polymer fuel cell systems. In: Fuel cell systems. Blomen L, Mugerwa M, editors. New York: Plenum Press, 1993: 493–530.
73. Hirschenhofer JH, Stauffer DB, Engleman RR. Fuel cells: a handbook. 3rd rev. Reading: Gilbert/Commonwealth, Inc., 1994.
74. Bellows RJ, Marucchi-Soos EP, Buckley DT. Analysis of reaction kinetics for carbon monoxide and carbon dioxide on polycrystalline platinum relative to fuel cell operation. Ind Eng Chem Res 1996;35:1235–42.
75. Divisek J, Oetjen H-F, Peinecke V, Schmidt VM, Stimming U. Components for PEM fuel cell systems using hydrogen and CO containing fuels. Electrochim Acta 1998;43:3811–5.
76. Beden B, Bewick A, Lamy C. A study by electrochemically modulated infrared reflectance spectroscopy of the electrosorption of formic acid at a platinum electrode. J Electroanal Chem 1983;148:147–60.
77. Villegas I, Weaver MJ. Carbon monoxide adlayer structures on platinum (111) electrodes: A synergy between in-situ scanning tunneling microscopy and infrared spectroscopy. J Chem Phys 1994;101:1648–60.
78. Petukhov AV. Effect of molecular mobility on kinetics of an electrochemical Langmuir-Hinshelwood reaction. Chem Phys Lett 1997;277:539–44.
79. Petukhov AV, Akemann W, Friedrich KA, Stimming U. Kinetics of electrooxidation of a CO monolayer at the platinum/electrolyte interface. Surf Sci 1998;402–404:182–6.
80. Koper MTM, Jansen APJ, Santen RAv, Lukien JJ, Hilbers PAJ. Monte Carlo simulations of a simple model for the electrocatalytic CO oxidation on platinum. J Chem Phys 1998;109:6051–62.
81. Koper MTM, Jansen APJ, Lukkien J. Lattice–gas modeling of electrochemical Langmuir–Hinshelwood surface reactions. Electrochim Acta 1999;45:645–51.
82. Koper MTM, Lukien JJ, Jansen APJ, van Santen RA. Lattice gas model for CO electrooxidation on Pt-Ru bimetallic surfaces. J Phys Chem B 1999;103:5522–9.
83. Massong H, Tillmann S, Langkau T, Abd El Meguid EA, Baltruschat H. On the influence of tin and bismuth UPD on Pt(111) and Pt(332) on the oxidation of CO. Electrochim Acta 1998;44:1379–88.
84. Lebedeva NP, Koper MTM, Feliu JM, van Santen RA. Role of crystalline defects in electrocatalysis: mechanism and kinetics of CO adlayer oxidation on stepped platinum electrodes. J Phys Chem B 2002;106:12938–47.
85. Lebedeva NP, Koper MTM, Herrero E, Feliu JM, van Santen RA. Cooxidation on stepped Pt[n(111)×(111)] electrodes. J Electroanal Chem 2000;487:37–44.
86. Samjeské G, Xiao X-Y, Baltruschat H. Ru decoration of stepped Pt single crystals and the role of the terrace width on the electrocatalytic CO oxidation. Langmuir 2002;18:4659–66.
87. Watanabe M, Motoo S. Electrocatalysis by ad-atoms part II. Enhancement of the oxidation of methanol on platinum by ruthenium ad-atoms. J Electroanal Chem 1975;60:267–73.
88. Ralph TR, Hards GA. Powering the cars and homes for tomorrow. Chem Ind (London) 1998;9:337–42.

89. Watanabe M, Motoo S. Electrocatalysis by ad-atoms: part III. Enhancement of the oxidation of carbon monoxide on platinum by ruthenium ad-atoms. J Electroanal Chem 1975;60:275–83.
90. Liu P, Norskov JK. Kinetics of the anode processes in PEM fuel cells - the promoting effect of Ru in PtRu anodes. Fuel Cells 2001;1:192–201.
91. Parsons R, Vandernoot T. The oxidation of small organic molecules: A survey of recent fuel cell related research. J Electroanal Chem 1988;257:9–45.
92. Hamnett A. Mechanism of methanol electro-oxidation. In: A.Wieckowski, editor. Interfacial electrochemistry: theory, experiment, and applications. New York: Marcel Dekker, 1999: 843–83.
93. Samjeské G, Wang H, Löffler T, Baltruschat H. CO and methanol oxidation at Pt-electrodes modified by Mo. Electrochim Acta 2002;47:3681–92.
94. Berenz P, Tillmann S, Massong H, Baltruschat H. Decoration of steps at Pt single crystal electrodes and its electrocatalytic effect. Electrochim Acta 1998;43:3035–43.
95. de Becdelievre AM, de Becdelievre J, Clavilier J. Electrochemical oxidation of adsorbed carbon monoxide on platinum spherical single crystals. Effect of anion adsorption. J Electroanal Chem 1990;294:97–110.
96. Baschuk J, Li X. Carbon monoxide poisoning of proton exchange membrane fuel cells. Int J Energy Res 2001;25:695–713.
97. Dhar HP, Christner LG, Kush AK. Nature of CO adsorption during H_2 oxidation in relation to modeling for CO poisoning of a fuel cell anode. J Electrochem Soc 1987;134:3021–6.
98. Gilman S. The mechanism of electrochemical oxidation of carbon monoxide and methanol on platinum II: the “reactant pair” mechanism for electrochemical oxidation of carbon monoxide and methanol. J Phys Chem 1964;68:70–80.
99. Stonehart P, Ross P. The commonality of surface processes in electrocatalysis and gas-phase heterogeneous catalysis. Cat Rev – Sci Eng 1975;12:1–35.
100. Vogel W, Lundquist J, Ross P, Stonehart P. Reaction pathways and poisons-II. The rate controlling step for electrochemical oxidation of hydrogen on Pt in acid and poisoning of the reaction by CO. Electrochim Acta 1975;20:79–93.
101. Wilson M, Derouin C, Valerio J, Gottesfeld S. Electrocatalysis issues in polymer electrolyte fuel cells. Proceedings of the Intersociety Energy Conversion Engineering Conference 1993;1:1203–8.
102. Oetjen H-F, Schmidt VM, Stimming U, Trila F. Performance data of a proton exchange membrane fuel cell using H_2/CO as fuel gas. J Electrochem Soc 1996;143:3838–42.
103. Iwase M, Kawatsu S. Optimized CO tolerant electrocatalysts for polymer electrolyte fuel cells. In: Proton conducting membrane fuel cells I. Gottesfeld S, Halpert G, Landgrebe A, editors. Electrochemical Society Proceedings 1995;95–23:12–23.
104. Schmidt VM, Ianneillo R, Oetjen H-F, Reger H, Stimming U, Trila F. 1995. Oxidation of H_2/CO in a proton exchange membrane fuel cell. In: Proton conducting membrane fuel cells I. Gottesfeld S, Halpert G, Landgrebe A, editors. Electrochemical Society Proceedings 1995;95–23:1–11.
105. Zawodzinski TA, Karuppaiah C, Uribe F, Gottesfeld S. Aspects of CO tolerance in polymer electrolyte fuel cells: some experimental findings. In: Electrode materials and processes for energy conversion and storage I. Srinivasan S, McBreen J, Khandkar AC, Tilak VC, editors. Proceedings of the Electrochemical Society 1997;97(13):139–146.
106. Lu C, Rice C, Masel RI, Babu PK, Waszczuk P, Kim HS, et al. UHV, electrochemical NMR, and electrochemical studies of platinum/ruthenium fuel cell catalysts. J Phys Chem B 2002;106:9581–9.

107. Lu C, Masel RI. The effect of ruthenium on the binding of CO, H_2, and H_2O on Pt(110). J Phys Chem B 2001;105:9793–7.
108. Yajima T, Uchida H, Watanabe M. In-situ ATR-FTIR spectroscopic study of electro-oxidation of methanol and adsorbed CO at Pt-Ru alloy. J Phys Chem B 2004;108:2654–9.
109. Brankovic SR, Wang JX, Adžić RR. Pt submonolayers on Ru nanoparticles: a novel low Pt loading, high CO tolerance fuel cell electrocatalyst. Electrochem Solid-State Lett 2001;4:A217–20.
110. Gasteiger HA, Markovic NM, Ross PN. H_2 and CO electrooxidation on well-characterized Pt, Ru, and Pt-Ru. 2. Rotating disk electrode studies of CO/H_2 mixtures at 62 degree C. J Phys Chem 1995;99:16757–67.
111. Gasteiger HA, Markovic NM, Ross PN. H_2 and CO electrooxidation on well-characterized Pt, Ru, and Pt-Ru. 1. Rotating disk electrode studies of the pure gases including temperature effects. J Phys Chem 1995;99:8290–301.
112. Friedrich KA, Geyzers KP, Linke U, Stimming U, Stumper J. CO adsorption and oxidation on a Pt(111) electrode modified by ruthenium deposition: an IR spectroscopic study. J Electroanal Chem 1996;402:123–8.
113. Zawodzinski TA, Springer TE, Gottesfeld S. The 1997 joint international meeting of ECS and ISE. ECS Meeting Abstracts 1997;97–2:1228.
114. Kua J, Goddard WA III. Oxidation of methanol on 2nd and 3rd row group VIII transition metals (Pt, Ir, Os, Pd, Rh, and Ru): application to direct methanol fuel cells. J Am Chem Soc 1999;121:10928–41.
115. Denis MC, Gouerec P, Guay D, Dodelet JP, Lalande G, Schulz R. Improvement of the high energy Ball-Milling preparation procedure of CO tolerant Pt and Ru containing catalysts for polymer electrolyte fuel cells. J Appl Electrochem 2000;30:1243–53.
116. Tong YY, Kim HS, Babu PK, Waszczuk P, Wieckowski A, Oldfield E. An NMR investigation of CO tolerance in a Pt/Ru fuel cell catalyst. J Am Chem Soc 2002;124:468–473.
117. Lamouri A, Gofer Y, Luo Y, Chottiner GS, Scherson DA. Low energy electron diffraction, X-ray photoelectron spectroscopy, and CO-temperature-programmed desorption characterization of bimetallic ruthenium–platinum surfaces prepared by chemical vapor deposition. J Phys Chem B 2001;105:6172–7.
118. Camara GA, Giz MJ, Paganin VA, Ticianelli EA. Correlation of electrochemical and physical properties of PtRu alloy electrocatalysts for PEM fuel cells. J Electroanal Chem 2002;537:21–9.
119. Lin WF, Zei MS, Eiswirth M, Ertl G, Iwasita T, Vielstich W. Electrocatalytic activity of Ru-modified Pt(111) electrodes toward CO oxidation. J Phys Chem B 1999;103:6968–77.
120. Qi Z, Kaufman A. CO-tolerance of low-loaded Pt/Ru anodes for PEM fuel cells. J Power Sources 2003;113:115–23.
121. Viswanathan R, Hou G, Liu R, Bare SR, Modica F, Mickelson G, et al. In-situ XANES of carbon-supported Pt-Ru anode electrocatalyst for reformate-air polymer electrolyte fuel cells. J Phys Chem B 2002;106:3458–65.
122. Koper MTM, Lebedeva NP, Hermse CGM. Dynamics of CO at the solid/liquid interface studied by modeling and simulation of CO electro-oxidation on Pt and PtRu electrodes. Faraday Discuss 2002;121:301–11.
123. Koper MTM, Shubina TE, van Santen RA. Periodic density functional study of CO and OH adsorption on Pt-Ru alloy surfaces: Implications for CO tolerant fuel cell catalysts. J Phys Chem B 2002;106:686–92.
124. Lebedeva NP, Koper MTM, Feliu JM, van Santen RA. Mechanism and kinetics of the electrochemical CO adlayer oxidation on Pt(111). J Electroanal Chem 2002;524–525:242–51.

125. Camara GA, Ticianelli EA, Mukerjee S, Lee SJ, McBreen J. The CO poisoning mechanism of the hydrogen oxidation reaction in proton exchange membrane fuel cells. J Electrochem Soc 2002;149:A748–53.
126. Mukerjee S, Urian RC. Bifunctionality in Pt alloy nanocluster electrocatalysts for enhanced methanol oxidation and CO tolerance in PEM fuel cells: electrochemical and in situ synchrotron spectroscopy. Electrochim Acta 2002;47:3219–31.
127. Mukerjee S, Urian RC, Lee SJ, Ticianelli EA, McBreen J. Electrocatalusis of CO tolerance by carbon-supported PtMo electrocatalysts in PEMFCs. J Electrochem Soc 2004;151:A1094–103.
128. Russell AE, Maniguet S, Mathew RJ, Yao J, Roberts MA, Thompsett D. In situ X-ray absorption spectroscopy and X-ray diffraction of fuel cell electrocatalysts. J Power Sources 2001;96:226–32.
129. Goetz M, Wendt H. Composite electrocatalysts for anodic methanol and methanol-reformate oxidation. J Appl Electrochem 2001;31:811–7.
130. Skelton DC, Tobin RG, Lambert DK, DiMaggio CL, Fisher GB. Oxidation of CO on gold-covered Pt(335). J Phys Chem B 1999;103:964–71.
131. Hammer B, Norskov JK. Electronic factors determining the reactivity of metal surfaces. Surf Sci 1995;343:211–20.
132. Liu P, Logadottir A, Norskov JK. Modeling the electro-oxidation of CO and H_2/CO on Pt, Ru, PtRu and Pt_3Sn. Electrochim Acta 2003;48:3731–42.
133. Krausa M, Vielstich W. Study of the electrocatalytic influence of Pt/Ru and Ru on the oxidation of residues of small organic molecules. J Electroanal Chem 1994;379:307–14.
134. Frelink T, Visscher W, Vanveen JAR. On the role of Ru and Sn as promotors of methanol electro-oxidation over Pt. Surf Sci 1995;335:353–60.
135. Buatier de Mongeot F, Scherer M, Gleich B, Kopatzki E, Behm RJ. CO adsorption and oxidation on bimetallic Pt/Ru(0001) surfaces – a combined STM and TPD/TPR study. Surf Sci 1998;411:249–62.
136. Watanabe M, Zhu YM, Igarashi H, Uchida H. Mechanism of CO tolerance at Pt-Alloy anode catalysts for polymer electrolyte fuel cells. Electrochemistry 2000;68:244–51.
137. Roth C, Benker N, Buhrmester T, Mazurek M, Loster M, Fuess H, et al. Determination of O[H] and CO coverage and adsorption sites on PtRu electrodes in an operating PEM fuel cell. J Am Chem Soc 2005;127:14607–15.
138. El-Shafei AA, Hoyer R, Kibler LA, Kolb DM. Methanol oxidation on Ru-modified preferentially oriented Pt electrodes in acidic medium. J Electrochem Soc 2004;151:F141–5.
139. Davies JC, Hayden BE, Pegg DJ. The modification of Pt(110) by ruthenium: CO adsorption and electro-oxidation. Surf Sci 2000;467:118–30.
140. Frelink T, Visscher W, Cox AP, Vanveen JAR. Ellipsometry and dems study of the electrooxidation of methanol at Pt and Rupromoted and Sn-promoted Pt. Electrochim Acta 1995;40:1537–43.
141. Roth C, Benker N, Buhrmester T, Mazurek M, Loster M, Fuess H, et al. Determination of O[H] and CO coverage and adsorption sites on PtRu electrodes in an operating PEM fuel cell. J Am Chem Soc 2005;127:14607–15.
142. Waszczuk P, Lu GQ, Wieckowski A, Lu C, Rice C, Masel RI. UHV and electrochemical studies of CO and methanol adsorbed at platinum/ruthenium surfaces, and reference to fuel cell catalysis. Electrochim Acta 2002;47:3637–52.
143. Iwasita T. Progress in the study of methanol oxidation by in situ, ex situ and on-line methods. In: Advances in electrochemical science and engineering. Gerischer H, Tobias Ch, editors. Verlag Chemie 1990;1:127–70.
144. Wolter O, Giordano C, Heitbaum J, Vielstich W. Proceedings of the symposium on electrocatalysis. Pennington, NJ: The Electrochemical Society, 1982: 235.

145. Bittins-Cattaneo B, Cattaneo E, Königshoven P, Vielstich W. New developments in electrochemical mass spectroscopy. In: Electroanalytical chemistry: a series of advances. Bard AJ, editor. New York: Marcel Dekker, New York: vol 17, ch 3, 181–220.
146. Iwasita T, Nart FC. In situ infrared spectroscopy at electrochemical interfaces. Prog Surf Sci 1997;55:271–340.
147. Clavilier J, Armand D, Sun SG, Petit M. Electrochemical adsorption behaviour of platinum stepped surfaces in sulphuric acid solutions. J Electroanal Chem 1986;205:267–77.
148. Ocko BM, Wang J, Davenport A, Isaacs H. In situ x-ray reflectivity and diffraction studies of the Au(001) reconstruction in an electrochemical cell. Phys Rev Lett 1990;65:1466–9.
149. Faguy PW, Markovic N, Adzic RR, Fierro CA, Yeager EB. A study of bisulfate adsorption on Pt(111) single crystal electrodes using in situ Fourier transform infrared spectroscopy. J Electroanal Chem 1990;289:245–62.
150. Tidswell IM, Markovic NM, Ross PN. Potential dependent surface relaxation of the Pt(001)/electrolyte interface. Phys Rev Lett 1993;71:1601–4.
151. Sawatari Y, Inukai J, Ito M. The structure of bisulfate and perchlorate on a Pt(111) electrode surface studied by infrared spectroscopy and ab-initio molecular orbital calculation. J Electron Spec 1993;64/65:515–22.
152. Nart FC, Iwasita T, Weber M. Vibrational spectroscopy of adsorbed sulfate on Pt(111). Electrochim Acta 1994;39:961–8.
153. Lucas C, Markovic NM, Ross PN. Observation of an ordered bromide monolayer at the Pt(111)-solution interface by in-situ surface X-ray scattering. Surf Sci 1995;340:L949–54.
154. Kolb DM. Reconstruction phenomena at metal-electrolyte interfaces. Prog Surf Sci 1996;51:109–73.
155. Itaya K. In situ scanning tunneling microscopy in electrolyte solutions. Prog Surf Sci 1998;58:121–247.
156. Hughes VB, Miles R. cyclic voltammetric investigation of adsorbed residues derived from methanol on platinum-based electrocatalysts. J Electroanal Chem 1983;145:87–107.
157. Ticanelli E, Beery JG, Paffett MT, Gottesfeld S. An electrochemical, ellipsometric, and surface science investigation of the PtRu bulk alloy surface. J Electroanal Chem 1989;258:61–77.
158. Richardz E, Wohlmann B, Vogel U, Hoffschulz H, Wandelt K. Surface and electrochemical characterization of electrodeposited PtRu alloys. Surf Sci 1995;335:361–71.
159. Markovic NM, Ross PN Jr. Surface science studies of model fuel cell electrocatalysts. Surf Sci Rep 2002;45:117–229.
160. Watanabe M, Zhu Y, Uchida H. Oxidation of CO on a Pt-Fe alloy electrode studied by surface enhanced infrared reflection-absorption spectroscopy. J Phys Chem B 2000;104:1762–8.
161. Miki A, Ye S, Osawa M. Surface-enhanced IR absorption on platinum nanoparticles: an application to real-time monitoring of electrocatalytic reactions. Chem Commun 2002;1500–1.
162. Futamata M, Luo L, Nishihara C. ATR–SEIR study of anions and water adsorbed on platinum electrode. Surf Sci 2005;590:196–211.
163. Chen YX, Miki A, Ye S, Sakai H, Osawa M. Formate, an active intermediate for direct oxidation of methanol on Pt electrode. J Am Chem Soc 2003;125:3680–1.

164. Friedrich KA, Geyzers KP, Dickson AJ, Stimming U. Fundamental aspects in electrocatalysis: from the reactivity of single-crystals to fuel cell electrocatalysts. J Electroanal Chem 2002;524–525:261–72.
165. Cramm S, Friedrich KA, Geyzers K-P, Stimming U, Vogel R. Surface structural and chemical characterization of Pt/Ru composite electrodes: a combined study by XPS, STM and IR spectroscopy. Fres J Anal Chem 1997;358:189–92.
166. Futamata M, Luo L. Adsorbed water and CO on Pt electrode modified with Ru. J Power Sources 2007;164:532–7.
167. García G, Silva-Chong JA, Guillén-Villafuerte O, Rodríguez JL, González ER, Pastor E. CO tolerant catalysts for PEM fuel cells: spectroelectrochemical studies. Catal Today 2006;116:415–21.
168. Vericat C, Wakisaka M, Haasch R, Bagus PS, Wieckowski A. Binding energy of ruthenium submonolayers deposited on a Pt(111) electrode. J Solid State Electrochem 2004;8:794–803.
169. Igarashi H, Fujino T, Zhu Y, Uchida H, Watanabe M. CO tolerance of Pt alloy electrocatalysts for polymer electrolyte fuel cells and the detoxification mechanism. Phys Chem Chem Phys 2001;3:306–14.
170. Tillmann S, Samjeské G, Friedrich KA, Baltruschat H. The adsorption of Sn on Pt(1 1 1) and its influence on CO adsorption as studied by XPS and FTIR. Electrochim Acta 2003;49:73–83.
171. Frances J, Scott E, Mukerjee S, Ramaker DE. CO coverage/oxidation correlated with PtRu electrocatalyst particle morphology in 0.3 M Methanol by in situ XAS. J Electrochem Soc 2007;154:A396–406.
172. Stamenković V, Arenz M, Blizanac BB, Mayrhofer KJJ, Ross PN, Marković NM. In situ CO oxidation on well characterized Pt_3Sn(hkl) surfaces: A selective review. Surf Sci 2005;576:145–57.
173. Tong YY, Wieckowski A, Oldfield E. NMR of electrocatalysts. J Phys Chem B 2002;106:2434–46.
174. Babu PK, Oldfield E, Wieckowski A. Nanoparticle surfaces studied by electrochemical NMR. In: Modern aspects of electrochemistry, vol. 36. Vayenas C, Conway BE, White RE, editors. New York: Kluwer Academic/Plenum Publishers, 2003: 1–50.
175. Rudaz SL, Ansermet J-P, Wang P-K, Slichter CP. NMR study of chemosorption bond of carbon monoxide on platinum. Phys Rev Lett 1985;54:71.
176. Yahnke MS, Rush BM, Reimer JA, Cairns EJ. Quantitative solidstate NMR spectra of CO adsorbed from aqueous solution onto a commercial electrode. J Am Chem Soc 1996;118:12250–1.
177. Babu PK, Kim HS, Chung J-H, Oldfield E, Wieckowski A. Bonding and motional aspects of CO adsorbed on the surface of Pt nanoparticles decorated with Pd. J Phys Chem B 2004;108:20228–32.
178. Iwasita T, Hoster H, John-Anacker A, Lin WF, Vielstich W. Methanol oxidation on PtRu electrodes. Influence of surface structure and Pt-Ru atom distribution. Langmuir 2000;16:522–9.
179. Slichter CP. Principles of magnetic resonance. 3rd ed. Berlin: Springer-Verlag, 1992.
180. Davies JC, Hayden BE, Pegg DJ. The electrooxidation of carbon monoxide on ruthenium modified Pt(110). Electrochim Acta 1998;44:1181–90.
181. Blyholder G. Molecular orbital view of chemisorbed carbon monoxide. J Phys Chem 1964;68:2772–7.
182. Hammer B, Morikawa Y, Norskov JK. CO chemisorption at metal surfaces and overlayers. Phys Rev Lett 1996;76:2141–4.
183. Schlapka A, Lischka M, Gross A, Kasberger U, Jakob P. Surface strain versus substrate interaction in heteroepitaxial metal layers: Pt on Ru(0001). Phys Rev Lett 2003;91:016101.

184. Shubina TE, Koper MTM. Quantum-chemical calculations of CO and OH interacting with bimetallic surfaces. Electrochim Acta 2002;47:3621–36216.
185. Diemant T, Hager T, Hoster HE, Rauscher H, Behm RJ. Hydrogen adsorption and coadsorption with CO on well-defined bimetallic PtRu surfaces—a model study on the CO tolerance of bimetallic PtRu anode catalysts in low temperature polymer electrolyte fuel cells. Surf Sci 2003;541:137–46.
186. Leng YJ, Wang X, Hsing IM. Assessment of CO-tolerance for different Pt-alloy anode catalysts in a polymer electrolyte fuel cell using ac impedance spectroscopy. J Electroanal Chem 2002;528:145–52.
187. Wang X, Hsing IM, Leng Y-J, Yue PL. Model interpretation of electrochemical impedance spectroscopy and polarization behavior of H_2/CO mixture oxidation in polymer electrolyte fuel cells. Electrochim Acta 2001;46:4397–405.
188. Wang X, Hsing IM. Kinetics investigation of H_2/CO electro-oxidation on carbon supported Pt and its alloys using impedance based models. J Electroanal Chem 2003;556:117–26.
189. Koper MTM, Lukkien JJ. Modeling the butterfly: influence of lateral interactions and adsorption geometry on the voltammetry at (1 1 1) and (1 0 0) electrodes. Surf Sci 2002;498:105–15.
190. Ge Q, Desai S, Neurock M, Kourtakis K. CO adsorption on Pt-Ru surface alloys and on the surface of Pt-Ru bulk alloy. J Phys Chem B 2001;105:9533–6.
191. Liao M-S, Cabrera CR, Ishikawa Y. A theoretical study of CO adsorption on Pt, Ru and Pt–M (M=Ru, Sn, Ge) clusters. Surf Sci 2000;445:267–82.
192. Ishikawa Y, Cabrera CR, Liao M-S. Oxidation of methanol on platinum, ruthenium and mixed Pt–M metals (M=Ru, Sn): a theoretical study. Surf Sci 2000;463:66–80.
193. Igarashi H, Fujino T, Watanabe M. Hydrogen electro-oxidation on platinum catalysts in the presence of trace carbon monoxide. J Electroanal Chem 1995;391:119–23.
194. Markovic NM, Lucas CA, Grgur BN, Ross PN. Surface electrochemistry of CO and H_2/CO mixtures at Pt(100) interface: Electrode kinetics and interfacial structures. J Phys Chem B 1999;103:9616–23.
195. Jusys Z, Kaiser J, Behm RJ. Electrooxidation of CO and H_2/CO mixtures on a carbon-supported Pt catalyst—a kinetic and mechanistic study by differential electrochemical mass spectrometry. Phys Chem Chem Phys 2001;3:4650–60.
196. Gűlmen MA, Sűmer A, Aksoylu AE. Adsorption properties of CO on low-index Pt_3Sn surfaces. Surf Sci 2006;600:4909–21.
197. Napporn WT, Leger J-M, Lamy C. Electrocatalytic oxidation of carbon monoxide at lower potentials on platinum-based alloys incorporated in polyaniline. J Electroanal Chem 1996;408:141–7.
198. Ley KL, Liu R, Pu C, Fan Q, Leyarovska N, Segree C, et al. Methanol oxidation on single-phase Pt-Ru-Os ternary alloys. J Electrochem Soc 1997;144:1543–8.
199. Chen KY, Shen PK, Tseung ACC. Anodic oxidation of impure H_2 on Teflon-bonded Pt-Ru/WO_3/C electrodes. J Electrochem Soc 1995;142:L185–6.
200. Mukerjee S, Srinivasan S. Enhanced electrocatalysis of oxygen reduction on platinum alloys in proton exchange membrane fuel cells. J Electroanal Chem 1993;357:201–24.
201. Mukerjee S, Srinivasan S, Soriaga MP, McBreen J. Role of structural and electronic properties of Pt and Pt alloys on electrocatalysis of oxygen reduction. J Electrochem Soc 1995;142:1409–22.
202. Gasteiger HA, Markovic NM, Ross PN. Structural effects in electrocatalysis: electrooxidation of carbon monoxide on Pt_3Sn single-crystal alloy surfaces. Catal Lett 1996;36:1–8.
203. Stalnionis G, Tamasauskaite-Tamasiunaite L, Pautieniene A, Sudavicius VA, Jusys Z. Modification of a Pt surface by spontaneous Sn deposition for electrocatalytic applications. J Solid State Electrochem 2004;8:892.

204. Mukerjee S, Lee SJ, Ticianelli EA, McBreen J, Grgur BN, Markovic NM, et al. Investigation of enhanced CO tolerance in proton exchange membrane fuel cells by carbon supported PtMo alloy catalyst. Electrochem Solid State Lett 1999;2:12–5.
205. Crabb EM, Ravikumar MK. Synthesis and characterisation of carbon-supported PtGe electrocatalysts for CO oxidation. Electrochim Acta 2001;46:1033–41.
206. Aberdam D, Durand R, Faure R, Gloaguen F, Hazemann JL, Herrero E, et al. X-ray absorption near edge structure study of the electro-oxidation reaction of CO on $Pt_{50}Ru_{50}$ nanoparticles. J Electroanal Chem 1995;398:43–7.
207. Gasteiger HA, Markovic N, Ross PN, Cairns EJ. Methanol electrooxidation on well-characterized platinum-ruthenium bulk alloys. J Phys Chem 1993;97:12020–9.
208. Gasteiger HA, Markovic N, Ross PN, Cairns EJ. Electro-oxidation of small organic molecules on well-characterized Pt-Ru alloys. Electrochim Acta 1994;39:1825–32.
209. Watanabe M, Uchida M, Motoo S. Preparation of highly dispersed Pt + Ru alloy clusters and the activity for the electrooxidation of methanol. J Electroanal Chem 1987;229:395–406.
210. Papageorgopoulos DC, Keijzer M, de Bruijn FA. The inclusion of Mo, Nb and Ta in Pt and PtRu carbon supported electrocatalysts in the quest for improved CO tolerant PEMFC anodes. Electrochim Acta 2002;48:197–204.
211. Gasteiger HA, Kocha SS, Sompalli B, Wagner FT. Activity benchmarks and requirements for Pt, Pt-alloy, and non-Pt oxygen reduction catalysts for PEMFCs. Appl Catal B Environ 2005;56:9–35.
212. Wiese W, Emonts B, Peters R. Methanol steam reforming in a fuel cell drive system. J Power Sources 1999;84:187–93.
213. Vielstich W, Lamm A, Gasteiger H, editors. Handbook of fuel cells, vol. 3, part 3. West Sussex, UK: Wiley, 2003: 349–464.
214. Tremiliosi G, Kim H, Chrzanowski W, Wieckowski A, Grzybowska B, Kulesza P. Reactivity and activation parameters in methanol oxidation on platinum single crystal electrodes 'decorated' by ruthenium adlayers. J Electroanal Chem 1999;467:143–56.
215. Chrzanowski W, Wieckowski A. Ultrathin films of ruthenium on low index platinum single crystal surfaces: an electrochemical study. Langmuir 1997;13:5974–59716.
216. Chrzanowski W, Wieckowski A. Surface structure effects in platinum/ruthenium methanol oxidation electrocatalysis. Langmuir 1998;14:1967–70.
217. Waszczuk P, Solla-Gullon J, Kim HS, Tong YY, Montiel V, Aldaz A, et al. Methanol electrooxidation on platinum/ruthenium nanoparticle catalysts. J Catal 2001;203:1–6.
218. Maillard F, Lu G-Q, Wieckowski A, Stimming U. Ru-decorated Pt surfaces as model fuel cell electrocatalysts for CO electrooxidation. J Phys Chem B 2005;109:16230–43.
219. Maillard F, Gloaguen F, Hahn F, Léger J-M. Electrooxidation of carbon monoxide at ruthenium-modified platinum nano-particles: evidence for CO surface mobility. Fuel Cells 2002;2:143–52.
220. Maillard F, Gloaguen F, Léger JM. Preparation of methanol oxidation electrocatalysts: ruthenium deposition on carbon-supported platinum nanoparticles. J Appl Electrochem 2003;33:1–8.
221. Dubau L, Hahn F, Coutanceau C, Léger JM, Lamy C. On the structure effects of bimetallic PtRu electrocatalysts towards methanol oxidation. J Electroanal Chem 2003;554:407–15.
222. Dubau L, Coutanceau C, Garnier E, Léger JM, Lamy C. Electrooxidation of methanol at platinum–ruthenium catalysts prepared from colloidal precursors: atomic composition and temperature effects. J Appl Electrochem 2003;33:419–29.
223. Holleck GL, Pasquariello DM, Clauson SL. Carbon monoxide tolerant anodes for proton exchange membrane (PEM) fuel cells. II. Alloy catalyst development In: proceedings of the 2nd international symposium on proton conducting membrane fuel cells 1998;2:150.

224. Lima A, Coutanceau C, Léger JM, Lamy C. Investigation of ternary catalysts for methanol electrooxidation. J Appl Electrochem 2001;31:379–86.
225. Götz M, Wendt H. Binary and ternary anode catalyst formulations including the elements W, Sn and Mo for PEMFCs operated on methanol or reformate gas. Electrochim Acta 1998;43:3637–44.
226. Aricò AS, Cretì P, Giordano N, Antonucci V. Chemical and morphological characterization of a direct methanol fuel cell based on a quaternary Pt-Ru-Sn-W/C anode. J Appl Electrochem 1996;26:959–67.
227. Liu R, Iddir H, Fan Q, Hou G, Bo A, Ley KL, et al. Potential-dependent infrared absorption spectroscopy of adsorbed CO and X-ray photoelectron spectroscopy of arc-melted single-phase Pt, PtRu, PtOs, PtRuOs, and Ru electrodes. J Phys Chem B 2000;104:3518–31.
228. Watanabe M, Igarashi H, Fujino T. Design of CO tolerant anode catalysts for polymer electrolyte fuel cell. Electrochemistry 1999;67:1194–6.
229. Uribe FA, Valerio JA, Garzon FH, Zawodzinski TA. PEMFC reconfigured anodes for enhancing CO tolerance with air bleed. Electrochem Solid-State Lett 2004;-7:A376–9.
230. Ishikawa Y, Liao MS, Cabrera CR. Energetics of H_2O dissociation and CO_{ads}+OH_{ads} reaction on a series of Pt–M mixed metal clusters: a relativistic density-functional study. Surf Sci 2002;513:98–110.
231. Dinh HN, Ren X, Garzon FH, Zelenay P, Gottesfeld S. Electrocatalysis in direct methanol fuel cells: in-situ probing of PtRu anode catalyst surfaces. J Electroanal Chem 2000;491:222–33.
232. Janssen MMP, Moolhuysen J. Binary systems of platinum and a second metal as oxidation catalysts for methanol fuel cells. Electrochim Acta 1976;21:869–716.
233. Liu R, Ley KL, Pu C, Fan Q, Leyarovska N, Segre C, et al. In: Electrode processes, VI. Wieckowski A, Itaya K, editors. Electrochemical Society Proceedings Series 1996;96–8:341–55.
234. Gottesfeld S, Zawodzinski TA. Polymer electrolyte fuel cells. In: Advances in electrochemical science and engineering. Alkire RC, Gerischer H, Kolb DM, Tobias CW, editors. New York: Wiley-VCH, 1997: vol 5, ch 4, 195–301.
235. Stevens DA, Rouleau JM, Mar RE, Bonakdarpour A, Atanasoski RT, Schmoeckel AK, et al. Characterization and PEMFC testing of $Pt_{1-x}M_x$ (M = Ru,Mo,Co,Ta,Au,Sn) anode electrocatalyst composition spreads. J Electrochem Soc 2007;154:B566–76.
236. Attwood PA, McNicol BD, Short RT. The electrocatalytic oxidation of methanol in acid electrolyte: preparation and characterization of noble metal electrocatalysts supported on pre-treated carbon-fibre papers. J Appl Electrochem 1980;10:213–22.
237. Frelink T, Visscher W, van Veen JAR. Particle size effect of carbon-supported platinum catalysts for the electrooxidation of methanol. J Electroanal Chem 1995;382:65–72.
238. Kabbabi A, Gloagen F, Andolfatto F, Durand R. Particle size effect for oxygen reduction and methanol oxidation on Pt/C inside a proton exchange membrane. J Electroanal Chem 1994;373:251–4.
239. Mukerjee S, McBreen J. Effect of particle size on the electrocatalysis by carbon-supported Pt electrocatalysts: an in situ XAS investigation. J Electroanal Chem 1998;448:163–71.
240. Knights SD, Colbow KM, St-Pierre J, Wilkinson DP. Aging mechanisms and lifetime of PEFC and DMFC. J Power Sources 2002;127:127–34.
241. Pozio A, Silva RF, De Francesco M, Cardellini F, Giorgi L. Erratum to “A novel route to prepare stable Pt–Ru/C electrocatalysts for polymer electrolyte fuel cell”: [Electrochim Acta 48 (3): 255–262]. Electrochim Acta 2003;48:1625.

242. Chen W, Sun G, Liang Z, Mao Q, Li H, Wang G, et al. The stability of a PtRu/C electrocatalyst at anode potentials in a direct methanol fuel cell. J Power Sources 2006;160:933–9.
243. Gancs L, Hakim N, Hult B, Mukerjee S. Dissolution of Ru from PtRu electrocatalysts and its consequences in DMFCs. ECS Trans 2006;3(1):607–18.
244. Gancs L, Hult BN, Hakim N, Mukerjee S. The impact of Ru contamination of a Pt/C electrocatalyst on its oxygen-reducing activity. Electrochem Solid-State Lett 2007;10:B150–4.
245. Piela P, Eickes C, Brosha E, Garzon F, Zelenay P. Ruthenium crossover in direct methanol fuel cell with Pt-Ru black anode. J Electrochem Soc 2004;151:A2053–9.
246. Shi M, Anson FC. Mobilities and concentration profiles of counterion catalysts incorporated in Nafion coatings on electrodes. Electrochim Acta 1998;44:1301–5.
247. Okada T. Effect of ionic contaminants. In: Handbook of fuel cells: fundamentals, technology, applications. Vol 3. Vielstich W, Gasteiger HA, Lamm A, editors. New York: John Wiley & Sons, 2003: 627.
248. LaConti AB, Hamdan M, McDonald RC. Mechanism of membrane degradation. In: Handbook of fuel cells: fundamentals, technology, applications. Vol 3. Vielstich W, Gasteiger HA, Lamm A, editors. New York: John Wiley & Sons, 2003: 647.
249. Zelenay P. In: Fuel cells durability: stationary, automotive, portable. 1st ed. Brookline, MA: Knowledge Press, 2006: 61.
250. Stamenkovic V, Grgur BN, Ross PN, Markovic NM. Oxygen reduction reaction on Pt and Pt-bimetallic electrodes covered by CO. J Electrochem Soc 2005;152:A277–82.
251. Cao D, Wieckowski A, Inukai J, Alonso-Vante N. Oxygen reduction reaction on ruthenium and rhodium nanoparticles modified with selenium and sulfur. J Electrochem Soc 2006;153:A869–74.
252. Choban ER, Spendelow JS, Gancs L, Wieckowski A, Kenis PJA. Membraneless laminar flow-based micro fuel cells operating in alkaline, acidic, and acidic/alkaline media. Electrochim Acta 2005;50:5390–8.
253. Ranga JS, Gancs L, Choban ER, Primak A, Natarajan D, Markoski LJ, et al. Air-breathing laminar flow-based microfluidic fuel cell. J Am Chem Soc 2005;127:16758–9.
254. Ghenciu AF. Review of fuel processing catalysts for hydrogen production in PEM fuel cell systems. Curr Opin Solid State Mater Sci 2002;6:389–99.
255. Mehta V, Cooper JS. Review and analysis of PEM fuel cell design and manufacturing. J Power Sources 2003;114:32–53.
256. Costamagna P, Srinivasan S. Quantum jumps in the PEMFC science and technology from the 1960s to the year 2000; Part II. Engineering, technology development and application aspects. J Power Sources 2001;102:253–69.
257. Schaller KV, Gruber C. Fuel cell drive and high dynamic energy storage systems–opportunities for the future city bus. Fuel Cells Bull 2000;3:9–13.
258. Grgur BN, Markovic NM, Ross PN. Electrochemical oxidation of carbon monoxide: from platinum single crystals to low temperature fuel cells catalysts. Part II. Electrooxidation of H_2, CO and H_2/CO mixtures on well characterized PtMo alloy. J Serb Chem Soc 2003;68:191–206.
259. Gouérec P, Denis MC, Guay D, Dodelet JP, Schulz R. High energy ballmilled Pt-Mo catalysts for polymer electrolyte fuel cells and their tolerance to CO. J Electrochem Soc 2000;147:3989–96.
260. Ball S, Hodgkinson A, Hoogers G, Maniguet S, Thompsett D, Wong B. The proton exchange membrane fuel cell performance of a carbon supported PtMo catalyst operating on reformate. Electrochem Solid-State Lett 2002;-5:A31–4.

261. Crabb EM, Ravikumar MK, Qian Y, Russell AE, Maniguet S, Yao J, et al. Controlled modification of carbon supported platinum electrocatalysts by Mo. Electrochem Solid-State Lett 2002;-5:A5–9.
262. Santiago EI, Giuseppe GA, Camara A, Ticianelli EA. CO tolerance on PtMo/C electrocatalysts prepared by the formic acid method. Electrochim Acta 2003;48:3527–34.
263. Santiago EI, Batista MS, Assaf EM, Ticianelli EA. Mechanism of CO tolerance on molybdenum-based electrocatalysts for PEMFC. J Electrochem Soc 2004;151:A944–9.
264. Grgur BN, Markovic NM, Ross PN. In: Second international symposium on proton conducting membrane fuel cells II. Gottesfeld S, Fuller TF, Halpert G, editors. Pennington, NJ: The Electrochemical Society, 1998: PV 98–27, p. 176.
265. Janssen GJM. Modelling study of CO_2 poisoning on PEMFC anodes. J Power Sources 2004;136:45–54.
266. Moss TS, Peachey NM, Snow RC, Dye RC. Multilayer metal membranes for hydrogen separation. Int J Hydrogen Energy 1998;23:99–106.
267. Crabb EM, Marshall R, Thompsett D. Carbon monoxide electr-oxidation properties of carbon-supported PtSn catalysts prepared using surface organometallic chemistry. J Electrochem Soc 2000;147:4440–7.
268. Honma I, Toda T. Temperature dependance of kinetics of methanol electro-oxidation on PtSn alloys. J Electrochem Soc 2003;150:A1689–92.
269. Zhou WJ, Zhou B, Li WZ, Zhou ZH, Song SQ, Sun GQ, et al. Performance comparison of low-temperature direct alcohol fuel cells with different anode catalysts. J Power Sources 2004;126:16–22.
270. Lamy C, Rousseau S, Belgasir EM, Coutanceau C, Leger J-M. Recent progress in the direct ethanol fuel cell: development of new platinum–tin electrocatalysts. Electrochim Acta 2004;49:3901–8.
271. Arenz M, Stamenkovic V, Blizanac BB, Mayrhofer KJ, Markkovic NM, Ross PN. Carbon-supported Pt–Sn electrocatalysts for the anodic oxidation of H_2, CO, and H_2/CO mixtures.: Part II: the structure–activity relationship. J Catal 2005;232:402–10.
272. Colmati F, Antolini E, Gonzalez ER. Pt–Sn/C electrocatalysts for methanol oxidation synthesized by reduction with formic acid. Electrochim Acta 2005;50:5496–503.
273. Lee D-Y, Hwang S-W, Lee I-S. A study on composite PtRu(1:1)-PtSn(3:1) anode catalyst for PEMFC. J Power Sources 2005;145:147–53.
274. Jiang L, Sun G, Sun S, Liu J, Tang S, Li H, et al. Structure and chemical composition of supported Pt–Sn electrocatalysts for ethanol oxidation. Electrochim Acta 2005;50:5384–9.
275. Srinivasan R, De Angeles RJ, Davis BH. Alloy formation in Pt-Sn-alumina catalysts: In situ X-ray diffraction study. J Catal 1987;106:449–57.
276. Srinivasan R, De Angeles RJ, Davis BH. Structural studies of Pt-Sn catalysts on high and low surface area alumina supports. Catal Lett 1990;4:303–8.
277. Srinivasan R, Rice LA, Davis BH. Electron microdiffraction study of Pt-Sn-alumina reforming catalysts. J Catal 1991;129:257–68.
278. Srinivasan R, Davis BH. X-ray diffraction and electron microscopy studies of platinum-tin-silica catalysts. Appl Catal A Gen 1992;87:45–67.
279. Liu ZL, Lin XH, Lee JY, Zhang W, Han M, Gan LM. Preparation and characterization of platinum-based electrocatalsyts on multiwalled carbon nanotubes for proton exchange membrane fuel cells. Langmuir 2002;18(10):4054–60.
280. Yu RQ, Chen LW, Liu QP, Lin JY, Tan KL, Ng SC, et al. Platinum deposition on carbon nanotubes via chemical modification. Chem Mater 1998;10(3):718–22.
281. Lim D-H, Choi D-H, Lee W-D, Park D-R, Lee H-I. The effect of Sn addition on a Pt/C electrocatalyst synthesized by borohydrode reduction and hydrothermal treatment for a low-temperature fuel cell. Electrochem Solid-State Lett 2007;10:B87–90.

282. Neto AO, Vasconcelos TRR, Da Silva RWRV, Linardi M, Spinace EV. Electro-oxidation of ethylene glycol on PtRu/C and PtSn/C electrocatalysts prepared by alcohol-reduction process. J Appl Electrochem 2005;35:193–8.
283. Zhu Y, Uchida H, Watanabe M. Oxidation of carbon monoxide at a platinum film electrode studied by Fourier transform infrared spectroscopy with attenuated total reflection technique. Langmuir 1999;15:8757–64.
284. Kwak C, Park TJ, Suh DJ. Preferential oxidation of carbon monoxide in hydrogen-rich gas over platinum–cobalt–alumina aerogel catalysts. Chem Eng Sci 2005;60:1211–7.
285. Yan J, Ma JX, Cao P, Li P. Preferential oxidation of CO in H_2-rich gases over Co-promoted Pt-γ-Al_2O_3 catalyst. Catal Lett 2004;93:55–60.
286. Page T, Johnson R, Hormes J, Noding S, Rambabu B. A study of methanol electro-oxidation reactions in carbon membrane electrodes and structural properties of Pt alloy electro-catalysts by EXAFS. J Electroanal Chem 2000;485:34–41.
287. Mukerjee S, Srinivasan S. Enhanced electrocatalysis of oxygen reduction on platinum alloys in proton exchange membrane fuel cells. J Electroanal Chem 1993;357:201–24.
288. Antolini E, Salgado JRC, Giz MJ, Gonzalez ER. Effects of geometric and electronic factors on ORR activity of carbon supported Pt–Co electrocatalysts in PEM fuel cells. Int J Hydrogen Energy 2005;30:1213–20.
289. Antolini E, Salgado JRC, Gonzalez ER. The methanol oxidation reaction on platinum alloys with the first row transition metals: The case of Pt–Co and –Ni alloy electrocatalysts for DMFCs: A short review. Appl Catal B 2006;63:137–49.
290. Bonakdarpour A, Lobel R, Sheng S, Monchesky TL, Dahn JR. Acid stability and oxygen reduction activity of magnetron-sputtered $Pt_{1-x}Ta_x$ ($0 \leq x \leq 1$) films. J Electrochem Soc 2006;153:A2304–13.
291. Gómez R, Gutiérrez de Dios FJ, Feliu JM. Carbon monoxide oxidation and nitrous oxide reduction on Rh/Pt(1 1 1) electrodes. Electrochim Acta 2004;49:1195–1208.
292. Llorca MJ, Feliu JM, Aldaz A, Chavilier J. Formic acid oxidation on Pd_{ad} + Pt(100) and Pd_{ad} + Pt(111) electrodes. J Electroanal Chem 1994;376:151–60.
293. Baldauf M, Kolb DM. Formic acid oxidation on ultrathin Pd films on Au(hkl) and Pt(hkl) electrodes. J Phys Chem 1996;100:11375–81.
294. Lu GQ, Crown A, Wieckowski A. Formic acid decomposition on polycrystalline platinum and palladized platinum electrodes. J Phys Chem B 1999;103:9700–11.
295. Stonehart P. Fuel cell with Pt/Pd electrocatalyst electrode. United States Patent US4407906. 1983 Oct 4.
296. Stonehart P. Electrocatalyst advances for hydrogen oxidation in phosphoric acid fuel cells. J Hydrogen Energy 1984;9:921–8.
297. Papageorgopoulos DC, Keijzer M, Veldhuis JBJ, de Bruijn FA. CO tolerance of Pd-rich platinum palladium carbon-supported electrocatalysts. J Electrochem Soc 2002;149:A1400–4.
298. He C, Kunz HR, Fenton JM. Evaluation of platinum-based catalysts for methanol electro-oxidation in phosphoric acid electrolyte. J Electrochem Soc 1997;144:970–9.
299. Stonehart P, Watanabe M, Yamamoto N, Nakamura T, Hara N, Tsurumi K, inventors. Tanaka, Precious Metal Ind., Stonehart Ass. Inc., assignees. Electrocatalyst. United States Patent US5208207. 1993 May 4.
300. Zhang H, Wang Y, Fachini ER, Cabrera CR. Electrochemically codeposited platinum/molybdenum oxide electrode for catalytic oxidation of methanol in acid solution. Electrochem Solid State 1999;2:437–9.
301. Pinheiro ALN, Oliveira-Neto A, de Souza EC, Perez J, Paganin VA, Ticianelli E, et al. Electrocatalysis on noble metal and noble metal alloys dispersed on high surface area carbon. J New Mater Electrochem Syst 2003;6(1):1–16.

302. Stevens DA, Rouleau JM, Mar RE, Atanasoski RT, Schmoeckel AK, Debe MK, et al. Enhanced CO-tolerance of Pt–Ru–Mo hydrogen oxidation catalysts. J Electrochem Soc 2007;154:B1211–9.
303. Wu G, Swaidan R, Cui G. Electrooxidations of ethanol, acetaldehyde and acetic acid using PtRuSn/C catalysts prepared by modified alcohol-reduction process. J Power Sources 2007;172:180–8.
304. Venkataraman R, Kun HR, Fenton JM. Development of new CO tolerant ternary anode catalysts for proton exchange membrane fuel cells. J Electrochem Soc 2003;150:A278–84.
305. Verbeek H, Sachtler WHM. The study of the alloys of platinum and tin by chemisorption. J Catal 1976;42:257–67.
306. Wise H. Role of surface composition in co adsorption on Pd-Ag catalysts. J Catal 1976;43:373–5.
307. Fleischmann R, Boehm H. Dechema Monographs 1982;92:309.
308. Ioroi T, Fujiwara N, Siroma Z, Yasuda K, Miyazaki Y. Platinum and molybdenum oxide deposited carbon electrocatalyst for oxidation of hydrogen containing carbon monoxide. Electrochem Commun 2002;4:442–6.
309. Ioroi T, Yasuda K, Siroma Z, Fujiwara N, Miyazaki Y. Enhanced CO-tolerance of carbon-supported platinum and molybdenum oxide anode catalyst. J Electrochem Soc 2003;150:A1225–30.
310. Matsui T, Fujiwara K, Okanishi T, Kikuchi R, Takeguchi T, Eguchi K. Electrochemical oxidation of CO over tin oxide supported platinum catalysts. J Power Sources 2006;155:152–6.
311. Ioroi T, Akita T, Yamazaki S, Siroma Z, Fujiwara N, Yasuda K. Comparative study of carbon-supported Pt/Mo-oxide and PtRu for use as CO-tolerant anode catalysts. Electrochim Acta 2006;52:491–8.
312. Machida K, Enyo M, Adachi G, Shiokawa J. Methanol oxidation characteristics of rare earth tungsten bronze electrodes doped with platinum. J Electrochem Soc 1988;135:1955–61.
313. Shen PK, Tseung ACC. Anodic oxidation of methanol on Pt/WO_3 in acidic media. J Electrochem Soc 1994;141:3082–90.
314. Shukla AK, Ravikumar MK, Aricò AS, Candiano G, Antonucci V, Giordano N, et al . Methanol electrooxidation on carbon-supported Pt-WO_{3-x} electrodes in sulphuric acid electrolyte. J Appl Electrochem 1995;25:528–32.
315. Tseung ACC, Chen KY. Hydrogen spill-over effect on Pt/WO_3 anode catalysts. Catal Today 1997;38:439–43.
316. Shen PK, Chen KY, Tseung ACC. CO oxidation on Pt-Ru/WO_3 electrodes. J Electrochem Soc 1995;142:L85–6.
317. Chen KY, Sun Z, Tseung ACC. Preparation and characterization of high-performance Pt-Ru/WO_3-C anode catalysts for the oxidation of impure hydrogen. Electrochem Solid State Lett 2000;3:10–2.
318. Roth C, Goetz M, Fuess H. Synthesis and characterization of carbon-supported Pt–Ru–WO_x catalysts by spectroscopic and diffraction methods. J Appl Electrochem 2001;31:793–8.
319. Hou Z, Yi B, Yu H, Lin Z, Zhang H. CO tolerance electrocatalyst of PtRu-H_xMeO_3/C (Me = W, Mo) made by composite support method. J Power Sources 2003;123:116–25.
320. Maillard F, Peyrelade E, Soldo-Olivier Y, Chatenet M, Chaînet E, Faure R. Is carbon-supported Pt-WO_x composite a CO-tolerant material? Electrochim Acta 2007;52:1958–67.
321. Gustavo L, Pereira S, dos Santos FR, Pereira ME, Paganin VA, Ticianelli EA. CO tolerance effects of tungsten-based PEMFC anodes. Electrochim Acta 2006;4061–6.

322. Giordano N, Aricò AS, Hocevar S, Staiti P, Antonucci PL, Antonucci V. Oxygen reduction kinetics in phosphotungstic acid at low temperature. Electrochim Acta 1993;38:1733–41.
323. Giordano N, Staiti P, Aricò AS, Passalacqua E, Abate L, Hocevar S. Analysis of the chemical cross-over in a phosphotungstic acid electrolyte based fuel cell. Electrochim Acta 1997;42:1645–52.
324. Aricò AS, Modeca E, Ferrara I, Antonucci V. CO and CO/H_2 electrooxidation on carbon supported Pt–Ru catalyst in phosphotungstic acid ($H_3PW_{12}O_{40}$) electrolyte. J Appl Electrochem 1998;28:881–7.
325. Gatto I, Saccà A, Carbone A, Pedicini R, Urbani F, Passalacqua E. CO-tolerant electrodes developed with phosphomolybdic acid for polymer electrolyte fuel cell (PEFCs) application. J Power Sources 2007;171:540–5.
326. Herrero E, Franaszczuk K, Wieckowski A. A voltammetric identification of the surface redox couple effective in methanol oxidation on a ruthenium-covered platinum (110) electrode. J Electroanal Chem 1993;361:269–73.
327. Franszczuk K, Sobkowski J. The influence of ruthenium adatoms on the oxidation of chemisorbed species of methanol on a platinum electrode by a radiochemical method. J Electroanal Chem 1992;327:235–45.
328. Fachini ER, Diaz-Ayala R, Casado-Rivera E, File S, Cabrera CR. Surface coordination of ruthenium clusters on platinum nanoparticles for methanol oxidation catalysts. Langmuir 2003;19:8986–93.
329. Crabb EM, Ravikumar MK, Thompsett D, Hurford M, Rose A, Russell AE. Effect of Ru surface composition on the CO tolerance of Ru modified carbon supported Pt catalysts. Phys Chem Chem Phys 2004;6:1792–8.
330. Crown A, Moraes IR, Wieckowski A. Examination of Pt(111)/Ru and Pt(111)/Os surfaces: STM imaging and methanol oxidation activity. J Electroanal Chem 2001;500:333–43.
331. Szabo S, Bakos I. Investigation of ruthenium deposition onto a platinized platinum-electrode in sulfuric-acid media. J Electroanal Chem 1987;230:233–40.
332. Friedrich KA, Geyzers KP, Marmann A, Stimming U, Vogel R. Bulk metal electrodeposition in the sub-monolayer regime: Ru on Pt(111). Z Phys Chem 1999;208:137–50.
333. Morimoto Y, Yeager EB. CO oxidation on smooth and high area Pt, Pt-Ru and Pt-Sn electrodes. J Electroanal Chem 1998;441:77–81.
334. Jarvi TD, Madden TH, Stuve EM. Vacuum and electrochemical behavior of vapor deposited ruthenium on platinum (111). Electrochem Solid-State Lett 1999;2:224–7.
335. Davies JC, Hayden BE, Pegg DJ, Rendall ME. The electrooxidation of carbon monoxide on ruthenium modified Pt(111). Surf Sci 2002;496:110–20.
336. Cao DX, Bergens SH. An organometallic deposition of ruthenium adatoms on platinum that self poisons at a specific surface composition. A direct methanol fuel cell using a platinum–ruthenium adatom anode catalyst. J Electroanal Chem 2002;533:91–100.
337. Crown A, Johnston C, Wieckowski A. Growth of ruthenium islands on Pt(hkl) electrodes obtained via repetitive spontaneous deposition. Surf Sci 2002;506:L268–74.
338. Jiang Q, Lu HM, Zhao M. Modelling of surface energies of elemental crystals. J Phys Condens Matter 2004;16:521–30.
339. Ianniello R, Schmidt VM, Stimming U, Stumper J, Wallau A. Co adsorption and oxidation on Pt and Pt-Ru alloys – dependence on substrate composition. Electrochim Acta 1994;39:1863–9.
340. Brankovic SR, McBreen J, Adzic RR. Spontaneous deposition of Pt on the Ru(0001) surface. J Electroanal Chem 2001;503:99–104.

341. Brankovic SR, McBreen J, Adzic RR. Spontaneous deposition of Pd on a Ru(0 0 0 1) surface. Surf Sci 2001;479:L363–8.
342. Adzic RR, Brankovic SR, Wang JX. Carbon monoxide tolerant electrocatalyst with low platinum loading and a proces for its preparation United State patent pending, 2001.
343. Sasaki K, Wang JX, Balasubramanian M, McBreen J, Uribe F, Adzic RR. Ultra-low platinum content fuel cell anode electrocatalyst with a long-term performance stability. Electrochim Acta 2004;49:3873–7.
344. Campbell CT. Bimetallic surface chemistry. Annu Rev Phys Chem 1990;41:775–837.
345. Rubin AV, Skriver HL, Nørskov JK. Surface segregation energies in transition-metal alloys. Phys Rev B 1999;59:15990–6000.
346. Lasch K, Hayn G, Jörissen L, Garche J, Besenhardt O. Mixed conducting catalyst support materials for the direct methanol fuel cell. J Power Sources 2002;105(2):305–10.
347. Somorjai G. Introduction to surface chemistry and catalysis. New York: Wiley, 1994: 442–595.
348. Nakamura T, Yamada M, Yamaguchi T. Catalytic properties of $Mo(CO)_6$ supported on activated carbon for ethene homologation. Appl Catal A Gen 1992;87(1):69–79.
349. de la Fuente JLG, Martinez-Huerta MV, Rojas S, Peňa MA, Terreros P, Fierro JLG. Enhanced methanol electrooxidation activity of PtRu nanoparticles supported on H_2O_2-functionalized carbon black. Carbon 2005;43(14):3002–5.
350. de la Fuente JLG, Rojas S, Martínez-Huerta MV, Terreros P, Peňa MA, Fierro JLG. Functionalization of carbon support and its influence on the electrocatalytic behaviour of Pt/C in H_2 and CO electrooxidation. Carbon 2006;44:1919–29.
351. Iijima S. Helical microtubules of graphitic carbon. Nature 1991;354(6348):56–7.
352. Ebbesen TW, Ajayan PM. Large-scale synthesis of carbon nanotubes. Nature 1992;358(6383):220–2.
353. Li WZ, Xie SS, Qian LX, Chang BH, Zou BS, Zhou WY, et al. Large-scale synthesis of aligned carbon nanotubes. Science 1996;274(5293):1701–3.
354. Ebbesen TW, Lezec HJ, Hiura H, Bennett JW, Ghaemi HF, Thio T. Electrical conductivity of individual carbon nanotubes. Nature 1996;382(6586):54–6.
355. Che GL, Lakshmi BB, Martin CR, Fisher ER. Metal-nanocluster filled carbon nanotubes: catalytic properties and possible applications in electrochemical energy storage and production. Langmuir 1999;15(3):750–16.
356. Joo SH, Choi SJ, Oh I, Kwak J, Liu Z, Terasaki O, et al. Ordered nanoporous arrays of carbon supporting high dispersions of platinum nanoparticles. Nature 2001;412(6848):169–72.
357. Sun X, Li R, Villers D, Dodelet JP, Desilets S. Composite electrodes made of Pt nanoparticles deposited on carbon nanotubes grown on fuel cell backings. Chem Phys Lett 2003;379(1–2):99–104.
358. Pyun SI, Rhee CK. An investigation of fractal characteristics of mesoporous carbon electrodes with various pore structures. Electrochim Acta 2004;49(24):4171–80.
359. He ZB, Chen JH, Liu DY, Zhou HH, Kuang YF. Electrodeposition of PtRu nanoparticles on carbon nanotubes and their electrocatalystic properties for methanol electrooxidation. Diam Relat Mater 2004;13:1764–79.
360. Liu ZL, Lee JY, Chen WX, Han M, Gan LM. Physical and electrochemical characterizations of microwave-assisted polyol preparation of carbon-supported PtRu nanoparticles. Langmuir 2004;20(1):181–7.
361. Yu JS, Kang S, Yoon SB, Chai G. Fabrication of ordered uniform porous carbon networks and their application to a catalyst supporter. J Am Chem Soc 2002;124(32):9382–3.

362. Li WZ, Liang CH, Qiu JS, Xin Q. Carbon nanotubes as support for cathode catalyst of a direct methanol fuel. Carbon 2002;40(5):791–4.
363. Li WZ, Liang CH, Zhou WJ, Xin Q. Preparation and characterization of multiwalled carbon nanotube-supported platinum for cathode catalysts of direct methanol fuel cells. J Phys Chem B 2003;107(26):6292–9.
364. Li L, Wu G, Xu B-Q. Electro-catalytic oxidation of CO on Pt catalyst supported on carbon nanotubes pretreated with oxidative acids. Carbon 2006;44:2973–2983.
365. Carmo M, Paganin VA, Rosolenand JM, Gonzalez ER. Alternative supports for the preparation of catalysts for low-temperature fuel cells: the use of carbon nanotubes. J Power Sources 2005;142:169–76.
366. Rodrigues NM, Chambers A, Baker RTK. Catalytic engineering of carbon nanostructures. Langmuir 1995;11:3862–6.
367. Gadd GE, Blackford M, Moricca S, Weebb N, Evans PJ, Smith AM, et al. The world's smallest gas cylinders. Science 1997;277:933–6.
368. Luo J, Maye MM, Kariuki NN, Wang LY, Njoki P, Lin Y, et al. Electrocatalytic oxidation of methanol: carbon-supported gold–platinum nanoparticle catalysts prepared by two-phase protocol. Catal Today 2005;99:291–7.
369. Cameron D, Holliday R, Thompson D. Gold's future role in fuel cell systems. J Power Sources 2003;118:298–303.
370. Ullmann's encyclopedia of industrial chemistry, Vol. A21. Gerhartz W, Elvers B, editors, Weinheim, Germany: VCH, 1992: 113.
371. Machida K, Enyo M. In situ X-ray diffraction study of hydrogen entry into Pd and Pd-Au alloy electrodes during anodic HCHO oxidation. J Electrochem Soc 1987;134:1472–4.
372. Lewis FA. The palladium hydrogen system. London: Academic Press, 1967.
373. Thompsett D, Cooper SJ, Hards GA. Report ETSU F/02/00014/REP/1, 1998.
374. Yepez O, Scharifker BR. Oxidation of CO on hydrogen-loaded palladium. J Appl Electrochem 1999;29:1185–90.
375. Fishman JH, inventor; Leesona Corp., assignee. Method of generating electricity comprising contacting a Pd/Au alloy black anode with a fuel containing carbon monoxide. United State Patente US3510355. 1970 May 5.
376. Eley DD, Moore PB. The adsorption and reaction of CO and O_2 on Pd---Au alloy wires. Surf Sci 1981;111:325–43.
377. Okanishi T, Matsui T, Takeguchi T, Kikuchi R, Eguchi K. Chemical interaction between Pt and SnO_2 and influence on adsorptive properties of carbon monoxide. Appl Catal A 2006;298:181–7.
378. Takeguchi T, Anzai Y, Kikuchi R, Eguchi K, Ueda W. Preparation and characterization of CO-tolerant Pt and Pd anodes modified with SnO_2 nanoparticles for PEFC. J Electrochem Soc 2007;154:B1132–7.
379. Okumura M, Masuyama N, Konishi E, Ichikawa S, Akita T. CO oxidation below room temperature over Ir/TiO_2 catalyst prepared by deposition precipitation method. J Catal 2002;208:485–9.
380. Wasmus S, Küver A. Methanol oxidation and direct methanol fuel cells: a selective review. J Electroanal Chem 1999;461:14–31.
381. Bonnemann H, Brinkmann R, Britz P, Endruschat U, Mortel R, Feldmeyer G, et al. J New Mater Electrochem Syst 2000;3:199.
382. Paulus U, Endruschat U, Feldmeyer G, Schmidt T, Behm R. New PtRu alloy colloids as precursors for fuel cell catalysts. J Catal 2000;195:383–93.
383. Luna A, Camara G, Paganin V, Ticianelli E, Gonzalez E. Effect of thermal treatment on the performance of CO-tolerant anodes for polymer electrolyte fuel cells. Electrochem Commun 2000;2:222–5.

384. Antolini E, Giorgi L, Cardellini F, Passalacqua E. Physical and morphological characteristics and electrochemical behaviour in PEM fuel cells of PtRu/C catalysts. J Solid State Electrochem 2001;5:131–40.
385. Pozio A, Silva R, De Francesco M, Cardellini F, Giorgi L. A novel route to prepare stable Pt–Ru/C electrocatalysts for polymer electrolyte fuel cell. Electrochim Acta 2002;48:255–62.
386. Che G, Lakeshmi B, Fisher E, Martin C. Carbon nanotubule membranes for electrochemical energy storage and production. Nature 1998;393:346–9.
387. Antolini E, Cardellini F. Formation of carbon supported PtRu alloys: an XRD analysis. J Alloys Compd 2001;315:118–22.
388. Steigerwalt E, Deluga G, Cliffel D, Lukehart C. A Pt-Ru/graphitic carbon nanofiber nanocomposite exhibiting high relative performance as a direct-methanol fuel cell anode catalyst. J Phys Chem B 2001;105:8097–101.
389. Fujiwara N, Shiozaki Y, Tanimitsu T, Yasuda K, Miyazaki Y. Precursor effects in PtRu electrocatalysts as a direct methanol fuel cell anode. Electrochemistry 2002;70:988–90.
390. Hills C, Mack N, Nuzzo R. The size-dependent structural phase behaviors of supported bimetallic (Pt-Ru) nanoparticles. J Phys Chem B 2003;107:2626–36.
391. Liu Y, Qiu X, Chen Z, Zhu W. A new supported catalyst for methanol oxidation prepared by a reverse micelles method. Electrochem Commun 2002;4:550–3.
392. Zhang X, Chan KY. Water-in-oil microemulsion synthesis of platinum-ruthenium nanoparticles, their characterization and electrocatalytic properties. Chem Mater 2003;15:451–9.
393. Roth C, Martz N, Fuess H. Characterization of different Pt–Ru catalysts by X-ray diffraction and transmission electron microscopy. Phys Chem Chem Phys 2001;3:315–9.
394. Goodenough JB, Hamnett A, Kennedy BJ, Manoharam R, Weeks SA. Porous carbon anodes for the direct methanol fuel cell—I. The role of the reduction method for carbon supported platinum electrodes. Electrochim Acta 1990;35:199–207.
395. Lizcano-Valbuena WH, Paganin VA, Leite CA, Galembeck F, Gonzalez ER. Catalysts for DMFC: relation between morphology and electrochemical performance. Electrochim Acta 2003;48:3869–78.
396. Colmati F Jr, Lizcano-Valbuena WH, Camara GA, Ticianelli EA, Gonzalez ER. Carbon monoxide oxidation on Pt-Ru electrocatalysts supported on high surface area carbon. J Braz Chem Soc 2002;13:474–82.
397. Shukla AK, Neegat M, Bera P, Jayaram V, Hegde MS. An XPS study on binary and ternary alloys of transition metals with platinized carbon and its bearing upon oxygen electroreduction in direct methanol fuel cells. J Electroanal Chem 2001;504:111–9.
398. Watson DJ, Attard GA. The electro-oxidation of glucose using platinum–palladium bulk alloy single crystals. Electrochim Acta 2001;46:3157–61.
399. Watson DJ, Attard GA. Surface segregation and reconstructive behaviour of the (1 0 0) and (1 1 0) surfaces of platinum–palladium bulk alloy single crystals: a voltammetric and LEED/AES study. Surf Sci 2002;515:87–93.
400. Schmidt TJ, Markovic NM, Stamenkovic V, Ross PN, Attard GA, Watson DJ. Surface characterization and electrochemical behavior of well-defined Pt-Pd{111} single-crystal surfaces: a comparative study using Pt{111} and palladium-modified Pt{111} electrodes. Langmuir 2002;18:6969–75.
401. Clavilier J, Feliu JM, Aldaz A. An irreversible structure sensitive adsorption step in bismuth underpotential deposition at platinum electrodes. J Electroanal Chem 1988;243:419–33.
402. Feliu JM, Fernández-Vega A, Aldaz A, Clavilier J. New observations of a structure sensitive electrochemical behaviour of irreversibly adsorbed arsenic and antimony

from acidic solutions on Pt (111) and Pt (100) orientations. J Electroanal Chem 1988;256:149–63.
403. Gómez R, Llorca MJ, Feliu JM, Aldaz A. The behaviour of germanium adatoms irreversibly adsorbed on platinum single crystals. J Electroanal Chem 1992;340:349–55.
404. Feliu JM, Gómez R, Llorca MJ, Aldaz A. Electrochemical behavior of irreversibly adsorbed selenium dosed from solution on Pt(h,k,l) single crystal electrodes in sulphuric and perchloric acid media. Surf Sci 1993;289:152–62.
405. Feliu JM, Llorca MJ, Gómez R, Aldaz A. Electrochemical behaviour of irreversibly adsorbed tellurium dosed from solution on Pt(h, k, l) single crystal electrodes in sulphuric and perchloric acid media. Surf Sci 1993;297:209–22.
406. Clavilier J, Llorca MJ, Feliu JM, Aldaz A. Preliminary study of the electrochemical adsorption behaviour of a palladium modified Pt(111) electrode in the whole range of coverage. J Electroanal Chem 1991;310:429–35.
407. Clavilier J, Llorca MJ, Feliu JM, Aldaz A. Electrochemical structure-sensitive behaviour of irreversibly adsorbed palladium on Pt(100), Pt(111) and Pt(110) in an acidic medium. J Electroanal Chem 1993;351:299–319.
408. Gómez R, Feliu JM. Rhodium adlayers on Pt(111) monocrystalline surfaces. Electrochemical behavior and electrocatalysis. Electrochim Acta 1998;44:1191–205.
409. Gutiérrez de Dios FJ, Gómez R, Feliu JM. Preparation and electrocatalytic activity of Rh adlayers on Pt(1 0 0) electrodes: reduction of nitrous oxide. Electrochem Commun 2001;3:659–64.
410. Álvarez B, Climent V, Rodes A, Feliu JM. Potential of zero total charge of palladium modified Pt(111) electrodes in perchloric acid solutions. Phys Chem Chem Phys 2001;3:3269–76.
411. Álvarez B, Rodes A, Pérez JM, Feliu JM. Two-dimensional effects on the in situ infrared spectra of CO adsorbed at palladium-covered Pt(111) electrode surfaces. J Phys Chem 2003;107:2018–28.
412. Inukai J, Ito M. Electrodeposition processes of palladium and rhodium monolayers on Pt(111) and Pt(100) electrodes studied by IR reflection absorption spectroscopy. J Electroanal Chem 1993;358:307–15.
413. Attard GA, Al-Akl A. Palladium adsorption on Pt(111): a combined electrochemical and ultra-high vacuum study. Electrochim Acta 1994;39:1525–30.
414. Climent V, Markovic NM, Ross PN. Kinetics of oxygen reduction on an epitaxial film of palladium on Pt(111). J Phys Chem B 2000;104:3116–20.
415. Arenz M, Stamenkovic V, Schmidt TJ, Wandelt K, Ross PN, Markovic MN. The effect of specific chloride adsorption on the electrochemical behavior of ultrathin Pd films deposited on Pt(1 1 1) in acid solution. Surf Sci 2003;523:199–209.
416. Attard GA, Price R. Electrochemical investigation of a structure sensitive growth mode: palladium deposition on Pt(100)-hex-R0.7° and Pt(100)-(1×1). Surf Sci 1995;335:63–74.
417. Attard GA, Price R, Al-Akl A. Electrochemical and ultra-high vacuum characterisation of rhodium on Pt(111): a temperature dependent growth mode. Surf Sci 1995;335:52–62.
418. Tanaka K, Okawa Y, Sasahara A, Matsumoto Y. Chapter 18. In: Solid–liquid electrochemical interfaces. ACS symposium series. Washington DC: American Chemical Society, 1997.
419. Uosaki K, Ye S, Oda Y, Haba T, Kondo T. Electrochemical epitaxial growth of a Pt(111) phase on an Au(111) electrode. J Phys Chem B 1997;101:7566–72.
420. Brankovic SR, Wang JX, Adzic RR. Metal monolayer deposition by replacement of metal adlayers on electrode surfaces. Surf Sci L 2001;474:L173–9.

421. Keck L, Buchanan JS, Hards GA, inventors; Johnson Matthey PLC, assignee. Catalyst material. United States Patent US5068161. 1991 Nov 26.
422. Schmidt TJ, Noeske M, Gasteiger HA, Behm RJ, Britz P, Bönnemann H. PtRu alloy colloids as precursors for fuel cell catalysts. J Electrochem Soc 1998;145:925–31.
423. Boxall DL, Deluga GA, Kenik EA, King WD, Lukehart CM. Rapid synthesis of a Pt_1Ru_1/carbon nanocomposite using microwave irradiation: a DMFC anode catalyst of high relative performance. Chem Mater 2001;13:891–900.
424. Kim JY, Yang ZG, Chang C-C, Valdez TI, Narayanan SR, Kumta PN. A sol-gel-based approach to synthesize high-surface-area Pt-Ru catalysts as anodes for DMFCs. J Electrochem Soc 2003;150:A1421–31.
425. Kim T, Takahashi M, Nagai M, Kobayashi K. Preparation and characterization of carbon supported Pt and PtRu alloy catalysts reduced by alcohol for polymer electrolyte fuel cell. Electrochim Acta 2004;50:817–21.
426. Liu Z, Ling XY, Su X, Lee JY. Carbon-supported Pt and PtRu nanoparticles as catalysts for a direct methanol fuel cell. J Phys Chem B 2004;108:8234–40.
427. Bock C, Paquet C, Couillard M, Botton GA, MacDougall BR. Size-selected synthesis of PtRu nano-catalysts: reaction and size control mechanism. J Am Chem Soc 2004;126:8028–37.
428. Chan K-Y, Ding J, Ren J, Cheng S, Tsang KY. Supported mixed metal nanoparticles as electrocatalysts in low temperature fuel cells. J Mater Chem 2004;14:505–16.
429. Lizcano-Valbuena WH, de Azevedo DC, Gonzalez ER. Supported metal nanoparticles as electrocatalysts for low-temperature fuel cells. Electrochim Acta 2004;49:1289–95.
430. Sarma LS, Lin TD, Tsai Y-W, Chen JM, Hwang BJ. Carbon-supported Pt–Ru catalysts prepared by the Nafion stabilized alcohol-reduction method for application in direct methanol fuel cells. J Power Sources 2005;139:44–54.
431. Chu D, Gilman S. Methanol electro-oxidation on unsupported Pt-Ru alloys at different temperatures. J Electrochem Soc 1996;143:1685–90.
432. Jusys Z, Kaiser J, Behm RJ. Composition and activity of high surface area PtRu catalysts towards adsorbed CO and methanol electrooxidation—: A DEMS study. Electrochim Acta 2002;47:3693–706.
433. Lee SA, Park K-W, Choi J-H, Kwon B-K, Sung Y-E. Nanoparticle synthesis and electrocatalytic activity of Pt alloys for direct methanol fuel cells. J Electrochem Soc 2002;149:A1299–304.
434. Antolini E. Formation of carbon-supported PtM alloys for low temperature fuel cells: a review. Mater Chem Phys 2003;78:563–73.
435. Solla-Gullon J, Vidal-Iglesias FJ, Montiel V, Aldaz A. Electrochemical characterization of platinum–ruthenium nanoparticles prepared by water-in-oil microemulsion. Electrochim Acta 2004;49:5079–88.
436. Bock C, Blakely M-A, MacDougall B. Characteristics of adsorbed CO and CH_3OH oxidation reactions for complex Pt/Ru catalyst systems. Electrochim Acta 2005;50:2401–14.
437. Aricò AS, Antonucci PL, Modica E, Baglio V, Kim H, Antonucci V. Effect of Pt---Ru alloy composition on high-temperature methanol electro-oxidation. Electrochim Acta 2002;47:3723–32.
438. Sirk AHC, Hill JM, Kung SKY, Birss VI. Effect of redox state of PtRu electrocatalysts on methanol oxidation activity. J Phys Chem B 2004;108:689–95.
439. Park K-W, Sung Y-E. Catalytic activity of platinum on ruthenium electrodes with modified (electro)chemical states. J Phys Chem B 2005;109:13585–9.
440. Bönnemann H, Nagabhushana KS. Advantageous fuel cell catalysts from colloidal nanometals. J New Mater Electrochem Syst 2004;7:93–108.

441. Hui CL, Li XG, Hsing IM. Well-dispersed surfactant-stabilized Pt/C nanocatalysts for fuel cell application: dispersion control and surfactant removal. Electrochim Acta 2005;51:711–9.
442. Li X, Hsing I-M. Surfactant-stabilized PtRu colloidal catalysts with good control of composition and size for methanol oxidation. Electrochim Acta 2006;52:1358–65.
443. Sanchez MG, Park S, Maselli JM, City E, Graham JR. United States Patent 3830756, 1974.
444. Chen L, Guo M, Zhang H-F, Wang X-D. Characterization and electrocatalytic properties of PtRu/C catalysts prepared by impregnation-reduction method using Nd_2O_3 as dispersing reagent. Electrochim Acta 2006;52:1191–8.
445. Zeng J, Lee JY. More active PtRu/C catalyst for methanol electrooxidation by reversal of mixing sequence in catalyst preparation. Mater Chem Phys 2007;104:336–41.
446. Rolison DR. Catalytic nanoarchitectures--the importance of nothing and the unimportance of periodicity. Science 2003;299:1698–1701.
447. Rolison DR, Hagans PL, Swider KE, Long JW. Role of hydrous ruthenium oxide in Pt-Ru direct methanol fuel cell anode electrocatalysts: the importance of mixed electron/proton conductivity. Langmuir 1999;15:774–9.
448. Long JW, Stroud RM, Swider-Lyons KE, Rolison DR. How to make electrocatalysts more active for direct methanol oxidation-avoid PtRu bimetallic alloys. J Phys Chem B 2000;104:9772–6.
449. Grgur BN, Marković NM, Lucas CA, Ross PN. Electrochemical oxidation of carbon monoxide: from platinum single crystals to low temperature fuel cells catalysis. Part I: carbon monoxide oxidation onto low index platinum single crystals. J Serb Chem Soc 2001;66:785–97.